



University of Florence

Department of industrial engineering - DIEF

Thesis submitted in fulfilment of the requirements for the degree of

Doctor of Philosophy in

Energy Engineering and Innovative Industrial Technologies

PhD School in Industrial Engineering – XXVII Cycle (2012-2014)

Biomass pyrolysis for liquid biofuels: production and use

Tutor

Prof. Francesco Martelli

Candidate

Eng. Andrea Maria Rizzo

Co-Tutor

Prof. David Chiaramonti, PhD

External Advisor

Prof. Marco Baratieri, PhD

PhD Course Coordinator

Prof. Maurizio De Lucia

Florence, Italy, December 2014

*To Elena and Sibilla,
my two princesses*

Declaration

I hereby declare that this submission is my own work, and to the best of my knowledge and belief, it contains no material previously published or written by another person, nor material which to a substantial extent has been accepted for the award of any other degree or diploma at University of Florence or any other educational institution, except where due references are provided in the thesis itself.

Any contribution made to the research by others I have been working with is explicitly acknowledged in the thesis.

Andrea Maria Rizzo

Florence, December 2014

Acknowledgments

I would like to express my deepest and most sincere gratitude to all those people who gave me the opportunity and privilege of practicing Research, a profession amid the most fascinating. I'm indebted to David Chiamonti and my parents Miriam and Felice for this.

During the MSc it was just you and me, for my PhD we're going to be three. What about a Postdoc, my heart?

Crowded of colleagues and ideas, the office couldn't be a better place to stay: thanks to Daniela and the three musketeers (Renato, Marco & Marco), for making it possible!

Prof. Marco Baratieri of the Free University of Bozen reviewed this manuscript and provided several valuable suggestions; many thanks for his effort, encouragement, valuable suggestions and fruitful discussions.

Prof. Robert Ghirlando of the University of Malta kindly provided a thorough proofreading of the manuscript, greatly improving the language quality. His unsolicited and highly appreciated help was a notable example of academic commitment.

Last but not least, I gratefully acknowledge the help, support, friendship of all the important people of my life: my family – Giacomo & Nuschka, Lorenzo, Riccardo, Achille, Eva, Leonardo, Luca, Pino, Piera, Anna, all the aunts, uncles and cousins – and indeed all of my friends, colleagues and the group leader Prof. Francesco Martelli.

Contents

Declaration	I
Acknowledgments	III
Contents	VI
List of figures	IX
List of tables.....	XII
List of symbols and abbreviations	XIV
Summary.....	1
1 Pyrolysis for fuel, energy and chemicals	3
1.1 Schematic process pathway	4
1.2 General working principle.....	6
1.2.1 Plant design alternatives.....	7
1.2.2 Pyrolysis oil properties.....	8
1.2.3 Pyrolysis process energy balance.....	9
1.2.4 Pyrolysis process economics.....	11
1.3 Exploiting the potential of pyrolysis oil	12
1.3.1 Heat and power generation.....	13
1.3.2 Fuels.....	17
1.3.3 Chemicals.....	18
1.4 Industrial and demonstration project.....	20
1.4.1 Empyro B.V (The Netherlands)	20
1.4.2 Fortum (Finland)	21
1.5 Synthetic review of microalgae pyrolysis	22
1.6 Synthetic review of scrap tires pyrolysis.....	29
2 Bio-oil production in a pilot test bench	33
2.1 Description of the experimental apparatus.....	34

2.1.1	Pyrolysis reactor	34
2.1.2	Feeding system	35
2.1.3	Bio-oil condensation and collection	36
2.1.4	Char collection	37
2.2	Test procedure	37
2.2.1	Feedstock conditioning	38
2.2.2	Mass yield, energy recovery and carbon recovery of pyrolysis test	39
2.2.3	Products analysis.....	40
3	Experimental results	41
3.1	Pyrolysis oil from lignocellulosic feedstock.....	41
3.1.1	Analysis of the feedstock	41
3.1.2	Pyrolysis experiments	43
3.1.3	Bio-oil yield and characterization.....	44
3.2	Pyrolysis oil from microalgae	50
3.2.1	Analysis of the feedstock	50
3.2.2	Bio-oil yield.....	52
3.2.3	Bio-oil characterization	54
3.2.4	GC-MS analyses of bio-oils	59
3.3	Material compatibility test of bio-oil samples	61
3.3.1	Test procedure	64
3.3.2	Bio-oil samples	66
3.3.3	Results with elastomeric specimens	67
3.3.4	Results with metallic specimens	70
4	Use of bio-oils in a modified micro gas turbine	75
4.1	Description of the biofuel test bench	76
4.2	Turbine test of pine chips pyrolysis oil.....	78
4.2.1	Combustor redesign procedure	78
4.2.2	Firing test of new combustor with reference fuels	80
4.2.3	Firing test of new combustor with bio-oil and bio-oil blends	82
4.3	Turbine test of scrap tire pyrolysis oil.....	85

4.3.1 Firing test of STPO.....	85
5 Conclusions.....	88
6 References.....	90
Appendix A: analytical procedures	102
Appendix B: GC-MS of pyrolysis liquids	108

List of figures

Figure 1.1: Schematic of wood pyrolysis (adapted from [12–14]).	5
Figure 1.2 : Schematic flowsheet of a pyrolysis conversion process.	6
Figure 1.3 : Schematic flowsheet of the Joensuu scale-up plant fed with forest residues (adapted from [36]).	11
Figure 1.4: Range of products from BTX (adapted from [76]).	19
Figure 1.5: Quarterly market price of benzene, toluene and mixed xylenes compared to crude oil Brent between 2007 and 2013. Source: Bloomberg.	20
Figure 1.6: Pyrolysis plant integration at Joensuu premises. Source: Metso.	22
Figure 1.7: Possible pathways for microalgae conversion [90].	24
Figure 1.8: Schematic TGA (a) and DTG (b) during pyrolysis of <i>Chlorella P.</i> Source (ibid).	26
Figure 1.9: Schematic TGA (a) and DTG (b) during pyrolysis of <i>Chlorella P.</i> and <i>Spirulina P.</i> Source (ibid).	26
Figure 1.10: (a) Product yields (on the basis of the dry weight of samples) of fast pyrolysis from microalgae. (b) Product yields of HC <i>Chlorella P.</i> at temperatures from 400 to 600°C. Source (ibid).	27
Figure 2.1 : Schematic of the batch pyrolysis reactor.	35
Figure 2.2: Picture of the batch pyrolysis reactor (centre) and control panel (left).	35
Figure 3.1: TGA of mixed wood chips at 15 °C/min up 900 °C in nitrogen (triplicate). Green: actual samples weight loss profile. Violet: derivative of weight loss (calculated). Red: furnace temperature profile.	43
Figure 3.3: Nitrogen content of pyrolysis liquids vs. feedstock.	57

Figure 3.4: Measured HHV of bio-oils' organic phase vs. lipid content of original feed.	57
Figure 3.5: Viscosity of organic phase of bio-oils vs. temperature.	58
Figure 3.6: Viscosity of water-rich phase of bio-oils vs. temperature.	58
Figure 3.7: Relative distribution of compounds, grouped by classes, for the organic phases of the three bio-oil samples.	60
Figure 3.8: Experimental setup for material compatibility testing of bio-oils.	65
Figure 3.10: Elastomeric specimens before (left) and after (right) 72 h immersion at 80°C in the bio-oil from microalgae <i>Chlorella</i>	69
Figure 3.11: Elastomeric specimens before (left) and after (right) 72 h immersion at 80°C in the BTG bio-oil from pine chips.....	69
Figure 3.12: Weight change of metals after 48 and 72 hours of immersion at 80°C.....	71
Figure 3.13: Selected metal specimens after 72 h immersion at 80°C in bio-oils.	73
Figure 4.1: Layout of the interconnection of test bench basic sub-assemblies.....	77
Figure 4.2: Schematic of the biofuel test bench and measurement points.....	77
Figure 4.3: Cumulative area of air passages along the axial direction of the combustor.	79
Figure 4.4: Original and modified reverse flow, silo combustor of the micro gas turbine.	79
Figure 4.5: CO concentration @15 %vol oxygen in the exhaust for the original and modified combustor.	81
Figure 4.6: NOX concentration @15 %vol oxygen in the exhaust for the original and modified combustor.	82
Figure 4.7: Exhaust temperature and fuel flowrate during the blend test (PO:Ethanol 25:75).....	83
Figure 4.8: CO and NO concentration during the blend test (PO:Ethanol 25:75).....	83
Figure 4.9: Fuel injector before and after the test (left), and flame tube exit after test (right).....	84
Table 4.2: Chemical analysis of scrap tire pyrolysis oil.	85
Figure 4.10: Extract of exhaust gas measurements during a STOP firing test.	87
Figure B.1: Chromatogram of the bio oil from <i>Chlorella</i> Ingrepro.	109

Figure B.2: Chromatogram of the aqueous phase from Chlorella Ingrepro.	109
Figure B.3: Chromatogram of the bio oil from Nannochloropsis HCMR.....	109
Figure B.4: Chromatogram of the aqueous phase from Nannochloropsis HCMR.	110
Figure B.5: Chromatogram of the bio-oil from Chlorella HCMR.	110
Figure B.6: Chromatogram of the aqueous phase from Chlorella HCMR.	110

List of tables

Table 1.1: Yield of products (%wt) according to biomass pyrolysis mode [10].	4
Table 1.2: Typical properties and characteristics of wood-derived bio-oil (adapted from [26])	8
Table 2.1: Set point of process parameters in pyrolysis tests.	38
Table 3.1: Proximate and ultimate analysis of the feedstock (mixed wood chips).	42
Table 3.2: Mass yield, energy and carbon recovery in bio-oil from lignocellulosic feedstock.	48
Table 3.3: Properties of bio-oils from lignocellulosic feedstock.	49
Table 3.4: Compositional and ultimate analysis of microalgae feedstock.....	51
Table 3.5: Mass yield, energy and carbon recovery in bio-oil from microalgae feedstock.	53
Table 3.6: Chemical analysis of the bio-oil from microalgae pyrolysis.	55
Table 3.7: Chemical analysis of the aqueous phase from microalgae pyrolysis.	56
Table 3.8: ASTM Requirements for pyrolysis liquid biofuels [144].	63
Table 3.9: Chemical analysis of feedstock.	66
Table 3.10: Chemical analysis of BTG and microalgae bio-oils.	67
Table 4.1: Equivalence ratio (Φ) in the original and modified combustor at 20 and 12 kWe load.....	80
Table 4.2: Chemical analysis of scrap tire pyrolysis oil.	85
Table 4.3: Test conditions for the STPO test in micro gas turbine.....	86
Table 4.4: Timeline of STPO test in micro gas turbine.....	86

List of symbols and abbreviations

%wt	Weight percentage
AC	Alternate Current
ad	As determined
APU	Auxiliary Power Unit
BHP	Brake Horse Power
BTG	Biomass Technology Group
BTX	Benzene - Toluene - Xylene
CAD	Computer Aided Design
CFD	Computational Fluid Dynamics
CO	Carbon Monoxide
db	Dry basis
DTG(A)	Differential Thermo-Gravimetric (Analysis)
ECU	Engine Control Unit
EEC	Electronic Exciter Circuit
ELT	End-of-Life Tires
EU	European Union
FCU	Fuel Control unit
FP	Fast pyrolysis
GC-MS	Gas Chromatography - Mass Spectroscopy
HCMR	Hellenic Center for Marine Research
HP, HT	High Pressure, Temperature
HR	Heat Rate
LHV	Lower Heating Value (MJ/kg)
LT	Low Temperature
MGT	Micro gas turbine
Mtoe	Million ton of oil equivalent (1 kg oil equivalent = 41.87 MJ)
NO _x	Nitrogen Oxides
OD	Outer Diameter
PO	Pyrolysis oil
PBR	Photo bio-reactor
PPH - PHR	Pounds per Hour (lb _(US) /h)
RPM	Revolutions per Minute
SFC	Specific Fuel Consumption
STPO	Scrap tire pyrolysis oil
TGA	Thermo Gravimetric Analysis
TIT	Turbine Inlet Temperature, firing temperature
UHC	Unburned Hydrocarbons
wb	Wet basis

Summary

Biomass pyrolysis is an advanced process in which an organic material is rapidly heated in a controlled environment and in the absence of oxygen to produce a liquid intermediate, the bio-oil, composed of hundreds of oxygenated compounds, which can be used directly to generate heat or further upgraded to a fossil-fuel substitute with improved properties, more suitable to be fed into a conventional oil refinery.

This work deals with an experimental investigation in the production and use of biofuels and bioproducts from pyrolysis of several biomass species and alternative feedstock, for distributed energy generation or the production of chemical intermediates (biochemicals).

Within the doctoral studies, a dedicated laboratory reactor was built for this scope and samples of pyrolysis oils have been produced from several biomasses, both lignocellulosic and microalgae, in sufficient amount to assess their properties as a fuel.

Being a relatively novel bioliquid, material compatibility of microalgae bio-oil was addressed. Tests were carried out on selected metallic and elastomeric specimens to gain insight on handling and storage requirements and to compare the aggressiveness of pyrolysis oil from microalgae with the relatively more known pyrolysis oil from lignocellulosic biomasses.

The results from the experimental test campaign, aimed at investigating the possibility of feeding pyrolysis oils to a modified micro gas turbine for power generation, are then presented in the final part of the work.

The chapter “Pyrolysis for fuel, energy and chemicals” illustrates some generalities on the pyrolysis oil as a liquid intermediate, along with a brief state of the art of pyrolysis technologies and frontiers. The industrial perspective of generating energy from pyrolysis oils is also addressed, and examples of current demonstration activities in Europe are presented. A synthetic review of literature on two specialized subjects, microalgae and scrap tires pyrolysis, closes the chapter.

The chapter “Bio-oil production in a pilot test bench” describes the experimental set-up that was used in this thesis for the production and collection of bio-oil samples.

The chapter “Experimental results” discusses the results from production and analysis of pyrolysis oil from several biomass samples in a dedicated laboratory reactor. The yield and properties of the produced pyrolysis oils are presented, discussed and compared one against the other; a large quantity of microalgae from three distinct strains have been converted to pyrolysis oil for the first time in such amount. The chapter also reports the results from laboratory trials aimed at a preliminary assessment of the compatibility of pyrolysis oil from microalgae with 7 commercial specimens of metals and elastomers, commonly used in engineering practice for storage, handling and processing of fuels or organic fluids. Pyrolysis oil from microalgae was compared with pyrolysis oil from pine chips, which is almost commercially available, and for which larger data sets have been generated in the past.

Finally, the results of the test campaign on the micro gas turbine are presented in chapter “Use of bio-oils in a modified micro gas turbine”. The possibility to feed a modified micro gas turbine, previously adapted to biofuels, was evaluated and the unit tested with two distinct pyrolysis oils; the first was of biogenic origin (pine chips), the second was obtained from the pyrolysis of scrap tires. Test results are discussed along with the challenges associated with feeding pyrolysis oils to a stationary engine for distributed power generation.

1 Pyrolysis for fuel, energy and chemicals

Pyrolysis is the process of chemically decomposing organic materials by heating them in the absence of oxygen; the process is carried out at near atmospheric pressure and in the temperature range between 300 and 600 °C. Products of pyrolysis are a solid, also called char, a mixture of condensable vapours, and some permanent gases (mainly CO₂, CO, CH₄). The pyrolysis process is significantly flexible, as distribution of products, their relative abundance and properties can be influenced (steered) by properly tuning the process parameters or conditioning the feedstock, according to the desired final goal. A *resume* of the spectrum of products, in terms of relative abundance of liquid, solid and gas according to process conditions is reported in Table 1.1.

Lower temperature, slower heating rate, larger particle size and longer residence time (slow pyrolysis) are known to promote the formation of solids, while higher temperature, faster heating rate, smaller particle size and shorter residence time favour the formation of condensable vapours (fast pyrolysis) [1,2]. However, a clear distinction between processes does not exist [3] or is arbitrary in many respects [4], and since many of these parameters cannot be accurately defined nor measured during fast pyrolysis, high external heat transfer coefficient and efficient primary products removal have been suggested by Lédé and Authier recently as general conditions that must be fulfilled at the level of the reacting biomass sample in fast pyrolysis [5].

Research on slow pyrolysis (carbonization) for charcoal manufacturing dates back at least to mid-XIX century, when Violette reported on his investigation on the use of closed crucibles to enhance solid yield [6]. The process of carbonization has been applied since ancient times and it is still a widely diffused technique for the manufacturing of charcoal for household cooking and steel industries; according to Kammen & Lew, who reported FAO estimates, approx. 24 Mton of charcoal were already being produced annually in 1992 [7]. Systematic assessment of charcoal production technologies was carried out by Antal & Grønli [8], who devoted large efforts in optimizing process yields [9]. Nowadays, a renewed interest can be observed for the carbonization process in biochar manufacture for soil amendment, remediation and water treatment.

Table 1.1: Yield of products (%wt) according to biomass pyrolysis mode [10].

Mode	Conditions	Liquid %wt	Solid %wt	Gas %wt
fast	≈500 °C, short hot vapours residence time ≈1 s	75	12	13
intermediate	≈500 °C, hot vapours residence time 10-30 s	50 ^a	25	25
slow (carbonization)	≈400 °C, long vapours residence (hours up to days)	30	35	35
torrefaction	≈290 °C, solids residence time 10-60 min	0 ^b	80	20

^a: in 2 phases. ^b: unless condensed, then up to 5%.

When fast and intermediate pyrolysis is applied, the rapid condensation of pyrolysis vapours and aerosols produces a dark brown mobile liquid, the bio-oil, that has a heating value about half that of conventional fuel oil; synonyms for bio-oil include pyrolysis oils, pyrolysis liquids, bio-crude oil (BCO), wood liquids, wood oil, liquid smoke, wood distillates, pyroligneous acid, and liquid wood [4]. The interest in pyrolysis for the production of liquid fuels resides in the possibility to convert a solid biomass into a liquid intermediate with higher energy density, improving transportation cost, logistics, and further processing (upgrading or use).

1.1 Schematic process pathway

The simplified model of wood pyrolysis by Shafizadeh & Chin [11] helps in understanding the intricate sequence of reactions involved in the thermal degradation

of biomass. Provided there is a sufficient heating rate, the biomass particle is decomposed to char and pyrolysis vapours, i.e. permanent gases (CO₂, CO, CH₄) and condensable liquids (reaction water, biomass moisture and organic products). In a successive phase, the evolved pyrolysis vapours may undergo a great number of secondary reactions, e.g. cracking and condensation. Their nature and extent may considerably modify the yields and properties of vapours and consequently those of bio-oil. These secondary reactions include homogeneous gas phase and/or heterogeneous solids (char, catalysts)/vapours cracking and repolymerisations, and the extent of these reactions depends on the temperature fields, as well as gas and solid phase residence times distributions [3], which is of course also a function of the reactor geometry and working principle.

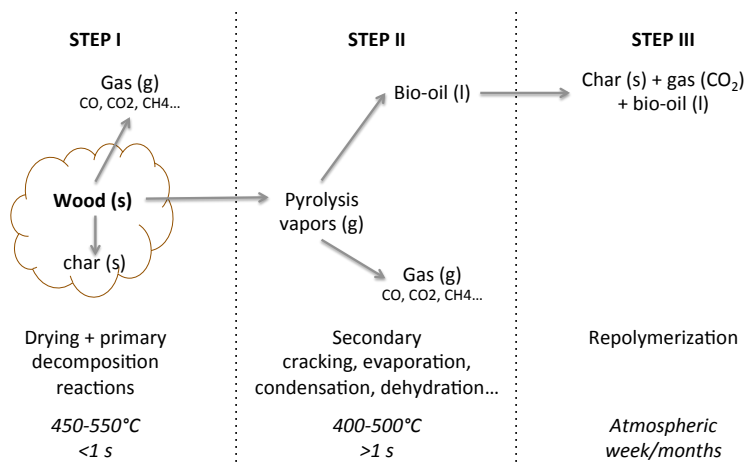


Figure 1.1: Schematic of wood pyrolysis (adapted from [12–14]).

The idea of being able to describe the intricate set of homogenous and heterogeneous reactions by means of analytical tools has intrigued the scientists involved in thermochemical biomass conversion since the beginning. Tens of different models have been proposed, described and (partially) validated for the decomposition pathways of several model compounds or biomass constituents. An outstanding review of the subject, that is beyond the scope of the present work, was carried out by Di Blasi [15].

Though the literature on thermal degradation is vast, an effective and elegant representation of the superposition of the degradation processes of elemental biomass constituents (extractives, hemicellulose, cellulose, lignin) was given by Grønli,

Várhegyi and Di Blasi [16] and Antal & Varhegyi [17]. More recently, Biagini and Tognotti [18], basing their work on a large and consistent data set of thermal analysis, derived a methodology to calculate the approximate chemical composition of a biomass sample, in terms of extractives, cellulose, hemicellulose and lignin content, from its thermal degradation pattern.

1.2 General working principle

In spite of their global complexity, several pyrolysis plants share not only the same physical working principle, i.e. a carbonaceous material is heated-up in a controlled manner to steer the composition and quality of products toward the desired result, but also, to a lesser extent, the number of sub-processes, variably interconnected, they are composed of. In particular, the observation applies for those lab scale rigs where heat is supplied by electrical resistors, and internal product recycling is limited or inexistent. The set of sub-processes, which describes also the working principle of the CREAR/RE-CORD pyrolysis reactor, is schematically represented in Figure 1.2 and will be detailed in the following paragraphs.

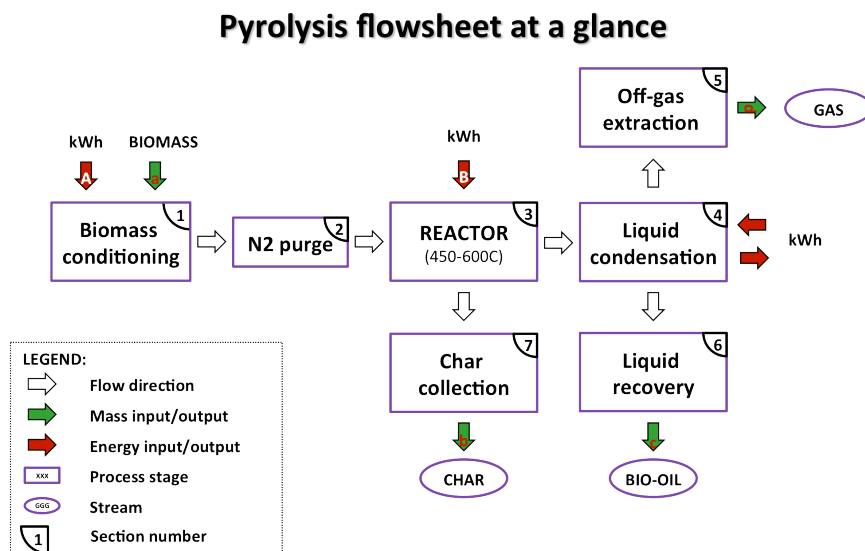


Figure 1.2 : Schematic flowsheet of a pyrolysis conversion process.

At first, biomass is properly conditioned in term of size and moisture content (step 1). At this stage, energy is supplied either in the form of mechanical work for size reduction or homogenization of the feed, or as process heat for reducing the moisture content to an *acceptable* level, or both input. The attained moisture content depends on the process itself but also on the desired amount of product, i.e. solid, liquid or gas, as it can influence, among others, their relative abundance.

The next step (2) involves the removal of the free oxygen, which is present in the volume of feed, to avoid undesired oxidation in the reactor, with a loss of carbonaceous material and uncontrolled release of energy due to combustion. The energy consumed in this step can be neglected, considered the very limited volume to be displaced of inert or off-gas; the latter can potentially be recycled from the process, as in the case for example of Tail Gas Reactive Pyrolysis [19].

Once the loading device forces the feedstock to enter the reactor, biomass falls into the hot section, and starts its conversion process (step 3); water vapour and organic volatiles are released from the particle, producing a complex and interconnected network of secondary and tertiary reactions, both homogeneous and heterogeneous, which modify the shape, structure and composition of the original particle and ultimately lead to the production of a mixture of volatiles, made up of permanent gases and vapours, and a solid carbonaceous residue.

Volatiles produced during pyrolysis are extracted by a fan (step 5) placed in the cold section, downstream of the condensation system (step 4), where they separate into a pyrolysis liquid, that is collected (step 6), and an off-gas stream composed of permanent gases, which is vented outside. The collection of solid residue (step 7), where possible, can be done either in a single or multiple locations, as is the case for fluid beds, where transport phenomena occur and part of the char is brought by the gas stream up to the cyclones.

1.2.1 Plant design alternatives

Several plant layouts have been proposed for biomass pyrolysis (ablative, auger, circulating fluidized bed, entrained flow, fluidized bed, rotating cone, transported bed,

vacuum moving bed), and the number of research organizations and private companies involved is large as well; a detailed list of both can be found in the review by Bridgwater [10].

1.2.2 Pyrolysis oil properties

Bio-oil has many very peculiar properties, which need to be considered carefully; Bridgwater reviewed extensively the matter [20].

Bio-oil is a mixture of hundreds of oxygenated compounds; the major chemical groups are water (15–30 %wt), monomeric carbonyls, sugars, organic acids, phenols, and oligomeric moieties from carbohydrates and lignin degradation [21,22], resulting in a wide range of molecular weights up to 8-10000 Da [23].

Water in pyrolysis oil comes from original moisture and as reaction product [24], the latter including both dehydration and degradation reactions [25]. A negative effect of high moisture content in the feed is that, for the same particle size, the release of water vapour by devolatilization slows down the heating up of the particle, resulting in a longer time to attain the desired process temperature, a slower heating rate and more energy consumed in the process, since enthalpy of vaporization of water is around $2.3 \text{ kJ}\cdot\text{g}^{-1}$, compared to a LHV around $14\text{-}18 \text{ kJ}\cdot\text{g}^{-1}$ for lignocellulosic feedstock.

Table 1.2: Typical properties and characteristics of wood-derived bio-oil (adapted from [26])

Property	Unit	Range (typical)
water	%wt	20-30
solids	%wt	<0.5
ash	%wt	0.01-0.2 ^a
nitrogen	%wt	<0.4
sulphur	%wt	<0.05
stability		unstable ^b
viscosity @40°C	cSt	15-35 ^c
density @15°C		1.1-1.3 ^c
flash point	°C	40-110
pour point	°C	9-36
LHV	MJ/kg	13-18 ^c
pH		2-3
distillability		not distillable

^a: note that metals form oxides during ashing and may yield ash values that are larger than the total solids in the liquid. ^b: unstable at high temperatures and for prolonged periods of time. ^c: depends on water content.

Pyrolysis liquids are highly polar, containing about 35-40 %wt oxygen, while mineral oils contain oxygen at ppm level. Moreover, they are not miscible with fossil fuels [27], but bio-oil/diesel emulsions have been successfully produced in laboratory equipment with the aid of surfactants and tested in lab scale combustion equipment [28–32]. Pyrolysis oil can be mixed with polar solvents such as methanol, acetone and isopropanol. It is a complex mixture of water, guaiacols, catecols, syringols, vanillins, furancarboxaldehydes, isoeugenol, pyrones, acetic acid, formic acid, and other carboxylic acids. It also contains other major groups of compounds, including hydroxyaldehydes, hydroxyketones, sugars, carboxylic acids, and phenolics [4]. Ageing of pyrolysis oil causes unusual time-dependent behaviour. Properties such as viscosity increases, volatility decreases, phase separation and deposition of gums change with time. A synthetic collection of typical PO properties is reported in Table 1.2.

1.2.3 Pyrolysis process energy balance

In fast pyrolysis, the limited amount of permanent gases produced by the thermal degradation of the feedstock does not allow to recover a substantial amount of heat; on the contrary, char is produced in more relevant quantity, and therefore it can be burnt to supply process heat. Several estimates have been done on the energy required for the pyrolysis process, often referred to as *heat of pyrolysis*, which was assessed by Daugaard & Brown at around $0.8 \pm 0.2 \text{ MJ} \cdot (\text{kg-dry-biomass})^{-1}$ for oat hulls and $1.6 \pm 0.3 \text{ MJ} \cdot (\text{kg-dry-biomass})^{-1}$ for pine [33]. In a recent work, Yang et al. developed a complex correlation for the estimate of the enthalpy of bio-oil vapours, which was then used to infer the heat of pyrolysis. According to their estimate, the heats of pyrolysis Q_{py} for five different biomass samples at $T_{py} = 823 \text{ K}$ were estimated to be $1.3\text{-}1.6 \text{ MJ} \cdot (\text{kg-dry-biomass})^{-1}$. For pyrolysis of cedar chips at $T_{py} = 733 \text{ K}$, Q_{py} was estimated to be $1.1\text{-}1.2 \text{ MJ} \cdot (\text{kg-dry-biomass})^{-1}$ and also to increase slightly with increasing heating rate [34].

For microalgae biomass under a slow heating rate, Grierson et al. derived by means of Computer Aided Thermal Analysis (CATA) the heat of pyrolysis of 6 distinct

microalgae species; the Authors found that the heat required for conversion was in the range $0.9\text{-}1 \text{ MJ}\cdot(\text{ kg-dry-biomass})^{-1}$ [35].

The energetic self-sustainability of a pyrolysis process is easily addressed by considering the following example, in which figures are conservative, i.e. the hypothetical plant is performing less than actual plants reported in literature. Let's consider a fast pyrolysis process producing around 70 %wt oil (on wet feed) at a calorific content (LHV) of around $16 \text{ MJ}\cdot\text{kg}^{-1}$ from pine chips ($\text{LHV}_{\text{dry}} \approx 19 \text{ MJ}\cdot\text{kg}^{-1}$) at 10 %wt db moisture; the energy recovered in the bio-oil makes up $\approx 65\%$ of feed energy content (wet). Allowing for a heat of pyrolysis of around $1.6 \text{ MJ}\cdot(\text{ kg-dry-biomass})^{-1}$, this amounts to $\approx 8.4\%$ of dry feed energy content. Considering that the solid residue is produced at around 20 %wt yield and has a calorific content (LHV) of up to $25 \text{ MJ}\cdot\text{kg}^{-1}$, it represents around 25 % of feed energy content (wet). Energy content in the gas stream ($<5\%$, considering losses) is therefore insufficient to provide process heat, that vice versa can be supplied by burning part of the char stream, as is actually done in operating plants, where the process heat for drying and pyrolysis is provided internally.

Onarheim et. al. [36] recently addressed the energy and carbon balances of an integrated fast pyrolysis-CHP facility in which 90 MW bio-oil are produced along with 50 MW electricity and 86 MW thermal power for district heating. The hypothetical integrated plant is a scaled-up version of the real Fortum/Metso/VTT integrated pyrolysis plant in Joensuu, Finland (under testing at the time of writing), that is expected to be delivering 30 MW bio-oil, 55 MW electricity, 110 MW district heating. The model that the Authors developed in ASPEN is based on the VTT PDU unit, with is derived from ENSYS technology. A schematic diagram is reported in Figure 1.3. According to the data provided by the Authors, the expected efficiency of the integrated plant is around 82.45%, considering as output the chemical energy in bio-oil, electricity and district heating and as input the chemical energy of the fuel (wood residues or pine chips) and electricity for auxiliary and equipment. All chemical energies are reported as LHV.

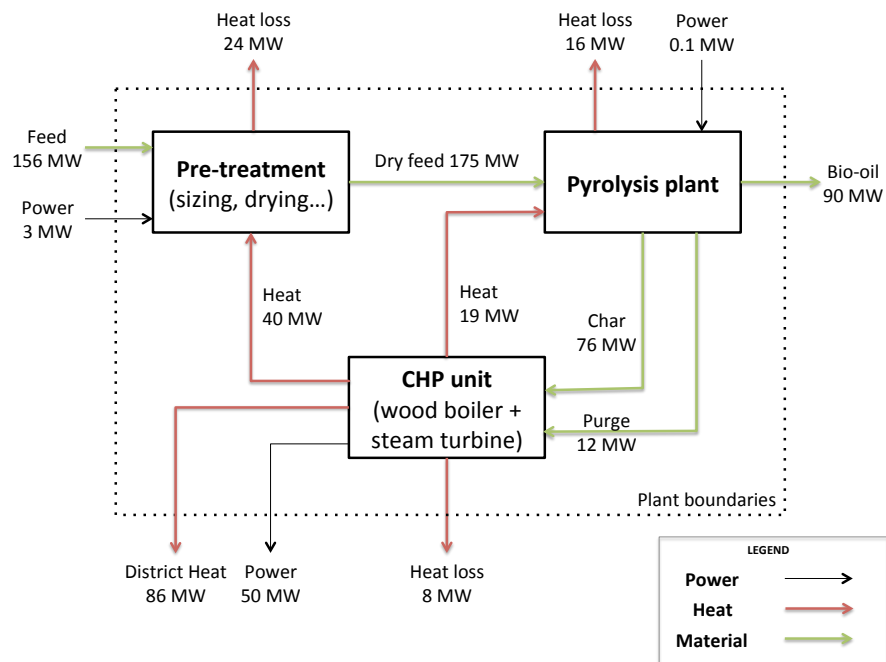


Figure 1.3 : Schematic flowsheet of the Joensuu scale-up plant fed with forest residues (adapted from [36]).

1.2.4 Pyrolysis process economics

In spite of the fact that commercial development of fast pyrolysis has not yet been achieved, a few studies on the economics of fast pyrolysis plants could be retrieved from literature, and in a recent article Rogers & Brammer developed a consensus techno-economic model of a pyrolysis plant with special attention to the UK [37].

Venderbosch & Prins, also relying on data from BTG, pointed out that the range of capital costs for the pyrolysis plant alone is between €200 and €500/kWth input biomass, depending on the technology, scale, degree of heat integration, location, etc. The main parts of the BTG pyrolysis plant are the reactor, riser, combustor, and condenser. The costs of pretreatment, feeding, buildings, and infrastructure are not included, but may add up to another 50 to 100%, depending on the initial feedstock properties. Costs related to the heat integration system (heat recovery, steam generation, drying, etc.) are usually not addressed in the studies of the economics [38].

Bridgwater, in a recent book, derived a cost estimate for the capital cost of pyrolysis plants in the following form [39]:

$$\text{capex (M€}_{2011}) = 6.98 \cdot BM^{0.67}$$

Eq. 1

Where BM is the dry biomass feed rate, in $\text{t}\cdot\text{h}^{-1}$; bio-oil production cost was given by the following equation:

$$\text{production cost bio-oil (€}_{2011} \cdot \text{t}^{-1}) = 1.1 \cdot [B + (H \cdot 16935 \cdot F^{-0.33})] \cdot Y^{-1}$$

Eq. 2

Where B is the biomass cost in € dry t^{-1} , H is the capital and capital-related charges (default value is 0.18), F is the biomass feed rate in $\text{t}_{\text{dry}}\cdot\text{y}^{-1}$, and Y is the fractional bio-oil yield by weight (default is 0.75 for wood and 0.6 for grasses). According to his estimates, for a plant capacity of $10000 \text{ t}_{\text{dry}}\cdot\text{yr}^{-1}$ the expected bio-oil production cost would be between 200 and around $320 \text{ €}\cdot\text{t}^{-1}$ ($12.5\text{-}20 \text{ €}\cdot\text{GJ}^{-1}$ at $16 \text{ MJ}\cdot\text{kg}^{-1}$ LHV of bio-oil) for a feed cost between 0 and $80 \text{ €}\cdot\text{t}_{\text{dry}}^{-1}$.

Studies from Ringer et al. [40] and Peacocke et al. [41] indicate that pyrolysis oils can be produced at costs in a range of $\text{€}4$ to $\text{€}14/\text{GJ}$ (corresponding to $\text{€}65$ to $\text{€}225/\text{t}$), with feedstock costing between $\text{€}0$ and $\text{€}100/\text{t}$ ($\text{€}0$ to $\text{€}6/\text{GJ}$); according to Venderbosch & Prins (ibid.), these figures match the BTG fast pyrolysis plant installed and operated in Malaysia between 2005-2008.

1.3 Exploiting the potential of pyrolysis oil

As an energy-efficient densification and conversion process, pyrolysis of biomass has been addressed in heat & power generation, and fuel & chemical production since the beginning. In the following paragraphs, a brief résumé of achievements in these fields is reported.

1.3.1 Heat and power generation

Heat generation

The highlighted properties of pyrolysis oil makes it a good candidate for fossil fuel substitution in medium and large boilers; indeed, these units already operate with heavier, less refined and more contaminated fuels, e.g. #4 and #6 fuel oil, are generally more tolerant toward chemical and physical aggression and their size can justify the investment needed to accommodate a dual fuel system or the fuel system replacement in case of feeding 100% bio-oil.

Co-firing of biomass pyrolysis oils with fossil fuels has been investigated and tested on a commercial scale, and the use of bio-oil in large coal and natural gas power station was demonstrated in the past. A valuable review of the combustion application of pyrolysis oil can be found in the work of Lehto et al. [42] and some highlights are given in the following paragraphs.

Bio-oil supplied by ENSYN was reported to be used commercially in co-firing with coal around in 1997 in a coal utility boiler for power generation at Manitowoc Public Utilities in Wisconsin (USA) [43]. As of 2010, over 60000 l of ENSYN bio-oil were successfully fired with stable combustion at Tolko Kraft Paper Mill in The Pas, Manitoba [24] with extensive emissions monitoring showing improved boiler performance; the same company announced in late 2014 to have started the commissioning of New Hampshire's Memorial Hospital heating system conversion, in North Conway (USA), from traditional petroleum fuels to Ensyn's renewable liquid fuel, commercially known as RFO™, with a 5 year agreement for supplying 300 kgal/year of bio-oil ($\approx 1.15 \cdot 10^6$ l/year).

In 2003, bio-oil from BTG has been successfully co-fired in a 350 MWe natural gas fired power station in Harculo, The Netherlands, where 15 tons of bio-oil (>1% bio-oil of the feed) was converted into 25 MWh of electricity [44].

Venderbosch & Prins reported that bio-oil from the BTG Malaysian plant¹ was routinely used to replace expensive diesel fuel for start-up purposes of a fluidized-bed combustor near Kuala Lumpur International Airport; moreover, BTG used the bio-oil from the Malaysian plant to replace diesel and/or natural gas in a dedicated 250 kW hot-water boiler in The Netherlands, and a dedicated fuel lance was developed [13].

Since 2010 bio-oil produced in Metso's integrated fast pyrolysis facility, based on VTT layout and expertise, was combusted in Fortum's 1 MW district heating plant in Masala, Finland. The existing burner was replaced with a new bio-oil burner consisting of a modified heavy fuel oil burner. The total amount of bio-oil combusted has been about 40 tons and the monitored emissions were close to those of heavy fuel oil [45].

Bio-oil has also been approved for use in utility boilers in Swedish district heating applications, where demonstration activities began in the late '90s at Årsta District Heating Plant.

Power generation

Electricity generation from pyrolysis oil is an attractive opportunity, because of the higher market value of electricity compared to process heat, the possibility to benefit from feed-in tariff for renewable energy sources, and the ease of distribution. The challenges associated with the use of bio-oil in energy conversion plants have been extensively reviewed by Shaddix & Hardesty [46], Czernik & Bridgwater [47], Chiamonti et al. [48] and Venderbosch & van Helden [49]. In the following sections, a brief introduction on the historical development of the use of bio-oil in turbines and internal combustion engines will be given.

Bio-oil in gas turbines

A limited number of independent researches have been carried out in the past on bio-oil combustion in gas turbines. The first reported successful demonstration of bio-oil combustion in a gas turbine combustor test rig was the work of Kasper et al. [50] in the '80s at Teledyne (USA). Authors fed bio-oil from forest and agricultural

¹ BTG built a 50 t/day pyrolysis plant in Malaysia; based on their proprietary technology (rotating cone reactor), and operating on empty fruit bunches from palm oil processing, the unit was operated daily from mid 2005 until 2008 [13].

residues to the annular combustor of a J69-T-29 turbine. The measured combustion efficiency in the rig using pyrolysis oil as fuel was 95%, emissions of CO were higher compared to fossil fuel, but CH and NO_x were within the limits observed for petroleum fuels. Also a slag build-up in the exhaust section resulting from ash in bio-oil was identified as a potential problem.

In the '90s Ardy et al. [51] at ENEL CRT (Italy) reported to have tested pure fast pyrolysis bio-oil produced by ENSYN and bio-oil/ethanol mixtures in a pressurized gas turbine combustor test rig, rated at 40 kWe. Authors found that bio-oil atomization and combustion quality were extremely sensible to the crude bio-oil feeding temperature; exhaust temperature had a strong influence on the combustion efficiency; CO concentration was relatively low only for high exhaust temperatures. Several problems arose in the fuel pumping section, especially in the throttling section of the valve. The combustor performance was influenced by gas residence time in the combustor, when air/fuel ratios and average exhaust outlet temperatures remained unchanged. Smoke (*Bacharach index, nda*) and CO were relatively low only for low loads, when increasing the air flow rate, smoke and CO rate increased by 1 order of magnitude. At the time, bio-oil stability was poor, owing to noticeable differences in test results over time under the same conditions.

In the '90s, Orenda Aerospace Corporation (Canada) and Zorya-Mashproekt (Ukraine) started a still ongoing R&D project on a 2.5 MWe industrial gas turbine, that was modified in its hot section and combustion system for alternative fuels applications and fed with fast pyrolysis bio-oils from ENSYN and Dynamotive [52,53]. Lupandin et al. [54] reported that emissions data generated during bio-oil operation showed that NO_x, CO and SO_x emissions were below the Ontario Emissions limits, and compared to measurements with #2 diesel fuel, NO_x and SO_x concentrations were lower, while CO concentration was higher when feeding both bio-oils.

Strenziok et al. [55] at University of Rostock (Germany) modified a T216 gas turbine, rated at 75 kWe. The combustion chamber of the turbine was adapted and equipped with a dual fuel system that included an ignition nozzle for diesel fuel and a main nozzle for bio-oil. The engine operated in a dual fuel mode at 73% of the full

power that would be generated in a standard fuel mode, with about 40% of total power produced from bio-oil and 60% from diesel. Compared to the operation on diesel fuel, CO and HC emissions were significantly higher and NO_x less for dual fuel operation. The use of bio-oil in the turbine resulted in deposits in the combustion chamber and on the blades.

At the University of Florence, tests with pyrolysis oil and blends of ethanol/pyrolysis oil were initiated in 2010; the combustion chamber of a Garrett GTP 30-67 gas turbine was modified to accommodate the requirements of bio-oil combustion and a new fuel line was set-up. Preliminary results gave encouraging feedback, but to date a sustained run on pure pyrolysis oil has not been achieved yet. Details of the combustion chamber development and testing activities can be found in references [56] and [57].

A recent development in the field was the work of Beran & Axelsson [58] at OPRA Turbine (The Netherlands) in the framework of a R&D project in partnership with Biomass Technology Group (BTG, The Netherlands) and University of Twente; Authors developed and tested a tubular combustor for low-calorific fuels to equip their OPRA OP16 radial gas turbine rated at 1.9MW. The experiments have been performed in an atmospheric combustion test rig. Authors reported to have burned pure pyrolysis oil in the load range between 70% and 100% with a combustion efficiency exceeding 99% and without creation of sediments on the combustor inner wall. They found that NO_x emissions were similar for pyrolysis oil and diesel, whereas the CO emissions were twice as high for pyrolysis oil. They found that an air blast nozzle was found to be more suitable than a pressure nozzle, due to its better performance over a wider operating range and its higher resistance to erosion and abrasion. Moreover, they found that the maximum allowed droplet size of the pyrolysis oil spray had to be 50–70% of the droplet size for diesel fuel.

Bio-oil in internal combustion engines

The possibility to use bio-oil in internal combustion engines was investigated worldwide by several research institutes (VTT, MIT, Aston University, University of Rostock and University of Florence, CNR-IM), sometimes in partnership with private

companies (Wartsila Diesel, Carterpillar, Ormrod Diesels) [28,59–62]; however, internal combustion engines present a larger number of technical barriers to overcome for the use of bio-oil, compared to gas turbines, mainly due to (1) limited time available for the combustion, which might be insufficient to accommodate the peculiar behaviour of bio-oil during combustion, and (2) material of construction of “wetted” parts, which are generally not tolerant toward harsh fuels.

Calabria et al., who performed several experiments in a single droplet combustion chamber, have addressed the fundamentals of bio-oil combustion recently. They reported that after an initial heat up phase, the bio-oil droplet starts swelling, volatiles are released and start burning, but the combustion time is dictated by the heterogeneous combustion of cenospheres, i.e. the solid carbonaceous particle formed by liquid phase pyrolysis during the last stages of droplet combustion [63].

According to Venderbosch & Prins (ibid.), the lack of available amounts of bio-oil was a key factor at that time for testing and development activities; however, in several tests, severe wear and erosion/corrosion phenomena were observed in the injector needles, due to fuel acidity and particulates; high viscosity and loss of stability with increasing temperature were major problems, and a carbon deposit build-up was reported in the combustion chamber and exhaust valve.

Chiaramonti et al. clearly pointed out that injector and fuel pump material as well as emissions are critical factors, and that development of effective and reliable pumping and injection systems and good combustion to avoid deposits on the hot parts (cylinder, piston, injector) are the main R&D needs [48].

1.3.2 Fuels

Due to its harsh properties, pyrolysis oil can hardly be directly used as a fossil fuel substitute in transportation, especially in small size, mobile applications, and upgrading is therefore highly recommended. Several routes for bio-oil upgrading have been postulated, and research groups have addressed some of them. Upgrading can be carried out either (1) in integrated process units, in which catalytic pyrolysis is applied, or (2) in distinct process units, in which conventional pyrolysis is coupled with

post-treatment of products; in both cases, the objective is to get a severe deoxygenation of the bio-oil to comply with standard fossil fuel refinery specifications. Example of (1) are the GTI IH² process [64], while an example of (2) can be found in the work of Jones et al. [65].

Bio-oil upgrading and catalytic pyrolysis are very specialized fields of investigation, and considerable amount of knowledge has been accumulated in decades of experimental activities and where often the protection of IPRs on catalyst or process hinder the possibility of independent examination. For a thorough examination of the matter, the reviews of Huber and Corma [66,67] should be consulted, while a panoramic view of the matter can be inferred from the work of French and Czernik [68] and the review from Mortensen et al. [69].

1.3.3 Chemicals

Owing to their much higher added value, when compared to fuels for heat and also electricity generation, chemicals recovery is a natural objective; an introduction to the subject can be found in the book Chapter from Bridgwater [20], while for a more thorough examination the comprehensive reviews of Amen-Chen [70] and Czernik & Bridgwater [47] should be referred to.

Being a collection of all types of (oxygen) functionalities - acids, sugars, alcohols, ketones, aldehydes, (poly-)phenols, furans and many others are all present - bio-oil has ever since attracted large research efforts for their isolation and recovery. Historically, bio-oil and its fractions have been regarded with interest for the production of resins for the production of particle or plywood boards [71], antimicrobial/anti-fungine agent for agriculture [72], phenolic compounds [70], hydroxyacetaldehyde, levoglucosan, acetic acid [73], food flavouring, and many other potential applications.

For example, the lignin-rich fraction of pyrolysis oil, and pyrolysis oil itself, have been patented as wood preservatives by ENSYN [74], and lignin as a phenol replacement in phenol formaldehyde resins has been proposed [4]. Due to the aromatic structure of lignin, fast pyrolysis has been considered as a process option for the production of high added-value compounds, like liquid fuel additives and

commodity chemicals like benzene, toluene and mixed xylene (BTX) or phenols that can be obtained through the functional chemical groups found in the lignin pyrolytic oil [75]. Such ubiquitous chemicals are globally traded and represent base commodities for the manufacturing of intermediate products used in many industrial sectors (e.g. plastics, adhesives, coatings, paints). An example of some of the possible intermediate and final use of BTX is reported in Figure 1.4.

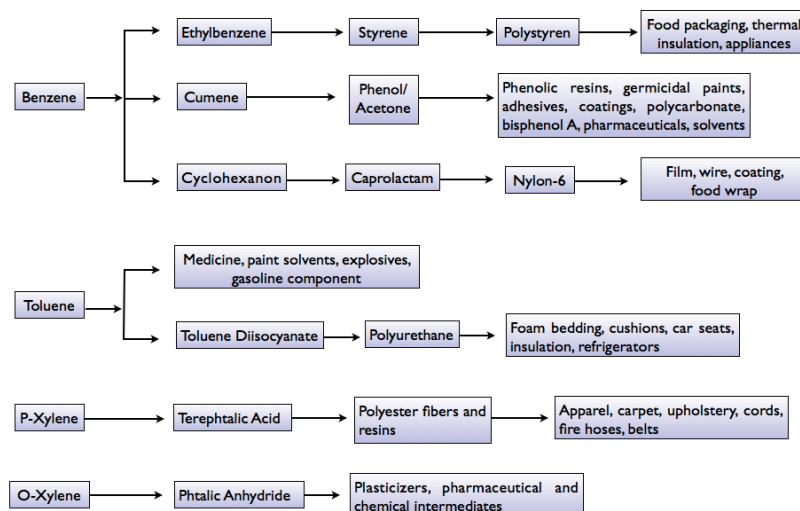


Figure 1.4: Range of products from BTX (adapted from [76]).

Figure 1.5 reports the quarterly prices of benzene, toluene and mixed xylenes compared to that of the barrel oil Brent between 2007 and 2013. The cost of such chemical commodities, in the price range of 850-1400 USD/ton for mixed xylenes and benzene respectively, is strongly affected by the price dynamics of crude oil, since it is the base feedstock for their production. By offsetting the production of BTX from fossil in favour of a renewable feedstock such as biomass, in principle it could be possible to reduce the influence of crude oil price fluctuations on supplies, thus limiting the market exposure of industries.

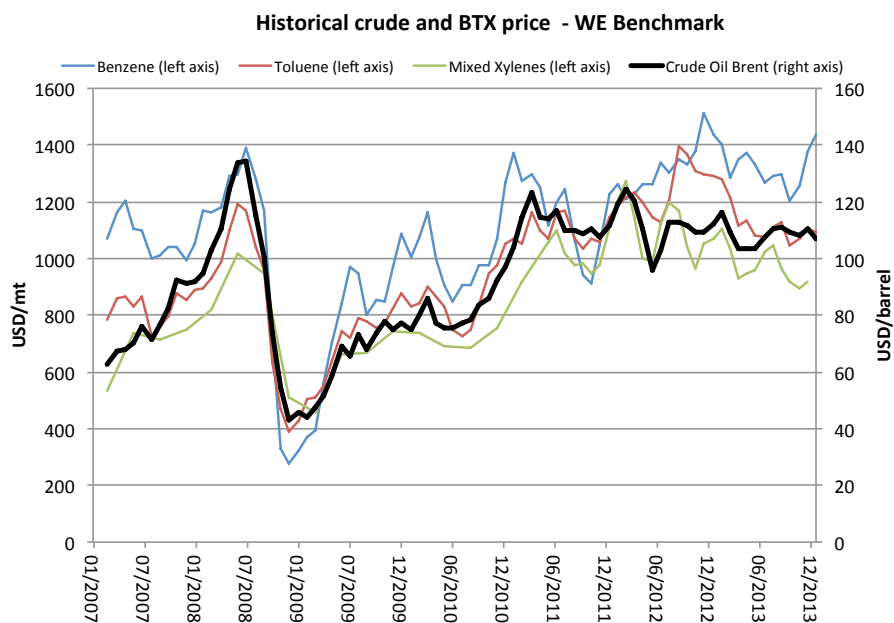


Figure 1.5: Quarterly market price of benzene, toluene and mixed xylenes compared to crude oil Brent between 2007 and 2013. Source: Bloomberg.

However, according to Venderbosch & Prins, even if the recovery of such pure compounds from the complex bio-oil may be technically feasible, it is probably economically unattractive because of the high cost of the recovery of the chemical and its (generally) low concentration in the oil [13].

1.4 Industrial and demonstration project

Current R&D, demonstration and commercial activities on fast pyrolysis have been reviewed by Meier et al. [24] in IEA countries. At the time of writing, two major demonstration projects based on fast pyrolysis of biomass are unwinding in the EU, with the potential of representing a breakthrough in liquid fuel production from biomass in the very short term. In the following paragraphs, a brief highlight will be given on both plants.

1.4.1 Empyro B.V (The Netherlands)

In January 2014 Empyro BV has started construction of its pyrolysis oil production facility in Hengelo, The Netherlands, on the premises of AkzoNobel. The

project is financially supported by the 7th Framework Programme of the European Commission (Grant number 239357), by the Dutch government via the *topsector Energy: TKI-BBE* funding scheme and by the province of Overijssel via the Energy Fund Overijssel. In late 2014 cold testing of the plant was started, after which production is expected to be initiated in a year's time. BTG BioLiquids, Tree power, the province of Overijssel and a private investor jointly own Empyro BV. The Empyro plant is based on the BTG rotating cone fast pyrolysis technology. The supply of biomass has been organized locally with a specialized partner. Part of the demo character of the plant is that in a later stage various types of feedstock will be tested. The complete design has been finalized in cooperation with the well-known industrial companies Stork-Thermeq, AkzoNobel, Zeton and HoSt, who have been subcontracted for several sections of the plant.

At full capacity, the plant is expected to deliver $22 \cdot 10^3 \text{ t} \cdot \text{year}^{-1}$ of bio-oil from used and clean wood and steam for the AzkoNobel facility.

1.4.2 Fortum (Finland)

The very first European industrial fast pyrolysis demonstration plant is being commissioned at Joensuu, integrated into an existing district heat CHP-plant by Fortum (55/110 MWe/MWth) with a production at full capacity of $50 \cdot 10^3 \text{ t} \cdot \text{year}^{-1}$ bio-oil. The Valmet FP reactor is integrated into the CHP boiler, which is employing a VTT license. In addition to the bio-oil, the integrated CHP plant in Joensuu will produce heat and electricity. The bio-oil raw materials will include forest residues and other wood based biomass. The new technology has been developed into a commercial scale concept in cooperation between Fortum, Metso, UPM and VTT as part of TEKES Biorefine research program. Construction of the bio-oil plant has been completed, and is now under testing. According to estimates, bio-oil production will increase the energy wood consumption at Joensuu power plant almost doubling the use from the existing $300 \cdot 10^3 \text{ m}^3$ per year.

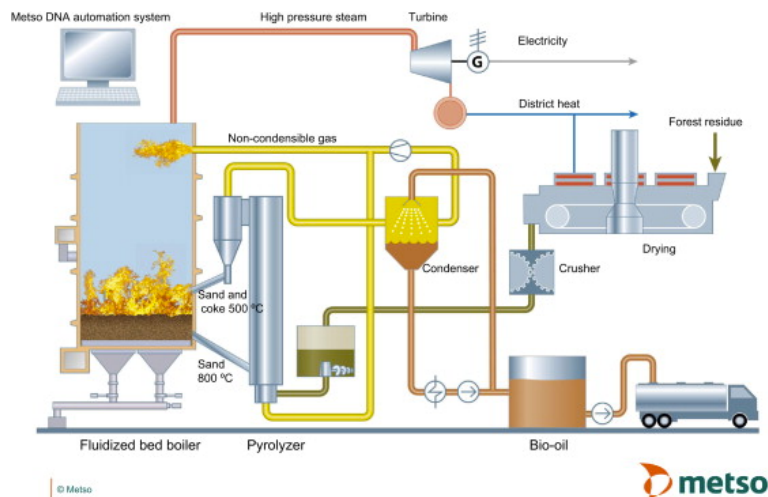


Figure 1.6: Pyrolysis plant integration at Joensuu premises. Source: Metso.

1.5 Synthetic review of microalgae pyrolysis

Microalgae are a diverse group of prokaryotic and eukaryotic photosynthetic and heterotrophic organisms that grow rapidly due to their simple structure and exhibit an extraordinary potential for energy production. Microalgae cultivation, or *algaculture*, using sunlight can be carried out in open or covered ponds or closed photobioreactors, based on different designs [77] and in several aqueous media, from fresh to extremely salty water and even on marginal or coastal areas avoiding land-use competition with food crops. Nowadays more than 40 different species of microalgae, isolated in different parts of the world, are cultured as pure strains in intensive systems. Microalgae can be extremely efficient in terms of land-use, as the potential oil productivity per hectare is considerably higher than traditional seed crops [77] and the productivity achievable with reactors is estimated at around 60-70 ton/ha/year [78], but the theoretical potential is assessed to be even higher [79].

Algaculture is performed worldwide to produce commodities with high economic value. Sometimes the entire alga is the final product, but more often several compounds are extracted, which are very difficult or impossible to produce in other ways. Some examples of these so-called “unique products” include oils, fats, vegetable protein, carbohydrates, bioactive compounds and chemicals as well as food, food-

additives and health-food, feed for fish, shrimp and shellfish, dyestuff and omega-3-fatty acids [80,81].

Under normal growing many species of microalgae exhibit a lipid yield between 10-30% on dry weight, but under special conditions the lipid content can be even doubled [82], and some Authors reported to have obtained oil content up to 80% by weight of dry biomass [83–85]. Growing of microalgae depends on the illumination that is available for photosynthesis, nutrients in the water as well as the intake of nutrients, which affects the production and accumulation of lipids.

The algal biomass is a valuable source of carbon, because its content can exceed 50% on dry weight [86] and some microalgae can produce larger amount of oil than the best dedicated energy-crop and can therefore represent a potential renewable source of oil for the biofuel chains.

Unlike lignocellulosic materials, which are mainly composed of cellulose, lignin and hemicellulose, microalgae are mainly composed of protein, lipid and water-soluble carbohydrate. The amount of hydrocarbons that can be obtained from any component of biomass is limited by its percentage of carbon and hydrogen [87] and thus lipids, proteins and carbohydrates appear to be preferable to convert into hydrocarbons than hemicelluloses, cellulose and lignin through pyrolytic reactions [88]. Microalgae are considered a promising source of biomass for some of their advantages over traditional biological renewable sources, like energy crop or forestry and agricultural residue. Mainly, these are [89]:

- Algae are considered to be a very efficient biological system for harvesting solar energy for the production of organic compounds.
- Algae are non-vascular plants, lacking (usually) complex reproductive organs.
- Many species of algae can be induced to produce particularly high concentrations of specific, commercially valuable compounds, such as proteins, carbohydrates, lipids and pigments.
- Algae are microorganisms that undergo a simple cell division cycle.
- The farming of microalgae can be grown using either sea or brackish water.
- Algal biomass production systems can be adapted to various levels of operational or technological skills.

- Higher oil yield, compared to other plant oils (e.g. palm, coconut, castor, sunflower).

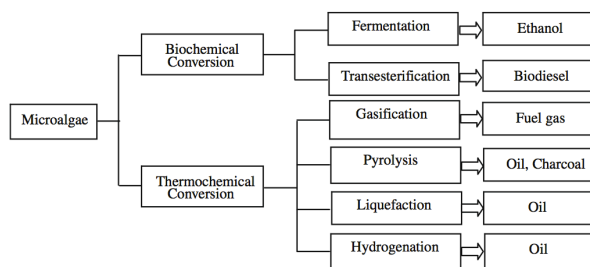


Figure 1.7: Possible pathways for microalgae conversion [90].

These significant potential benefits stimulated the scientific community to investigate the possibility of using microalgal biomass as a feedstock in several bioconversion technologies. Due to the high water content, direct combustion of microalgae is unfeasible, unless moisture content is reduced below 50%, so to date only thermochemical and biochemical options appear feasible [89]. Biochemical conversion of microalgae can include fermentation and transesterification. On the other hand, possible thermochemical conversion pathways of microalgae could be gasification, pyrolysis and liquefaction. Some of these pathways are shown in Figure 1.7. In the following paragraphs, some of the studies carried out on the pyrolytic processing of biomass will be further examined, and the most significant results presented.

In the '90 Ginzburg and co-workers [87] reported some pyrolysis experiments in autoclave (150-300°C) with *Dunaliella Parva*, a green microalga that can be found in oceans and salt lakes throughout the world. They could obtain a liquid fuel, low in nitrogen and sulphur, in the form of a mixture of hydrocarbons by pyrolysis of a suspension of the alga cells. Basing on their experience, the Authors found some difficulties in converting lipids to hydrocarbons by means of a thermal reaction, and that high lipid content could be found only in either old, or stressed algal culture. This means that the culture had to be left to grow for a long time, which was undesirable from an economic point of view. They also observed that high quality hydrocarbons could be obtained from pyrolysis of proteins; combining this observation with the fact that young algal culture have a high protein content, led them to conclude that protein

content of the biomass (*i.e. microalgae*) was the most important raw material for oil production.

Peng and co-worker [91] undertook both vacuum pyrolysis and thermogravimetric analysis (TGA) on small samples ($\approx 1\text{g}$) of autotrophic grown *Chlorella Protothecoides*. Pyrolysis conditions were between 200-600°C with holding times of 5-120 min separately. A high oil yield of approximately 41-52% was obtained at 300°C for 20-120 min or at 400°C for 5-20 min or at 500°C for 5 min. The maximum oil yield of 52.0% was achieved at 500°C for 5 min. On the other hand, the gas yield was generally increased with the increasing temperature and holding time. The yield of 64.4-69.0% was acquired at 400-500°C for 60-120 min. As the temperature rose to 600°C, the gas yield was up to 69.3-76.0%. TGA of HC *Chlorella P.*

In a successive study Peng and co-workers [92,93] performed a non-isothermal TGA on heterotrophic (HC) grown *Chlorella Protothecoides* sample, autotrophic (AC) grown samples of *Chlorella Protothecoides* and *Spirulina Platensis* under a heating rate (HR) of 15, 40, 60 and 80 °C/min up to a final temperature of 800 °C. From the analysis of TGA and DTG data, the Authors could infer the apparent kinetic parameters for a simplified, single step, global reaction scheme in which the solid biomass is converted to a solid residue and a volatile. It is reported that *Chlorella P.* HC sample proceeded its thermal degradation as three successive stages: dehydration, devolatilization and solid residue decomposition, all represented in Figure 1.8a. Its devolatilization stage consisted of two main temperature zones with a transition at 300–320°C (Figure 1.8b). The first stage (I) was from the initial temperature to T1 and was called dehydration, because of the elimination of water in the algal cells and external water bounded by surface tension; the second stage (II) was from T1 to T5 and was characterized by a major weight loss, which corresponded to the main pyrolysis process (devolatilization) and in which most of the volatiles were released; the third stage (III) was from T5 to the final temperature (800°C). Referring to the aforementioned figures, T1 was the temperature of initial devolatilization. T2 was the temperature of maximum reaction rate at Zone I. T3 was the transitional point between Zone I and II. T4 was the temperature of maximum reaction rate at Zone II. T5 was the end of devolatilization in

Stage II, taken as the point of an equal value of instantaneous reaction rate $d\alpha/dT^{-1}$ (weight loss rate, $\% \cdot ^\circ\text{C}^{-1}$) to T_1 . Two main temperature zones appeared in the devolatilization stage, as clearly shown by the DTG curves of *Chlorella* HC (Figure 1.8b). The lower temperature zone (Zone I) could be mainly correlated with the decomposition of protein and carbohydrate while the upper temperature zone (Zone II) correlated with the decomposition of lipid.

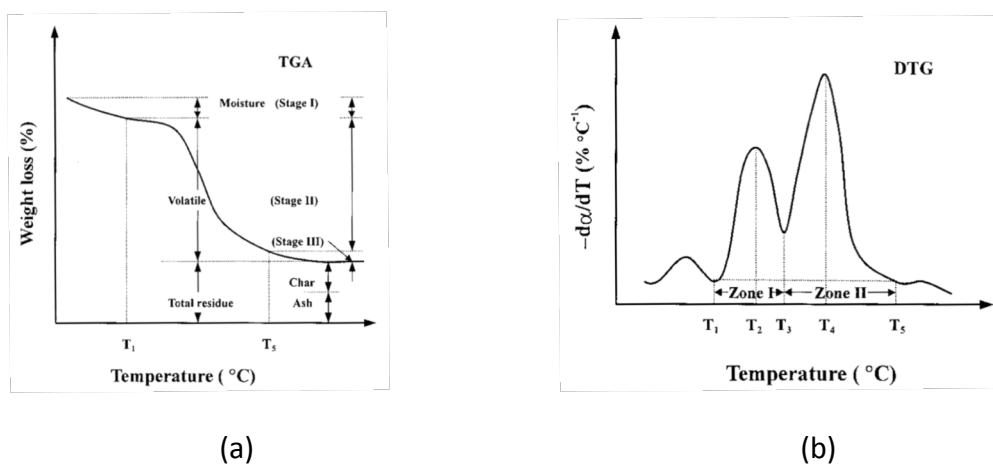


Figure 1.8: Schematic TGA (a) and DTG (b) during pyrolysis of *Chlorella P.* Source (ibid).

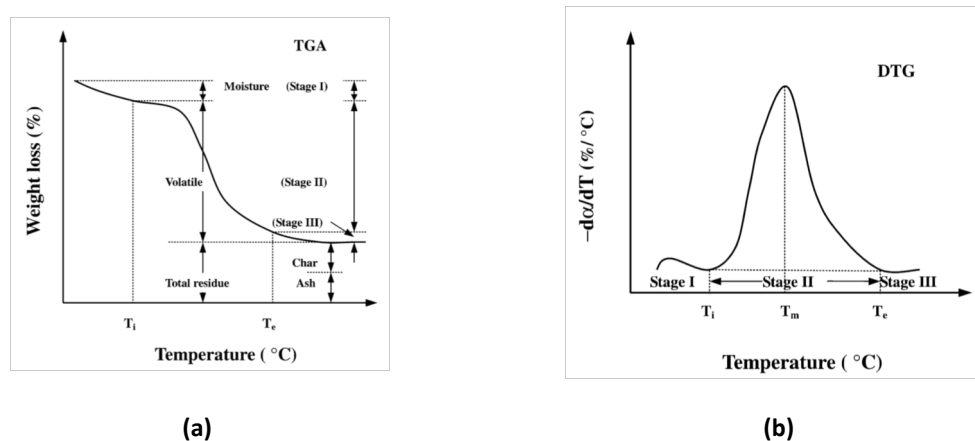


Figure 1.9: Schematic TGA (a) and DTG (b) during pyrolysis of *Chlorella P.* and *Spirulina P.* Source (ibid).

In their work, Miao and co-workers [88] subjected a lab culture of *Chlorella P.* (CP) and open-air grown *Microcystis Aeruginosa* (MA) to fast pyrolysis in a fluid bed reactor. The obtained bio-oil microalgae was characterized by low oxygen contents with high H/C ratios, HHV of about 29-30 MJ/kg and high nitrogen (10%wt), this last attributed mainly to chlorophyll and proteins.

Miao and Wu [94] subjected both autotrophic (AC) and heterotrophic (HC) grown *Chlorella P.* to fast pyrolysis in the same fluid bed reactor. The amounts of carbon and hydrogen in HC bio-oil were about 25 and 33% higher than those of AC bio-oil, whereas the amounts of oxygen and nitrogen were only about 58 and 10% of those in AC bio-oil. Compared to AC bio-oil, the HC bio-oil had higher HHV, lower density and lower viscosity.

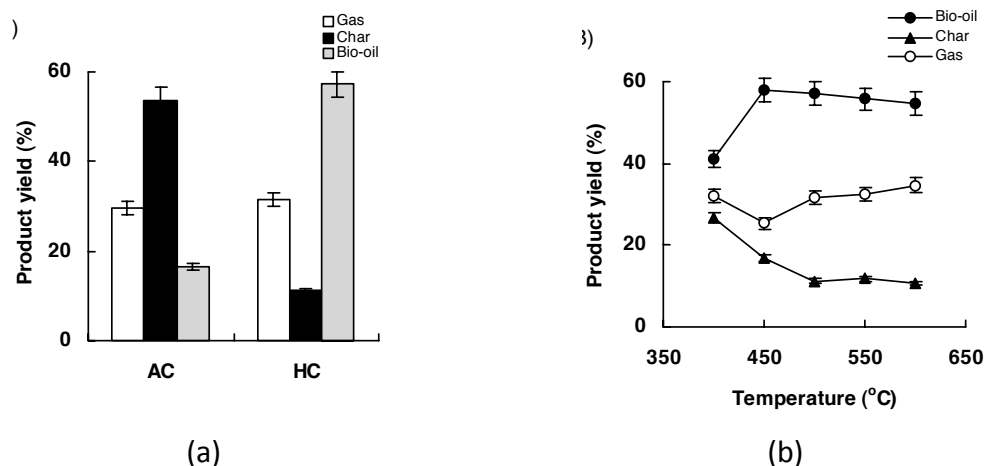


Figure 1.10: (a) Product yields (on the basis of the dry weight of samples) of fast pyrolysis from microalgae. (b) Product yields of HC *Chlorella P.* at temperatures from 400 to 600 °C. Source (*ibid*).

The heating value of HC bio-oil (41 MJ/kg) was 1.4 times that of AC bio-oil (30 MJ/kg). These results also show that the presence of lipids is favourable for proteins to produce fuel oil, both for the properties of the material as well as the energy produced. Compared with bio-oil from wood, bio-oil from HC has lower viscosity (0.02 Pa s), lower density (0.92 kg/l) and higher heating value (41 MJ/kg), about twice that of bio-oil from wood.

Demirbas [95] carried out a number of comparative studies of the pyrolysis of six small samples (~5g each) of mosses, one algae and microalga *Chlorella P.* in a tubular reactor, externally heated by a furnace. Pyrolysis was carried out in a temperature range from 525 to 825 K at a heating rate of 10 K/s. Demirbas found that the yield of bio-oil from pyrolysis of *Chlorella P.* increased with temperature up to 750 K, in order to reach a plateau value at 775 K, and maximum yield was 55.3% of the sample. The yield of bio-oil rose from 5.7 to 55.3% as the temperature rose from 525 to 775 K, and then gradually decreased to 51.8% at 875 K. The yield of gaseous products for *Chlorella*

P. increased from 4.6 to 39.5%, and the char yield decreased from 89.7 to 8.9% as the temperature rose from 525 to 825 K. Bio-oil comparable to fossil fuel, with a HHV of 39.7 MJ/kg and higher energy density than original feedstock was obtained from pyrolysis of microalgae. Moreover, higher quality bio-oil was obtained from pyrolysis of microalgae than from mosses.

Grierson and co-workers [35] carried out a study to evaluate the thermo-chemical properties of six species of microalgae biomass using a slow pyrolysis technique. In particular, using a Computer Aided Thermal Analysis (CATA) they could determine the specific heats of reaction that occur in each sample under unsteady-state heating conditions. The microalgae species were *T. Chui*, *Chlorella like*, *Chlorella Vulgaris*, *Chaetoceros Muelleri*, *Dunaliella Tertiolecta*, and *Synechococcus*. The total amount of process energy required to achieve thermal decomposition of all species of microalgae was calculated by the Authors, which found it to be similar at around 1 MJ/kg of dry microalgae biomass, whereas the calorific value of the combustible gas released up to 500°C (calculated under stoichiometric condition), was found to lie in the range 1.2-4.8 MJ/kg.

Torri and co-workers [96,97] subjected 2.85g of protein-rich residue of *Chlamidomonas Reinhardtii*, resulting from lipid extraction with chloroform/methanol, to pyrolysis at moderate temperature (350°C) in a quartz furnace. The Authors did not report the biomass heating rate during the process. Pyrolysis vapours were condensed with an ice bath. The ash content of the extraction residue was assessed in 17 wt.% of biomass weight, and the mass yield of char, bio-oil and gases was reported to be 44%, 28% and 28% respectively. The bio-char itself was found to be composed by 62 wt.% volatile matters, and 38 wt.% ash. The Authors performed an analytical characterisation of the organic fraction based on the solvent fractionation procedure. The liquid product (containing 9% water) was fractionated into a water-soluble fraction (55 wt.% of bio-oil), water insoluble matter (35% wt.% of bio-oil) and 0.5 wt.% of bio-oil insoluble solids (both chloroform and water insoluble fraction). Bio-oil was mainly composed by anhydrosugars, oligo- and poly-saccharides, relatively small amounts of

protein pyrolysis products and water insoluble components, that the Authors supposed to be formed by thermal cracking of un-extracted high polarity lipids.

1.6 Synthetic review of scrap tires pyrolysis

End-of-life tires (ELT), also called scrap tires (ST) represent an important concern in waste management for both developing and developed countries, because of the huge amount produced annually and the constraints associated with their environmentally sound management. The estimates of the 2010 annual production of scrap tires are about 2.5 million tons in North America, 0.5-1.0 million tons in Japan [98], 28 million tires in South Korea [99]; more recent data from ETRMA² reveals that in 2013 the amount of ELT treated in the European Union summed up to around 2 million tons [100,101], while in Brazil in the same year 0.4 million tons were estimated to have been collected by the RECICLANIP³ consortium [102].

To date, a limited number of alternatives have been adopted for processing the collected ELT [100,103]:

- Stockpiling or disposal in landfill (banned in the EU by Directive EC/31/99 [104]);
- Energy recovery
 - o incineration in cement plant
 - o incineration for urban heating or in power plants
- Material recovery
 - o material recycling
 - granulation to produce fillers, additives or asphaltic mixture
 - direct use (bumper, furniture)
 - in steel mills & foundries as carbon substitute
 - reuse for other purposes (e.g. devulcanization for rubber reclamation)
 - pyrolysis

² ETRMA is the European Tyre and Rubber Manufacturer Association.

³ RECICLANIP is a not-for-profit organization founded in 2007 by ANIP (Brazilian national association of tire industries). It is responsible for the creation of collection points, management of reverse logistics and product development for the reuse of waste tire in Brazil according to the provision of the law CONAMA, 258/99 and 416/09.

- civil engineering
 - public works
 - backfilling

While some of the solutions highlighted are well established, like incineration in cement kilns, carbon substitution in steel mills and foundries, granulation or landfilling, most of the remaining treatments either require further processing (pyrolysis), or have a very limited or niche application due to limited market size (additives, backfilling, public works, bumpers) or finally are subjected to uneven policy constraints (rubberized asphalt).

The scientific community devoted much attention to the theme of tire pyrolysis since the beginning of the '70s, with the technical report jointly prepared by the US Bureau of Mines and Firestone Co. [105] on the *“technical feasibility of carbonization for scrap tire management”*. Nowadays, comprehensive and independent reviews in literature [106–109] support the valuable properties of the pyrolysis oil that can be obtained from scrap tires when properly processed. Independently from the specific conversion technology adopted for tire pyrolysis, there is a general consensus on the characteristics of the oil, which results to be a distillable mixture of paraffins, olefins, and aromatic compounds, shows high calorific content (HHV 40-42 MJ/kg), has low viscosity (<5 cSt), and low sulphur (<2 %wt), nitrogen (<1%) and oxygen (<2%) content.

At least 10 companies worldwide claim to have developed commercial and semi-commercial plant for tire pyrolysis systems, ranging between 2 and 200 ton·day⁻¹, either batch or continuous, mostly rotary kiln [108]. Moreover, three European associations operating at national level in the framework of ETRMA and representing Turkey, Italy and Estonia, claimed respectively for 2013 (IT and TR) and 2012 (EE) that a grand total of around 14600 tons of ELT were destined to pyrolysis processing in their countries, which makes up less than 1% of the grand total of EU ELT annual generation. In spite of the ETRMA figures, it was not possible to gather further details on the owners of pyrolysis plants, working principle of their technology and final destination of products of these “operating” plants.

While the number of studies trying to assess the feasibility of power generation from scrap tire pyrolysis oil in internal combustion engine is significant - a Scopus

search on *title, abstract* and *keywords* with entries “*tire (or tyre) pyrolysis engine*” will yield more than 40 results - and several experiments have been carried out on either pure or upgraded, i.e. desulphured, pyrolysis oil, its fractions, or blend with fossil fuels, e.g. diesel, dimethyl-ether or gasoline, and biofuels, e.g. biodiesel or vegetable oil [110–120], barely one reference could be found on the use of STPO in micro gas turbine from Seljak et al. [121].

In their work, Seljak and co-workers [121] tested a distilled fraction of STPO, obtained in the temperature range 190-350°C, in a test rig dedicated to alternative fuels based on an automotive turbocharger and a gas turbine combustor. Their set-up, which mimics the geometry of a gas turbine operating in regenerative cycle, was operated at a turbine inlet temperature between 800 and 900 °C while measuring CO, NO_x and THC concentrations at the exhaust.

2 Bio-oil production in a pilot test bench

The present chapter reports on the experimental campaign aimed to investigate the yield and properties of pyrolysis oil from different biomass samples in an original intermediate pilot pyrolysis reactor for research applications. The R&D activity on the reactor was started in 2010 with the aim of expanding the capability of the group in the thermochemical field. After four years of work, the intermediate pyrolysis reactor represents a valuable asset for the Research Group, having been operated in the framework of both institutional research projects as well as for third-party contract research for the last four years.

In the following paragraphs, the results obtained with three microalgae species (marine and fresh water *chlorella* and marine *nannochloropsis*) and mixed hardwood and softwood used for wood-chips production are presented. For each feedstock, a comprehensive characterization of both raw material and its pyrolysis oil is presented and the results discussed in terms of oil properties, both chemical and physical, and process yield, in terms of mass as well as carbon and energy recovered in the pyrolysis liquids. Some of the results here reported and discussed have been published in an international journal [122] or presented in specialized conferences [123–125].

2.1 Description of the experimental apparatus

2.1.1 Pyrolysis reactor

The pyrolysis experiments were carried out in an innovative semi-continuous, intermediate pyrolysis reactor, jointly developed by CREAR-University of Florence and SEA Marconi Technologies. The unit, which has a capacity of up to $1.5 \text{ kg}\cdot\text{h}^{-1}$ of feed, mainly consists of a cylindrical body of corrosion resistant stainless steel (AISI 310), externally heated by two ceramic-shell resistors, regulated by a single PID controller, and capable of withstanding up to 600°C of continuous working temperature. Mixing of the feedstock inside the reactor is promoted by a variable speed stirrer, driven by an inverter, fitted with three plough-shares; in order to promote mixing and milling of the feedstock and contribute to transfer the heat from the surface of the reactor to the particle being converted, the system can be loaded with carbon-steel spheres of 22 mm diameter, which are continuously agitated by the stirrer. Besides the mechanical effects, metal spheres can potentially have a catalytic effect on the biomass conversion, for example if high-alloy steel with a large amount of Ni is used. The reactor is mounted on a reclining support; in normal operation it lies horizontally, but it can be reclined up to 15° to facilitate the discharge of solid residue and metal spheres in case of need.

The reactor is equipped with three openings: the first, on the front face of the reactor body, is for biomass loading; the second, on the top of the opposite side, connects the reactor to the post-treatment module which regulates extraction, condensation and collection of the liquid; the third, on the bottom of the rear face of the reactor, is equipped with a gate valve and an air-tight vessel, which allows the discontinuous removal of solid residue and allows the collected material to cool down to room temperature overnight.

Piping from the reactor to the condensers is heat-traced, and temperature control is actively supervised by three independent PID controllers; the scope of the measure is two-fold: it avoids premature and undesired condensation of liquid fractions before reaching the first condenser, and allows the user to set and maintain

the vapours stream either to the process temperature or to a lower value, to quench homogeneous reactions and avoid increasing the so called *hot vapours residence time*.

A schematic of the reactor is reported in Figure 2.1, while a picture of the unit installed at CREAR/RE-CORD premises is shown in Figure 2.2.

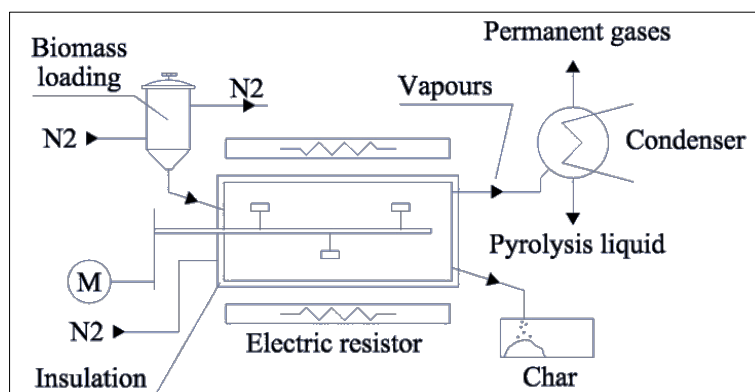


Figure 2.1 : Schematic of the batch pyrolysis reactor.



Figure 2.2: Picture of the batch pyrolysis reactor (centre) and control panel (left).

2.1.2 Feeding system

The reactor feeding system consists in a manually operated piston plunger, a cylindrical purging chamber with a capacity of around 0.5 L and a full-passage ball

valve, which separates the feeding vane from the reactor chamber. The sample is loaded into the purging chamber in variable amounts, ranging between 20 and 50 g, then the top cover is closed, sealed, and the feedstock flushed with nitrogen for few seconds to remove all the oxygen and prevent undesired oxidation before opening the valve and moving the piston downward several times, forcing the material to enter the process. Each cycle lasts less than 40 s, including the nitrogen flush.

2.1.3 Bio-oil condensation and collection

The bio-oil recovery system consists of two water-cooled, counter-current condensers made of grade AISI 316 stainless steel and connected in series. The first condenser is a tube-in-tube heat exchanger, with an inner diameter of 1" at the vapour side, while the second is a shell-and-tube, with 5 passages in the shell and 11x14 mm OD pipes in the tube side (vapours), allowing for a large surface to recover most of the low-boiling point species. In the first condenser pyrolysis vapour proceeds downward, and after a 180° turn enters the second condenser in upward direction, whereas condensate is collected by gravity in a pot placed at the bottom of the junction between the first and second condenser.

The difference in geometry is motivated by the complex composition of pyrolysis oil, comprising a mixture of hundreds of oxygenated compounds; the major chemical groups are water (15–30 %wt), monomeric carbonyls, sugars, organic acids, phenols, and oligomeric moieties from carbohydrates and lignin degradation [21,22], resulting in a wide range of molecular weights up to 8-10000 Da [23]. In practice, high boiling point species require larger passages because they are dense and present high viscosity, which could ultimately lead to pipe blockage, while lighter and more volatile compounds require larger surfaces due to their lower vapour pressure. Even if the product is collected in a single pot, by staging the condensation on two different surfaces it is possible to obtain an optimal recovery of liquid product.

2.1.4 Char collection

While vapour and permanent gases are continuously removed from the reactor and separated in the condenser, the solid residue produced during the conversion is accumulated inside the reactor along with the metal spheres. Once in a while, the reactor is reclined, the discharge port rotates to open and the metal spheres and the solid residue are discharged from the reactor and let fall inside an air-tight vessel (collection pot) saturated with nitrogen, where they cool down to room temperature before being collected.

The char produced in biomass pyrolysis, especially fast and intermediate, is known for being very reactive [126], and the one produced in CREAR/RE-CORD reactor is extremely fine, due to the combined actions of mixing and milling exerted by the stirrer and the metal spheres on the particles undertaking conversion. During a preliminary pyrolysis test with lignin-rich residues produced from a 2nd generation ethanol plant, around 500 ml of char was discharged from the reactor, let cool down in the collection pot for around 1 hour, until the material reached a temperature around 50 °C, and then left on the ground for around 1 hour. The result was that after the indicated time interval, most of the char was combusted in a flameless process, leaving only a white fine residue, which was speculated to mainly consist of ashes. Since then, the char discharging procedure was modified accordingly, and an overnight cooling cycle in inert environment was adopted as a precaution and safety measure to prevent auto-ignition of the sample when opening the collection pot.

2.2 Test procedure

The standard test procedure is reported in the following paragraphs. The empty and cold reactor is loaded with metal spheres and heated up to the desired process temperature; once the set point is stably reached, the reactor atmosphere is saturated with nitrogen, whose flow is then maintained at around 4 Nl·min⁻¹, and the stirrer starts rotating. Test begins with the first batch of feed being introduced in the reactor;

prior to loading the feedstock, the material is washed for 30 s with nitrogen to prevent oxygen from entering the process. During the test, the PID regulates the power supplied to the resistors to keep the process temperature constant and temperature measurements are acquired from several points of the system. The temperature on the surface of the reactor is used to control the PID, while the temperature measured in the middle of the reactor, inside the stirrer, is used as a reference for the process. Once the whole amount of feedstock is completely processed, a suitable time interval is allowed until condensate collection is completed, then the solid discharge port is opened to un-load the reactor from solid residue (char), and finally the stirrer is stopped.

Table 2.1: Set point of process parameters in pyrolysis tests.

Parameter		Value
Reactor temperature	°C	400-500
Nitrogen flowrate	$NI \cdot min^{-1}$	4-5
Size of feed batch	g	20-40 ¹
Loading cycle	min^{-1}	1-3

¹: depending on the bulk density of feedstock

The solid is collected in a closed vessel filled with nitrogen, and let to cool down to room temperature. Relevant process parameters are reported in Table 2.1.

2.2.1 Feedstock conditioning

As for most of the thermochemical conversion processes, pyrolysis is also extremely sensitive to all those properties of the feedstock affecting the degradation mechanisms and the subsequent complex set of secondary reactions. Among these properties, for a given raw material and process conditions (T,p), moisture content, absolute particle size and its distribution have a prominent influence, since they affect both heat transfer mechanisms and final oil properties.

Heat transfer to the particle, and especially the heating rate, strongly influence the yield and relative distribution of pyrolysis products, i.e. char, gas and oil (in its organic- and aqueous phases, when occurring) and is widely accepted as the

distinguishing parameter, along with attained temperature and to a minor extent residence time, between pyrolysis modes [10,127], i.e. slow, intermediate, fast, flash, etc.

In order to limit the influence of particle size and moisture on heat transfer to the particle, thus promoting a quick heat up to steer process conditions closer to fast pyrolysis, feedstock are properly conditioned in terms of size and water content before entering the reactor. As a rule of thumb, the unit was operated with moisture content below 10% and with feedstock ground below 1 mm.

2.2.2 Mass yield, energy recovery and carbon recovery of pyrolysis test

The results of the pyrolysis tests are presented in the form of chemical and physical properties of the oil samples, which were analysed according to the procedures described in appendix A and Appendix B. Three main parameters are calculated and compared for each tested feedstock: mass yield, carbon recovery and energy recovery.

Mass yield (Eq. 3) is defined as the ratio of the recovered bio-oil, either as a whole or considering the water- and organic-rich fractions, to the mass of feedstock.

$$mass\ yield = \frac{m_{bio-oil}}{m_{feed}} \quad \text{Eq. 3}$$

Carbon recovery (Eq. 4) is obtained as the ratio of the amount of carbon in the feed to that recovered in the bio-oil, as measured by CHN analysis and mass balance:

$$C\ recovery = \frac{\%C_{bio-oil} \cdot m_{bio-oil}}{\%C_{feed} \cdot m_{feed}} \quad \text{Eq. 4}$$

Neglecting process heat for pyrolysis and drying, that can be supplied by recovering by-products (char and permanent gases), power for feedstock conditioning and power for harvesting and cultivation, and by comparing the calorific content of the feed with that of the bio-oil, it is possible to make a reasonable estimate of the *energy*

recovery (Eq. 5) in the products for the pyrolysis process, according to the following expression:

$$ER = \frac{HHV_{\text{bio-oil}} \cdot m_{\text{bio-oil}}}{HHV_{\text{feed}} \cdot m_{\text{feed}}} \quad \text{Eq. 5}$$

The same expression applies if considering the LHV instead of the HHV.

It should be pointed out, however, that the energy balance of our plant is not meant to be representative of a real operating facility, neither demo nor industrial. The CREAR/RECORD pyrolysis unit was designed as a sturdy and robust tool for the production of bio-oils from as many feedstock as possible and to allow testing of several materials, each with distinct properties, from wood to industrial residues. The reactor volume is around 10 dm³, while each batch of material can be between 20 and 40 g, depending on its bulk density. Due to the large size of the reactor, it is therefore evident that the amount of energy required to keep the system at the process temperature (heat losses) can easily exceed the energy required for the conversion process itself, and its estimate can be difficult, since the batch-wise feeding does not have a precise timing, but is manually operated.

2.2.3 Products analysis

The produced bio-oils were analysed focusing on their chemical and physical properties according to common methodologies for pyrolysis liquids. In particular, the bio-oil samples were investigated for their acidity (TAN), pH, density, viscosity, elemental composition, calorific content, and solid content. When required, GC/MS qualitative analyses of constituents were also addressed. Details on analytical methods are reported in Appendix A and Appendix B.

3 Experimental results

3.1 Pyrolysis oil from lignocellulosic feedstock

3.1.1 Analysis of the feedstock

The CREAR/RE-CORD pyrolysis reactor was fed and tested with several wood based materials, like olive pruning, lignin-rich residue from 2nd generation bio-ethanol process, olive kernel residues, and mixed wood chips (MWC) from hardwood and softwood. This section reports on the pyrolysis experiments carried out with MWC. The feedstock was ground in a Retsch knife mill equipped with a 1 mm sieve. Since the moisture content was already low ($\approx 6-7$ %wt.) further drying was not necessary. Results from the operation of the CREAR/RE-CORD reactor are compared against data from Yang et al. [128], who operated an intermediate screw pyrolysis reactor at the University of Birmingham with wood and straw pellets.

Proximate and ultimate analyses of all the feedstock are reported in Table 3.1; measurements were carried out in triplicates according to the analytical procedures reported in Appendix A. Mixed wood chips do not differ substantially from the woody biomass tested by Yang et al. in their screw pyrolysis reactor except in the ash content, which is about 1/4th that of pine pellets; some differences can be found when considering barley straw pellets, which are higher in moisture and contain even higher amount of ash, up to 6 %wt.

Table 3.1: Proximate and ultimate analysis of the feedstock (mixed wood chips).

Property		Pine pellets	Barley straw pellets	Olive kernel residues	MWC ^b
		[128]	[128]	[129]	(this study)
<i>Ultimate analysis</i>					
C	<i>ad %wt</i>	47.5	44.2	47.2	48.1
H	<i>ad %wt</i>	5.3	6.1	5.5	5.8
N	<i>ad %wt</i>	0.4	0.4	0.3	0.1
O ^a	<i>ad %wt</i>	36.4	30.4	38.7	39.3
S	<i>ad %wt</i>	<0.1	0.6		
Cl	<i>ad %wt</i>	<0.1	0.4		
<i>Proximate analysis</i>					
Volatile matter	<i>ad %wt</i>	82.1	74.9	71.3	75.2
Moisture	<i>ad %wt</i>	7	11.9	7.9	6.1
Fixed carbon	<i>ad %wt</i>	7.7	7.2	20.4	18.0
Ash	<i>ad %wt</i>	3.2	6	0.4	0.8
HHV	<i>ad MJ·kg⁻¹</i>	18.2	17	20.5	18.4
LHV	<i>dry MJ·kg⁻¹</i>	18.3	17.8	21.0	18.2

^a: by difference.

^b: MWC = mixed wood chips

A TGA of the feedstock up to 900 °C with a 15 °C/min heating rate in nitrogen is reported in Figure 3.1, where triplicate runs are shown. The green line represents the actual weight loss measurement, the red line is the temperature profile of the oven versus time and the violet line is the time derivative of the weight loss, i.e. the rate of conversion. The expected behaviour of lignocellulosic biomass degradation can be here easily identified; the first peak in the violet line represents the release of moisture, while the largest peak is the convolution of two distinct degradation peaks, hemicellulose and cellulose. The second violet peak is right-skewed, i.e. the rate of conversion is faster before attaining the apex than after; this is due to at least two major factors: (1) hemicellulose conversion starts at a lower temperature than cellulose and ends right after cellulose decomposition had achieved its maximum, and (2) cellulose degradation is not symmetric. The smoother part of the degradation curve, from about 43 minutes onward, represents the decomposition peak of lignin, which compared to hemicellulose and cellulose is less intense, but lasts over a wider temperature range. The devolatilization of extractives, whose peak is expected to be between water and hemicellulose, is not identified in the graph on Figure 3.1 due to

mass transfer limitation of our instrument, which operates on a large sample size ($\approx 1\text{g}$).

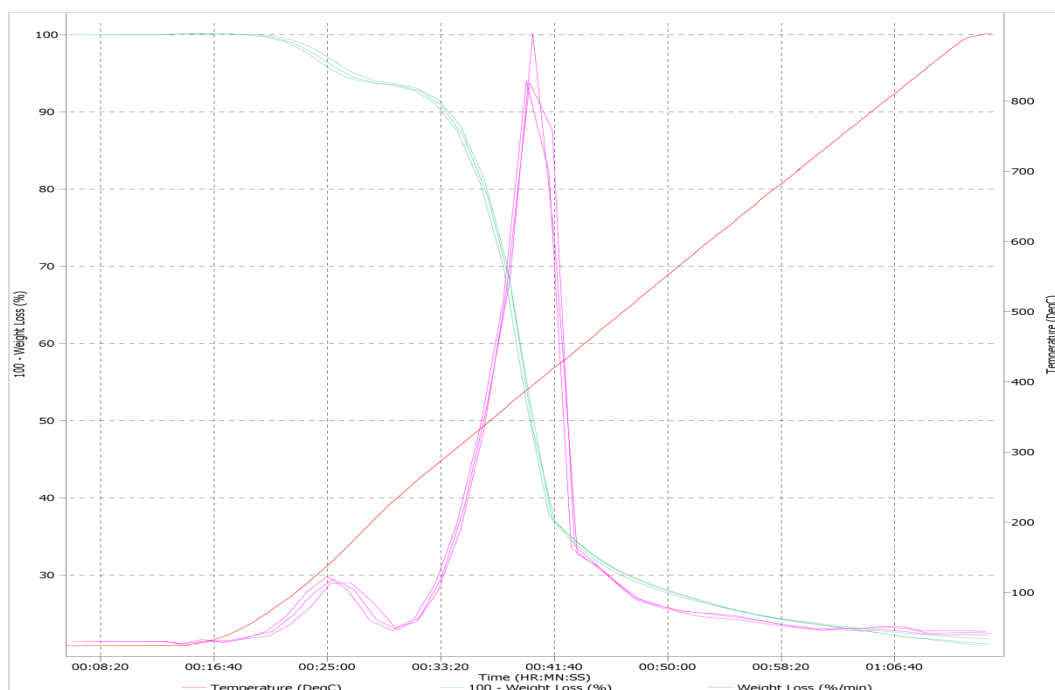


Figure 3.1: TGA of mixed wood chips at 15 °C/min up 900 °C in nitrogen (triplicate). Green: actual samples weight loss profile. Violet: derivative of weight loss (calculated). Red: furnace temperature profile.

3.1.2 Pyrolysis experiments

Four different experiments were carried out in our pyrolysis unit. At first, the reactor was operated at 450°C with pine chips in raw size ($\approx 2\text{x}1\text{x}2\text{ cm}$), i.e. not ground in a knife mill. The size of the particle was kept large in the first test to investigate the effect of particle size on the liquid product yield and quality. The temperature was selected from literature [1,10,38] and previous results obtained in our reactor, as the one yielding better quality product for fuel application, especially in terms of water content and heating value. Moreover, this choice was supported by the findings of Westerhof and co-workers at Twente University, that operated a lab-scale (1 kg/h) fluidized bed for biomass pyrolysis, and clearly showed how conditions maximizing the yield of bio-oil are not necessarily the ones resulting in bio-oils with higher quality for fuel applications [130].

The unit was later operated with ground biomass (<1mm) at 400, 450 and 500°C, to investigate the effect of process temperature on yield and quality of liquid products, minimizing the influence of heat transfer mechanisms to the particle. Process yields for all the investigated configurations are reported in Table 3.2 along with carbon recovery and energy recovery in the organic liquid phase.

3.1.3 Bio-oil yield and characterization

The bio-oils from the same mixed wood chips feedstock were collected and analysed in the laboratory according to the methodologies described in Appendix A. Table 3.3 reports the results from the analyses on the organic-rich phase (bio-oil) of the produced pyrolysis liquids, or the single-phase liquid in case of not-separating liquid product. Not-separating products are reported as “mixed” in the table. As produced, bio-oil generally looks like a mobile, black and viscous liquid. Depending on the process conditions, sometimes the collected liquid exhibited the tendency to separate spontaneously in two phases with distinct behaviours: in those cases, by agitating the collection vessel it was possible to identify the oil-rich phase (black, dense sticky and viscous liquid) and the water-rich phase (brownish, with water-like properties). When possible, the two phases were collected and separated in the laboratory with a funnel and weighted. The results from the analyses are compared to those carried out in the past on a sample of bio-oil from BTG (Biomass Technology Group, The Netherlands).

Sample MWC#1 did not phase separate right after production, but was reported to take around 1 week before separating into oil and aqueous phases. Sample MWC#2 was also homogeneous, while MWC#3 and 4 did phase-separate. MWC#3 was easily separated in the funnel, whereas MWC#4 was difficult to separate, due to its high solid loading (≈ 25 %wt). It was observed that bio-oil solid content increases with process temperature, from 0.25 %wt for MWC#2 to 24.6 for MWC#4; since stirring intensity (rpm), feeding rate and feedstock properties (particle size and moisture) are the same for MWC#2 to 4, this was attributed to the increased rate of volatiles and liquids released at increasing process temperatures, hence increased heating rate, and to

their disruptive effect on the structure of the solid particle that is undergoing conversion. A liquid release from cellulose undergoing thermal degradation under high heating rate was observed by Dauenhaer and co-workers, that investigated the formation of a liquid intermediate from microcrystalline cellulose particles in contact with a rhodium based reforming catalyst at 700°C by using high-speed micro-photography [131]. The liquids from the particle in this process could potentially be among the sources of aerosol generation.

The viscosity of bio-oils MWC#3 and 4 could not be measured at 40°C with a capillary viscosimeter ($k=0.3$), due to the fouling action of the bio-oil on the capillary tube wall, which prevented the optical sensor to determine the passage of the liquid meniscus. Therefore the viscosity values of our bio-oil samples were higher than those reported by Yang et al. [128] for bio-oils from pine pellets (14.8 cSt) and barley straw pellets (30.5 cSt) and BTG bio-oil (13 cSt). The viscosity of non-separating oils (olive kernel residues, MWC#1 and MWC#2) was low for all the samples, always below 2 cSt, due to the large amount of water.

Water content of MWC#1,2 and olive kernel residue obtained in our tests was quite high, >70, 74.7 and 48 %wt respectively, while water content of MWC#3 (23.5 %wt) was comparable to the one of BTG bio oil (22.5 %wt), and pine pellets (14.8 %wt).

The calorific content of the produced bio-oil varied with process conditions; it was poor for samples of olive kernel residues, MWC#1 and 2 (9.9, 7.8, 2.8 MJ·kg⁻¹ respectively) because of the high water content of the mixed phase, while it was higher for MWC#3 and 4 (18.5 and 26.8 MJ·kg⁻¹). However, the HHV of MWC#4 was affected by the excessive content of char, which has higher energy content than bio-oil.

Carbon recovery in pyrolysis liquid, for those phase-separating samples, was evenly distributed between the two phases; for sample MWC# 3, 18.1 %wt of the carbon was recovered in the bio-oil and 8.3 %wt in the aqueous phase, while for MWC#4, 7.3 %wt of the carbon was retained in the bio-oil and 8.2 %wt in the aqueous phase. The obtained carbon recovery is in line with the results obtained by Yang et al.

[128], who obtained 8.2 %wt in their intermediate screw pyrolysis reactor operated with barley straw pellets.

The energy recovery trend followed closely the one highlighted for carbon recovery; also in this case, the total energy content of the bio-oil and aqueous phases was almost equal, 10.4 vs. 9.5% for MWC#3 and 8.8 vs. 9.0% for MWC#4 samples, and comparable with that obtained from barley straw pellets (8.2%).

The effect of particle size on bio-oil quality can be inferred by comparing the products obtained with different feedstock particle size, i.e. large and ground material, at the same process temperature; comparing MWC#1 and MWC#3 it can be noticed that larger solid particle (hence lower heating rate) produced a single-phase liquid with a very high water content and a very low heating value. On the contrary, a smaller particle size leads to a phase-separating liquid product, in which the bio-oil has good calorific content ($18.5 \text{ MJ}\cdot\text{kg}^{-1}$ of MWC#3 vs. $7.8 \text{ MJ}\cdot\text{kg}^{-1}$ of MWC#1) and is lower in water (23.5 %wt for MWC#3, while water content of MWC#1 was too high to be precisely assessed with Karl-Fisher titration).

The effect of process temperature on the quality of the oil can be inferred by comparing samples MWC#2 to 4; at increasing temperatures, there is a tendency toward increasing TAN (respectively 42.4, 96.3, and $117 \text{ mgKOH}\cdot\text{g}^{-1}$) and decreasing pH (respectively 2.91, 2.52, and 2.6) of the organic fraction of the pyrolysis liquid, or the single phase if the pyrolysis liquid does not separate (MWC#2).

Compensating for the recovered organic fraction of MWC#4 to account for the unusual solid content, it can be noticed that MWC#3 shows a better mass yield, carbon and energy recovery among the tests carried out with the same particle size of the feedstock (<1 mm). Single phase samples like olive kernel residues and MWC#1 have better energy recovery due to the larger amount of mass considered in the calculation, but their quality is poorer since they have a lower heating value and much higher water content (48 %wt for olive kernel residue).

Table 3.3 reports the characterization of a commercial sample of pyrolysis oil from pine chips produced by BTG, The Netherlands, in their fast pyrolysis reactor. Comparing bio-oil from MWC#3 with BTG bio-oil, it can be seen that C-H-O contents,

calorific value, pH and water content are almost the same; MWC#3 shows higher viscosity, solid content and TAN. Though differences remain, especially considering the global process yield, it is a valuable result that in a relatively simple laboratory apparatus it was possible to obtain a bio-oil with energetic properties close to a commercially available fast pyrolysis bio-oil, by properly tuning the conversion parameters.

Table 3.2: Mass yield, energy and carbon recovery in bio-oil from lignocellulosic feedstock.

Parameter		Pine pellet [128]	Barley straw pellet [128]	Olive kernel residues [129]	MWC ^c #1 (this study)	MWC #2 (this study)	MWC #3 (this study)	MWC #4 (this study)
Particle size	mm			≈2-3	20x20x10 ^a	<1	<1	<1
Appearance		pellet	pellet	granulate	chips	powder	powder	powder
Process Temperature ^e	°C	450	450	450	450	400	450	500
<i>Mass balance</i>								
feedstock	kg	6	5	1.013	4.312	1.168	1.828	1.276
oil (mixed)	kg			0.446	1.734	0.396	0.722	0.490 ^d
oil (only organic phase)	kg	1.11	0.29				0.189	0.077 ^d
aqueous phase	kg	2.15	2.16				0.532	0.370 ^d
char	kg	1.71	1.51					
gas ^b	kg	1.03	1.05					
<i>Yield</i>								
oil (mixed)	% of feed	54.3	49.0	44.0	40.2	33.9	39.5	38.4 ^d
oil (organic phase)	% of feed	18.5	5.8				10.3	6.1 ^d
aqueous phase	% of feed	35.8	43.2				29.1	29.0 ^d
char	% of feed	28.5	30.2					
<i>Energy recovery</i>								
oil (organic phase)	% of feed HHV	24.6	9.9	21.3	17.0	5.1	10.4	8.8 ^d
oil (organic phase)	% of feed LHV _{dry}	22.7	8.8	16.9			9.5	8.5
aqueous phase	% of feed HHV						9.5	9.0 ^d
<i>Carbon recovery</i>								
oil (organic phase)	% wt of feed	21.7	8.2	20.8		5.1	8.1	7.3 ^d
aqueous phase	% wt of feed						8.3	8.2 ^d

^a: approximate size. ^b: by difference. ^c: MWC = mixed wood chips. ^d: data corrected to account for unusual solid content. ^e: nominal temperature.

Table 3.3: Properties of bio-oils from lignocellulosic feedstock.

Parameter		Feedstock / sample							
		Pine pellet [128]	Barley straw pellet [128]	Olive kernel residues [129]	BTG ^d bio-oil pine chips (fast)	MWC ^e #1 (this study)	MWC #2 (this study)	MWC #3 (this study)	MWC #4 (this study)
Particle size	mm					20x20x10 ^a	<1	<1	<1
Process T.	°C								
nominal		450	450	450	450	450	400	450	500
outer wall				525		525	475	525	575
<i>Ultimate analysis</i>									
C	%wt	55.69	62.57	22.3	38.9		7.3	37.56	58.33
H	%wt	7.93	8.12	8.62	7.4		9.97	8.31	6.18
N	%wt	0.36	1.41	0.03			0.22	0.41	0.61
O ^b	%wt	36.02	25.79	68.94	53.7		82.506	53.71	34.826
S	%wt			0.02			0.004	0.01	0.054
<i>Properties</i>									
phase reported	-	oil	oil	mixed	oil	mixed	mixed	oil	oil
TAN	mgKOH·g ⁻¹	47.5	30.9		72.4	71	42.4	96.3	117
pH	-			2.02	3	2.34	2.91	2.52	2.6
water	%wt	15.4	5.8	48	22.5	^f	74.7	23.5	8.59
HHV	MJ·kg ⁻¹	24.2	28.9	9.9	17.3	7.8	2.8	18.5	26.8
LHV	MJ·kg ⁻¹	22.5	27.1	8.1	15.7		0.6	16.7	25.5
viscosity @40°C	cSt	14.8	30.5	1.24	13	1.22	0.75	^c	^c
density @20°C	g·cm ⁻³	1.1	1.15	1.05	1.17		1.02	1.09	^c
carbon residue	%wt	3.55	6.5						
ash	%wt	0.18	0.2	0.09	0.016				
solid content	%wt			0.005	0.05		0.25	3.51	24.6

^a: approximate size. ^b: by difference. ^c: due to the excessive amount of solid entrained in the oil, it was not possible to measure viscosity and/or density at the specified temperature. ^d: MWC = mixed wood chips. ^e: Biomass Technology Group, The Netherlands, fast pyrolysis oil, produced mid-2010. ^f: the water content could not be measured with standard Karl-Fisher titration for pyrolysis oils (VTT method [26])

3.2 Pyrolysis oil from microalgae

3.2.1 Analysis of the feedstock

The samples here investigated are three different species of microalgae: freshwater and marine *Chlorella* and marine *Nannochloropsis*. Fresh water *Chlorella* was a proprietary strain supplied by Ingrepro B.V. (The Netherlands) in the form of dried powder. The algae were grown outdoors in two separate periods of 2011 in algal ponds with 30 cm deep raceways and under outdoor climatic conditions, i.e. sunlight and natural day/night rhythm. The growing medium was enriched with potassium nitrate (KNO_3), nitrate, mono ammonium phosphate ($\text{NH}_4\text{H}_2\text{PO}_4$), phosphate, and sodium bicarbonate (NaHCO_3) and pH kept constant. Microalgae were then harvested, dried, processed to obtain a fine powder and shipped. Marine *Chlorella* and *Nannochloropsis* samples were supplied by Hellenic Centre for Marine Research, Crete (Greece), grown in closed 20 l photo-bioreactor kept at 25-30°C in F2 medium and conditioned in the form of dry powder. The two batches were received during 2011 and stored at 4°C before analysis.

For each sample, around 1kg of material was processed at 450°C. Before pyrolysis, the microalgae samples were analysed in their elemental and macroscopic properties according to the analytical methods reported in Appendix A. Reports of the results from compositional and ultimate analyses of microalgae samples can be found in Table 3.4 along with the average composition of pine wood from 53 entries of the ECN Phyllis2 database [132].

All the three species of microalgae exhibited a very high ash content, up to 20 %wt db for freshwater *Chlorella*, which is more than 30 times the average ash content of pine wood, and similar to the level encountered with rice husks (11-22 %wt db [132]). Comparing the elemental composition of the three microalgae to the one of pine wood, it can be noticed that while H content is comparable, C content is in the lower end of the C range for pine, an S content is in the lower end of the S range for pine, microalgae biomass contains much more N (around 20 times more) and much

less O (around half). This leads to a *dry-ash-free* calorific content that is markedly higher for all the three microalgae species investigated compared to the one of pine wood (approx. +25%).

Table 3.4: Compositional and ultimate analysis of microalgae feedstock.

Parameter			Chlorella IP	Chlorella HCMR	Nannochl. HCMR	Pine [132] ^b
<i>General data</i>						
habitat			freshwater	marine	marine	
growth environment			open pond	PBR	PBR	
<i>Compositional analysis</i>						
lipid	%wt	db	17.2	10	14.8	
protein	%wt	db	41.8	52.8	35.6	
carbohydrate	%wt	db	20.2	22.7	23.1	
ash	%wt	db	20.1	16.1	15.4	0.07 - 1.03
water	%wt	wb	6.7	4.5	3.2	
<i>Ultimate analysis</i>						
C	%wt	db	46.1	47.3	48.4	48.6 - 54.8
H	%wt	db	6.1	6.4	6.8	5.8 - 7.0
N	%wt	db	6.7	8.4	5.7	0.01 - 0.39
O ^a	%wt	db	19	20.6	23.2	37.9 - 44.9
S	%wt	db	0.4	1	0.5	0 - 0.56
Cl	%wt	db	-	2.3	2.1	
P	%wt	db	1.6	2	2	
<i>Energy content</i>						
HHV	%wt	daf	24.5	25.6	26.5	17.8 - 23

^a: by difference

^b: database values for CHNOS are expressed as *daf*. An average ash content of 0.45 %wt *db* was adopted to convert from *daf* to *db*.

In addition to ash and unlike lignocellulosic biomasses, microalgae are also composed of proteins, lipids and carbohydrates. The determination of these three constituents in a biomass laboratory for energy can be somehow prone to errors: proteins are calculated from the nitrogen content by applying a conversion factor [133,134] that is not meant for a specific species, but groupings; lipids are measured gravimetrically after solvent extraction [135], but the choice of solvent system in combination with the extraction technique can markedly influence the amount and quality (i.e., chain length) of the fatty acid product recovered [136].

3.2.2 Bio-oil yield

During the test campaign, three different microalgae species were tested. Considering also the algal biomass (Chlorella) that was used in the commissioning of the pyrolysis reactor, a total of around 7 kg of microalgae were processed in the CREAR pyrolysis reactor. The first batch of 4 kg was used for testing the reactor performance and for analytical purposes, therefore data of product yield and bio-oil quality could not be used to assess the process performance or the characteristics of the produced bio-oil. Another 3 kg of material (≈ 1 each of Chlorella HCMR, Chlorella Ingrepro, and Nannochloropsis HCMR) were used for testing and production of pyrolysis oil, and the results are reported in the following paragraphs.

All the produced pyrolysis oil resulted to be prone to self-separation, exhibiting in few minutes from collection a less-dense phase floating over a heavier one. The top phase was dark-brown, highly dense and more viscous; the bottom phase was reddish, more transparent and less viscous. Conversely to lignocellulosic biomasses, the oil phase - richer in organics - was less dense than the water phase. The two phases were separately collected and weighed. A picture of the two distinct phases is shown in Figure 3.2. For lignocellulosic biomass, ash content in excess of 2.5% is known to promote phase separation of liquid products and to reduce liquid yield [48]; though specific investigations on the effect of ash content on microalgae pyrolysis are not reported in literature, the promptitude of the observed phenomenon and the extremely high amount of ash in the feed led one to suppose that the two elements could be correlated.

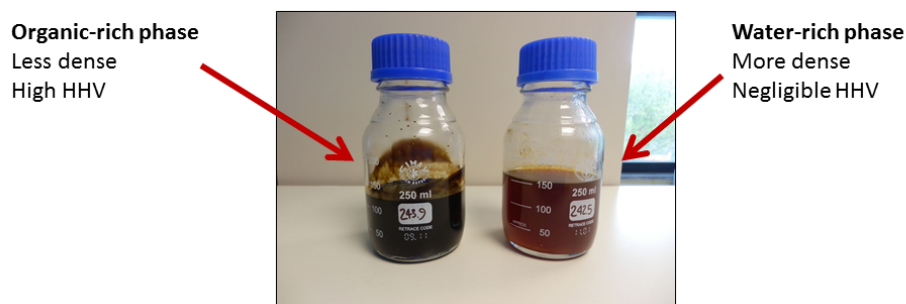


Figure 3.2: Organic- and water-rich phases of pyrolysis oil of Chlorella HCMR

Table 3.5 reports the mass yield, energy and carbon recovery from the three tests carried out on the microalgae biomass.

Table 3.5: Mass yield, energy and carbon recovery in bio-oil from microalgae feedstock.

Parameter		Chlorella IP	Chlorella HCMR	Nannochl. HCMR
<i>Mass balance - IN</i>				
feedstock	kg	1200	1030	1037
AF ^a mass	kg	974.4	974.4	974.4
C mass	kg	516.2	465.5	481.0
<i>Mass balance - OUT</i>				
pyrolysis liquid	kg	404	350.9	396
AF pyrolysis liquid	kg	402.9	349.8	392.7
oil	kg	228.0	256.0	237.3
aqueous phase	kg	168	94.9	105.2
<i>Yield</i>				
pyrolysis liquid	% feed	33.7	34.1	38.6
pyrolysis liquid	% on AF feed	41.5	40.3	45.3
oil	% on AF feed	23.9	29.4	31.4
aqueous phase	% on AF feed	17.6	10.9	13.9
<i>Nitrogen</i>				
total N in liquids	% feed	35.9	30.8	38.1
<i>Energy recovery</i>				
oil	% on HHV	31.7	32.9	34.8
aqueous phase	% on HHV	3.4	2.7	3.4
<i>Carbon recovery</i>				
oil	% on C feed	24.5	30.9	32.7
aqueous phase	% on C feed	3.5	2.6	3.4

^a: AF = ash-free (= water + organic matter).

Compared to lignocellulosic feedstock, microalgae biomass contains ash more than 10 times in excess. Hence in considering the mass yields of the pyrolysis process, distinction is made between *organic-to-organic* and *liquid-to-feed*; the former is the ratio between organic matter, i.e. the total mass excluding ash, in the recovered pyrolysis liquid (oil or water phases) to the organic matter in the feed, the latter is the ratio of the recovered mass of bio-oil to the total mass of the feed. The distinction is made because (1) in pyrolysis, the ash content of the feed is concentrated in the solid fraction of the products; (2) the amount of ash in the feed is relevant, but does not produce the liquid pyrolysis product. It is therefore necessary to exclude this term from the computation of the process yields.

In terms of *liquid-to-feed* yield, the results obtained in the CREAR/RE-CORD system at 450°C are in the range 33.7 - 38.6 %wt; if we consider the organic matter, the yields obtained are substantially higher, in the range 40.3 - 45.3 %wt, roughly divided in 1/3rd bio-oil (organic phase), 2/3rd aqueous phase.

In terms of energy recovery, between 31.7 and 34.8 % of the calorific content of the feed is recovered in the bio-oil, while the energy content of the aqueous phase is always \approx 1 order of magnitude less, i.e. around 2.7 - 3.4 % of feedstock HHV.

Finally, the elemental carbon recovered in the pyrolysis liquid follows very closely the energy content of the two phases: between 24.5 and 32.7% of the feed's C content is retained in the bio-oil, while between 2.6 and 3.5% in the aqueous phase.

3.2.3 Bio-oil characterization

The bio-oils from the three microalgae species were collected and analysed in the laboratory according to the methodologies described in Appendix A. The analyses on both bio-oil and aqueous phases are reported in Table 3.6 and Table 3.7.

Microalgae are very rich in nitrogen, and their pyrolysis liquids as well. N concentration resulted to be similar in both phases of all the three species, between 5.6-7.3 % wt in bio-oils and 5-8.1 %wt in aqueous phases; considering the N content of pyrolysis liquids and mass yields, the N retention in liquid products was calculated. It resulted that 35.9% of the nitrogen content of the feedstock is retained in liquid products during the pyrolysis of freshwater chlorella, 30.8% in marine chlorella and 38.1% in nanochloropsis. Considering that process temperatures are low (<550°C) and there are no oxidative reactions taking place inside the pyrolysis unit, it is quite unlikely that some of the nitrogen of the feedstock could migrate in the gas phase; this implies that most of the nitrogen content (around 60-70%) of the microalgae is concentrated in the pyrolytic char. Figure 3.3 reports the comparison between nitrogen content of bio-oils and feedstock.

All the collected bio-oils exhibited a high energetic content, respectively 29.8, 27.1 and 28.2 MJ·kg⁻¹ for chlorella IP, chlorella HCMR and nanochloropsis HCMR. These values are substantially higher than the corresponding HHV of lignocellulosic

bio-oils, i.e. 17-20 MJ·kg⁻¹. In Figure 3.4, the measured HHV of bio-oils are plotted against the lipid content of the intact feedstock. It can be seen that under the same process conditions, higher measured calorific values of the bio-oil correspond to higher lipid content of the intact feedstock.

Table 3.6: Chemical analysis of the bio-oil from microalgae pyrolysis.

Parameter		Chlorella IP	Chlorella HCMR	Nannochl. HCMR
<i>Elemental analysis</i>				
C	%wt	54.4	56.2	57.3
H	%wt	9.6	10	9.8
N	%wt	7.3	7	5.6
O ^a	%wt	28.5	26.3	26
S	%wt	0.2	0.2	0.2
P	%wt	-	0.00074	0.0017
<i>Fuel analysis</i>				
water	%wt	17.9	22.2	19.3
pH		9.6	9.36	8.9
solid content	%wt	1.6	1.56	4.32
ash	%wt	0.45	0.4	1.14
HHV	%wt ad	29.8	27.1	28.2
LHV ^b	%wt	27.8	25	26.1
CCR	%wt	9.3	6.01	9.8
density	g·cm ⁻³	≈1	≈1	≈1
viscosity	@ 40°C	cSt	43.2	50.76
	@ 50°C	cSt	30.6	
	@ 60°C	cSt	19.1	20.8

^a: by difference

^b: calculated

The viscosity of both water and organic-rich phases for all the three bio-oil samples was measured at several temperatures and results are reported in Figure 3.5 and Figure 3.6. Apart from nannochloropsis HCMR's organic phase, which exhibited a very high viscosity and could not be measured until attaining 60°C, all the samples tested showed a reduction in measured viscosity at increasing temperature. Bio-oil from chlorella IP had the lowest viscosity among samples (43.2 cSt at 40°C), viscosity of chlorella HCMR was higher (50.8 cSt at 40°C), while nannochloropsis featured the highest viscosity.

Table 3.7: Chemical analysis of the aqueous phase from microalgae pyrolysis.

Parameter		Chlorella IP	Chlorella HCMR	Nannochl. HCMR
<i>Elemental analysis</i>				
C	%wt	10.6	12.6	13.6
H	%wt	9.8	10.1	10.1
N	%wt	5.7	8.1	5
O ^a	%wt	73.9	69.2	71.1
S	%wt	0	0.1	0.1
P	%wt	nd	nd	nd
<i>Fuel analysis</i>				
water	%wt	80.4	nd	nd
pH		9.5	9.25	9
solid content	%wt	0.001	0.013	0.007
ash	%wt	0.05	0.05	0.15
HHV	%wt ad	4.4	6.1	6.2
LHV ^b	%wt ad	2.3	3.9	4
CCR	%wt	1.37	2.64	3.4
density	$g \cdot cm^{-3}$	1.05	1.1	1.1
viscosity	@ 40°C	cSt	1.56	2.04
	@ 50°C	cSt	1.08	1.44
	@ 60°C	cSt	1.05	0.96

^a: by difference

^b: calculated

A very peculiar characteristic of pyrolysis liquids from microalgae is their pH, that for all samples resulted to be pretty high, i.e. basic; the measured values of both phases of all samples was in the range 9-9.5 for aqueous phases and 8.9-9.6 for bio-oils. To draw a comparison, the corresponding values measured for the mixed wood chips samples reported in the previous chapter were in the range 2.3-2.9 for aqueous phases and 2.5-2.6 for bio-oils.

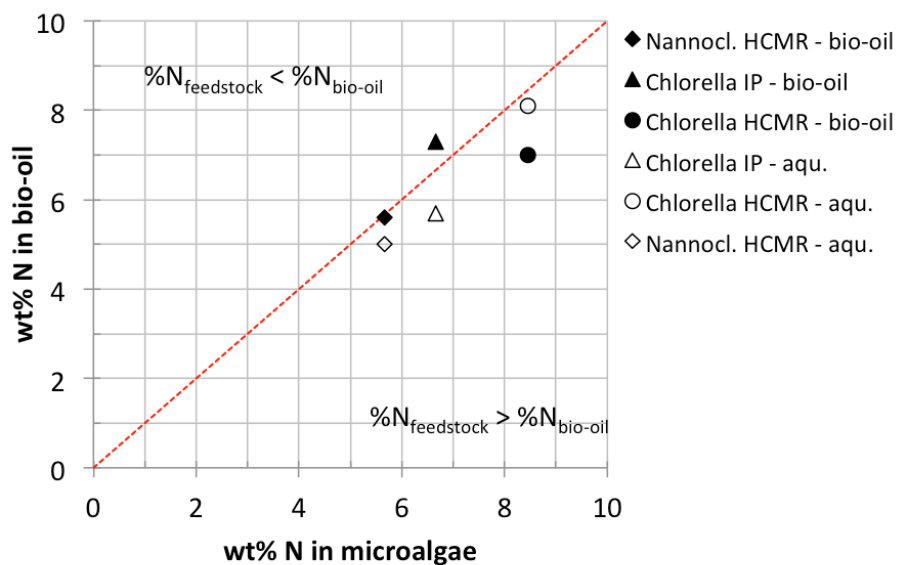


Figure 3.3: Nitrogen content of pyrolysis liquids vs. feedstock.

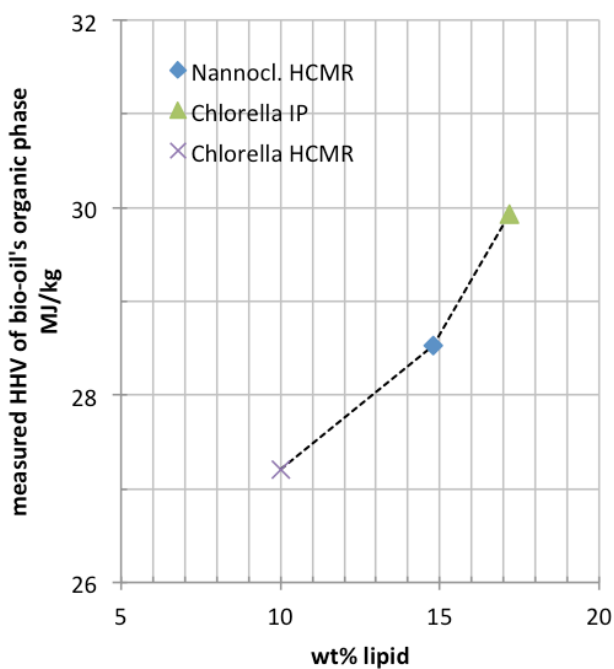


Figure 3.4: Measured HHV of bio-oils' organic phase vs. lipid content of original feed.

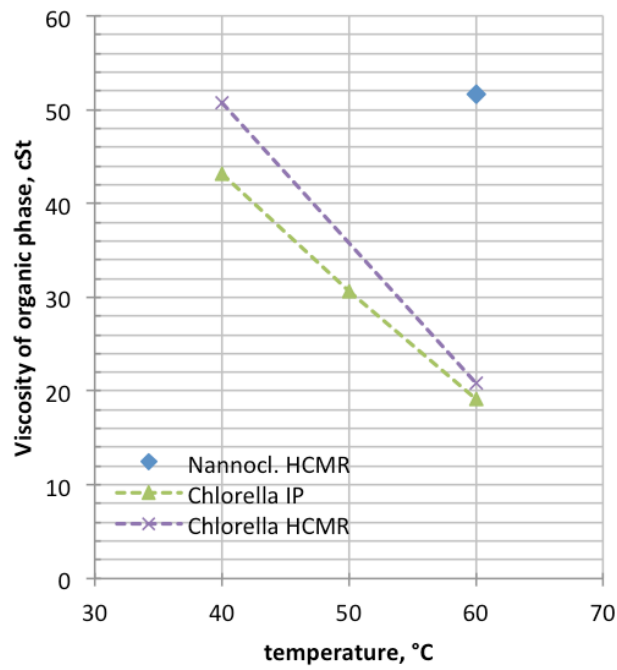


Figure 3.5: Viscosity of organic phase of bio-oils vs. temperature.

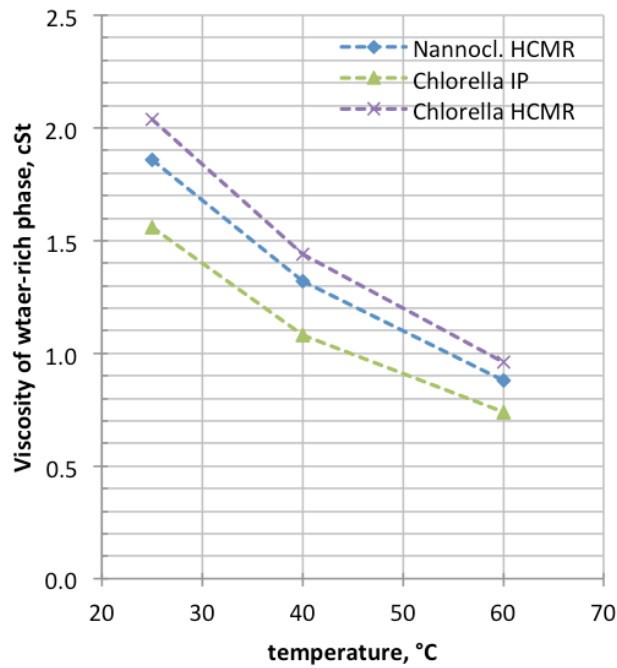


Figure 3.6: Viscosity of water-rich phase of bio-oils vs. temperature.

3.2.4 GC-MS analyses of bio-oils

A series of qualitative analyses in GC-MS were carried out on the organic and water-rich phases of bio-oils to identify the main constituents and draw a qualitative comparison of their relative abundance in the three bio-oils and aqueous samples, according to the procedure described in Appendix A.

Each chromatogram of each sample showed a large amount of peaks, both for organic phase and water-rich phase, but only a fraction (around 75%) could be identified with a reasonably high confidence due to the complexity of chromatograms, with frequently overlapping peaks. The identified molecules were grouped in hydrocarbons, nitrogen-containing compounds (ex. nitriles), aromatic hydrocarbons, others, nitriles, phenolics, BTEX, Free Fatty Acids (FFA), internal standard + unidentified. Compounds classified in *others* were mainly oxygenated compounds like alcohols or sterols, but some ketones, esters and aldehydes were also found.

Between 80 and 113 components could be identified in bio-oil samples, the two most numerous groups being hydrocarbons and nitrogen-compounds, while the number of compounds identified in aqueous phases was in the range 35-59, the most abundant group being nitrogen-compounds.

Figure 3.7 represents the area of each of the abovementioned group for each bio-oil. It can be noticed that the amount of phenolic compounds found in chlorella IP was almost triple than those measured for nanochloropsis and chlorella HCMR; moreover, chlorella IP showed the highest content of nitrogen compounds, nitriles, and aromatic hydrocarbons compared to the other bio-oils: this may suggest that cyclization of *Chlorella Ingrepro* algal cells during pyrolysis was more efficient than for other algal feedstock. FFA content of chlorella IP was negligible, while nanochloropsis HCMR content in FFA was twice that measured for chlorella HCMR. Chlorella HCMR, instead, had the largest amount of BTEX and hydrocarbons.

For each species, GC/MS outputs are reported in the Appendix B along with chromatograms of both phases.

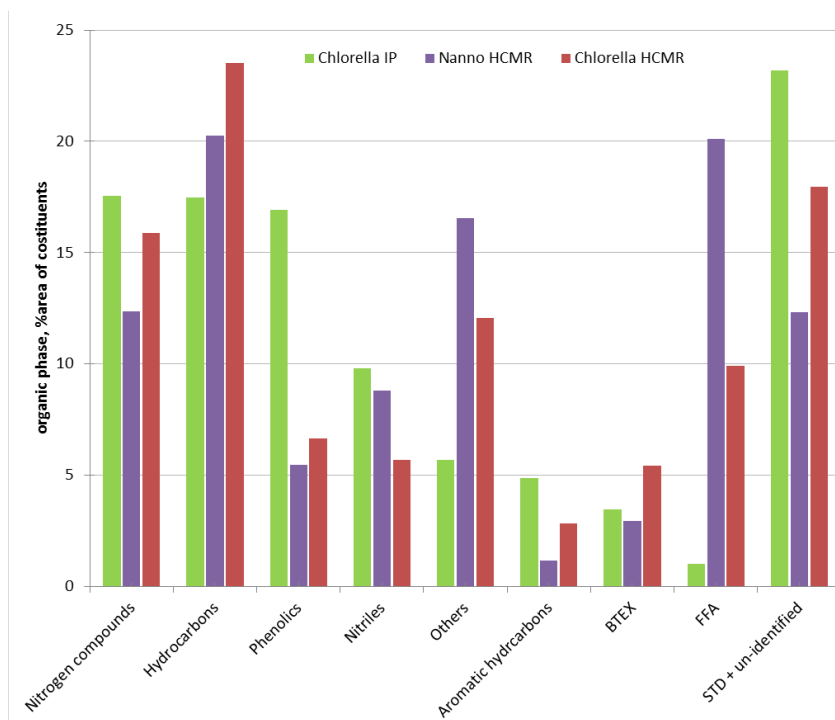


Figure 3.7: Relative distribution of compounds, grouped by classes, for the organic phases of the three bio-oil samples.

3.3 Material compatibility test of bio-oil samples

Material compatibility is of primary importance in engineering practice, because of its impacts on safety, operability and reliability of a machine. Bio-oil, due to its changing and aggressive nature, poses several challenges to process engineers because of the few published data set on material compatibility tests, the strong dependence of oil quality on the specific production process and the less developed standardization when compared to competing fossil fuels.

In organized and industrialized countries, norms and standards on product quality impact on the possibility of penetrating the market, being publicly traded locally or exported to foreign countries, not to mention quality assurance and quality management, traceability of test results and repeatability and reproducibility of test methods, or health, safety and environmental aspects (HSE). Pyrolysis oil is a relatively recent fuel and all these challenges have been only partially addressed and solved, as clearly pointed out by Oasmaa and Elliott [137]. In the EU, for example, a major source of concern for pyrolysis oil production and trading is the enforcement of the Regulation (EC) 1907/2006, entered into force on June 1st, 2007 and dealing with the Registration, Evaluation, Authorisation and Restriction of Chemicals (REACH). The regulation applies to substances manufactured or imported to the EU in annual quantities of one tonne or more per company, unless the regulation indicates otherwise. REACH requires that chemical substances on their own, in preparations and those that are intentionally released from articles, have to be registered to the European Chemicals Agency (ECHA). The chemicals currently on the EU market, which meet the definition of phase-in substances, were to be preregistered before December 1, 2008. A SIEF (Substance Information Exchange Forum) will be formed for each preregistered substance with the same identity. SIEF members need to nominate a "Lead Registrant". They will share and assess data and prepare common parts of the registration (joint submission). Compensation for sharing data is agreed among the respective SIEF members. A north European private initiative (FPBO REACH consortium) was established in January 2013 for registration of pyrolysis oils under

REACH, which was filed in November 2013 with the ECHA by the Lead Registrant; the agreed definition of the oil was: “*Liquid condensate recovered by thermal treatment of lignocellulosic biomass, at short hot vapour residence time (typically less than about 10 seconds) typically at between 450-600 °C at near atmospheric pressure or below, in the absence of oxygen*”. A CAS number (1207435-39-9) was also granted under the Public Name “Fast Pyrolysis Bio-Oil”; this registration adds to the already registered “wood, hydrolysed” (EC number 302-678-6, CAS number 94114-43-9), which was filed as a result of the EU project BIOTOX in 2005 [138].

The interest in providing the scientific community with valuable methodologies for the analysis of pyrolysis oil dates back to the ‘80s-‘90s, with the work of Elliott [139] Rick & Vix [140], Peacocke [141] and Oasmaa [142] and Meier [143]. This initiated the monumental work, done in the following years at VTT and in many other research centres, in the area of analytical determinations of pyrolysis oil properties.

With respect to norms and standards, in recent years the efforts from international research institutes (VTT, PNNL, TI), the IEA Bioenergy Task 34 and pyrolysis oil producers involved in technical committees of international standard organization, like ASTM and CEN, led to the achievement of valuable progress. In 2009 a first version of ASTM D7544 “Standard specification for pyrolysis liquid biofuel” was published, indicating the quality specification of a pyrolysis oil to be used in *industrial combustion equipment* and a set of norms for measurement of basic properties. The third version of the norm, published in 2012, was extended in its scope to cover “*grades of pyrolysis liquid biofuel produced from biomass intended for use in various types of fuel-burning equipment under various climatic and operating conditions*”; not meant to include residential heaters, engines, or marine applications yet, the norm defines two grades of pyrolysis oil, D and G, differing only in their maximum allowed contents of pyrolysis solids and ash. Requirement for grade D and G pyrolysis oil according to ASTM D7599 are reported in Table 3.8.

As can be noticed, Grade G and D only differ in their maximum allowed solid and ash contents, which are expected to impact the operation of small scale boilers, where

limited processing of the fuel, e.g. fine filtering, is desired and smaller nozzle passages could be affected by high solid content.

Table 3.8: ASTM Requirements for pyrolysis liquid biofuels [144].

Property		ASTM Test Method	Grade G	Grade D
Gross Heat of Combustion	$MJ \cdot kg^{-1}$, min	D240	15	
Water Content	% wt, max	E203	30	
Pyrolysis Solids Content	% wt, max	D7579	2.5	0.25
Kinematic Viscosity @ 40°C	$mm^2 \cdot s^{-1}$, max	D445 ¹	125	
Density at 20°C	$kg \cdot dm^{-3}$	D4052	1.1–1.3	
Sulphur Content	% wt, max	D4294	0.05	
Ash Content	% wt, max	D482	0.25	0.15
pH		E70	Report	
Flash Point	°C, min	D93, Procedure B	45	
Pour Point	°C, max	D97	–9	

¹: without filtering

Discussions are ongoing at CEN level in the EU, where Technical Committee 19, Working Group 41, which includes a working group chairman and secretary, as well as expert members from pyrolysis oil producers company, burner manufacturers and research institutions, is currently developing standards for fast pyrolysis oils in response to EC mandate M/525 (2013). Three standards will be developed for replacement of heavy fuel oil, light fuel oil and for use of bio-oils in stationary combustion engines. Later, two further technical specifications may also be introduced for use of fast pyrolysis oils as gasification feedstock and for mineral oil refinery co-processing, as and when required.

The present chapter reports on the results of material compatibility tests carried out on selected metallic (n.4) and elastomeric samples (n.3), representative of materials routinely adopted in process industry, with two distinct pyrolysis oil samples, one from pine chips, the other from microalgae. Though the data set is not extensive, to our best knowledge, it is the first time that a preliminary material compatibility test is carried out with bio-oil from pyrolysis of microalgae and results compared to an almost commercial sample of pyrolysis oil from pine chips.

3.3.1 Test procedure

Bio-oil from microalgae is a relatively new substance, and therefore there is a lack of information about its properties and compatibility with existing materials. In order to identify which materials could be safely used with bio-oil from microalgae, a screening test was performed on four metallic specimens of industrial grade alloys (AISI 304 and 316L, aluminium and copper) and three elastomers (silicone, VITON and NBR) commonly used in process engineering.

VITON is a fluoropolymer elastomer commonly used as sealing and material for o-rings, with good thermal and chemical resistance between -20 and +200°C to oils, aliphatic hydrocarbons, hydraulic fluids, fuels; silicone is a polymer of siloxane, frequently used in food handling for its compatibility with vegetable and animal fats and oils, water, diluted saline solutions, between -60 and 200°C; NBR (nitrile butadiene rubber) is a synthetic rubber copolymer of acrylonitrile and butadiene; it can withstand contact with mineral oil and grease, water and fuels between -30 to 120°C.

The test procedure was designed to assess the extent of weight change, either loss or uptake, of a technical material after prolonged submersion in a bath of bio-oil held at constant temperature; since a specific test for pyrolysis oils still does not exist, the experimental procedure that was developed mimics the basic layout and prescriptions of the copper strip corrosion test for petroleum products (UNI 20035 and ASTM D130) and previous work by Fuleki [145], Darmstadt [146], Zhiru [147], Kirk [148] and Hu [149]. Though tests like ASTM D130 or ASTM D665A were designed for petroleum fuels, are empirically based and bear little significance to the corrosion potential of pyrolysis liquids, as pointed out by Oasmaa and co-worker [27], they still provide valuable insights and visual information on the macroscopic behaviour of bio-oil compatibility and most of the aforementioned Authors retained the same approach. The observation especially applies to elastomers, since in a real application these are, most of the time, in a sort of static contact with the fluid and less subjected to physical attack (e.g. erosion by entrained particles).

When possible, thin metal specimens were used to maximize the surface area exposed to corrosion attack for copper and stainless steel; unfortunately it was not

possible to source a thin aluminium specimen, whose thickness was eventually around 2 mm. O-ring diameter was around 2 cm for all samples. Prior to the tests, o-rings were cleaned with demineralized water and dried; the surface of the metal strips was cleaned with abrasive paper (grade 60) until the surface looked homogeneous and no impurities could be visually identified. A second polishing was then performed on the specimen with a grade 120 abrasive paper and finally wiped with methanol-impregnated cotton. Glass vials filled with bio-oil were used to host the specimens, which were fully covered at all times during the test; vials were placed up-right in two larger glass containers filled with water acting as thermostatic bath, and kept at a constant temperature of 80°C. At specific intervals (48 and 72 hours) the samples were removed from the bio-oil and gently cleaned by hand wiping with cotton and methanol, to remove any traces of bio-oil and loose surface debris. After methanol evaporation, the samples were weighed with an analytical balance to ± 0.1 mg and returned to the vials until the next weight measurement. Due to the difference in diameter between o-rings and vial, elastomers were deformed to enter the vials; this allowed understanding to what extent the specimen could recover its shape after the test. The test rig for this essay is depicted in Figure 3.8, while results are shown in Figure 3.9 and Figure 3.12.



Figure 3.8: Experimental setup for material compatibility testing of bio-oils.

3.3.2 Bio-oil samples

Two different bio-oil samples were used for the material compatibility tests, one from lignocellulosic material and one from microalgae. The lignocellulosic bio-oil sample was produced by Biomass Technology Group (The Netherlands) in their rotating cone reactor, operated at a nominal temperature of 450°C; bio-oil from microalgae was produced in the CREAR/RE-CORD intermediate pyrolysis reactor.

Table 3.9: Chemical analysis of feedstock.

Parameter		Freshwater <i>Chlorella</i>	Pine chips
Carbon	%wt dry	46.1	49.3
Hydrogen	%wt dry	6.1	6.3
Nitrogen	%wt dry	6.7	0.01
Sulphur	%wt dry	0.4	<0.01
Oxygen ^a	%wt dry	19.1	44.1
Phosphorous	%wt dry	1.6	-
O/C	-	0.41	0.89
H/C	-	0.13	0.13
HHV	daf, MJ·kg ⁻¹	24.9	19.5

^a: by difference

The reactor was operated at the temperature of 450°C and the feedstock was a batch of dried freshwater *Chlorella* supplied by Ingrepro BV (The Netherland); characterization of feedstock and bio-oils used for the material compatibility test are reported in Table 3.9 and Table 3.10 respectively.

The two oils largely differ in their chemical and physical properties. In terms of elemental composition, the bio-oil from microalgae is higher in carbon, hydrogen, nitrogen and sulphur and lower in oxygen, compared to pine chips bio-oil. This reflects in a calorific value that is +70% higher on mass basis. On the contrary, the former has lower density compared to the latter. While pine chips bio-oil is acid (pH 2.3), microalgae bio-oil is basic (pH 9.6) and is lower in water.

Table 3.10: Chemical analysis of BTG and microalgae bio-oils.

Determination		Microalgae	BTG
		bio-oil	Bio- oil
		Chlorella	pine chips
<i>Elemental analysis</i>			
Carbon	% wt	54.4 ± 1.7	38.9 ± 0.4
Hydrogen	% wt	9.6 ± 0.2	7.4 ± 0.06
Nitrogen	% wt	7.3 ± 0.3	<0.01
Sulphur	% wt	0.2 ± 0.0	<0.01
Oxygen ^a	% wt	28.2 ± 2.1	53.7 ± 0.5
O/C	-	0.52	1.38
H/C	-	0.18	0.19
Ash	% wt	0.45	0.06
Water content	% wt	17.9 ± 0.8	22.5 ± 0.3
HHV	MJ·kg ⁻¹	29.8 ± 0.8	17.4 ± 0.2
density	kg·dm ⁻³	≈1	1.1-1.2
viscosity @ 20°C	cSt	- ^b	65.1
viscosity @ 40°C	cSt	43.2	20
viscosity @ 50°C	cSt	30.6	
viscosity @ 60°C	cSt	19.1	
pH	-	9.6	2.3

^a: by difference

^b: viscosity was too high to be measured in our Ubbelohde viscosimeter with $k=0.3$

3.3.3 Results with elastomeric specimens

Weight change of elastomers after 48 and 72h of immersion in bio-oils from pine chips and microalgae are compared in Figure 3.9⁴. Elastomeric specimens were generally affected by the prolonged contact with both bio-oils at 80°C. Out of the three elastomers tested (VITON, NBR and silicone), only silicone exhibited acceptable performance and a limited weight uptake after 72 h of immersion in both bio-oils, showing a limited increase in weight, though some swelling and permanent shape modification could be identified (see picture (b) in Figure 3.10). Neither VITON nor NBR proved to be compatible with any of the two bio-oil samples; both specimens showed permanent deformation, extensive weight uptake, surface damages and, in the case of VITON, severe crumbling (see picture (a) in Figure 3.10 and Figure 3.11).

⁴ Error bars are not inserted in the graph because too small to be noticeable, since the measured increase in weight overwhelmed the resolution of the instrument (± 0.1 mg).

With pine chips bio-oil, by the end of the test silicone had increased its mass by +11%, with a limited change from the weight uptake measured at 48 h (+10%), VITON by +71% and NBR by +91%. Even in this case VITON suffered the most severe permanent deformations, while silicone shape change was less severe than with bio-oil from microalgae.

With microalgae bio-oil, at the end of the test silicone was +14% of the original mass and no weight change was observed between 48 and 72h, NBR increased its weight by +69%, VITON by +123%. Moreover, NBR and VITON continued to increase their weight between 48 to 72h. The most severe permanent deformation observed was with VITON, which became fragile and retained the shape it was forced to acquire to enter the vial. A less pronounced deformation effected silicone, which acquired an elliptical shape instead of its original.

While comparable data for elastomers' compatibility with bio-oil from microalgae could not be found being this a pretty novel fuel, results with bio-oil from pine chips confirm what is found in literature from other Authors. Zhiru [147] and Kirk found that elastomeric materials were much more susceptible to swelling, weight gain and change of surface properties. The attack on elastomeric materials was quite rapid with significant volume expansion seen within 24 hours. Viton, Buna-N and EPDM had volume changes up to 100% during a 10-day test [148]. However, Oasmaa reported that in spite of the weight and volume changes, Viton and EPDM have been used very successfully at VTT as sealing material in pyrolysis units. Once inserted, it seemed to have good sealing properties. It could become fragile, however, and had to be changed when opening the connection [26].

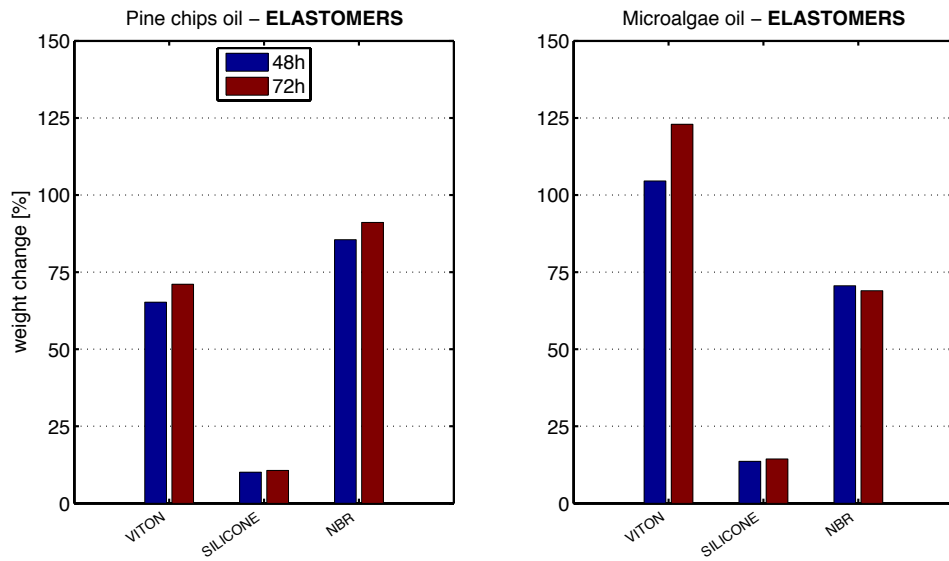


Figure 3.9: Weight change of metals after 48 and 72 hours of immersion at 80°C.

Surprisingly, it was not possible to find in literature other results of compatibility essay between silicone sealings and bio-oil, which however seemed to exhibit the best resistance to weight and volume change with both pine chips and microalgae bio-oils.

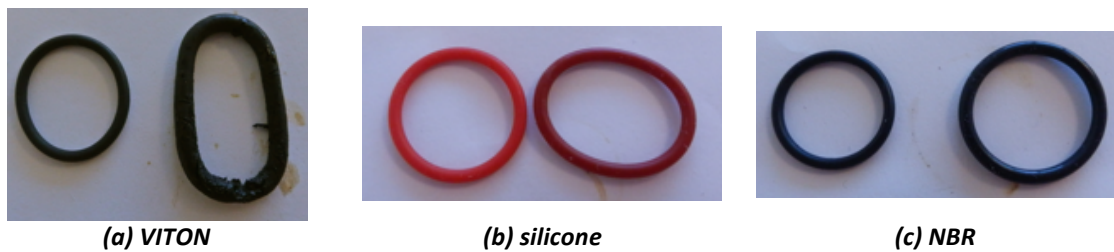


Figure 3.10: Elastomeric specimens before (left) and after (right) 72 h immersion at 80°C in the bio-oil from microalgae *Chlorella*.

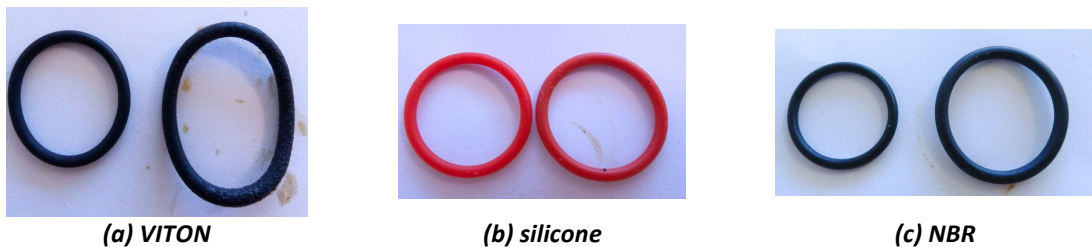


Figure 3.11: Elastomeric specimens before (left) and after (right) 72 h immersion at 80°C in the BTG bio-oil from pine chips.

3.3.4 Results with metallic specimens

Published data supports the finding that AISI 304 and 316L are tolerant to pyrolysis oil from lignocellulosic feedstock, copper can be corroded to a very small but noticeable extent, while aluminium is severely corroded. Darmstadt and co-workers noticed a slight increase in the weight of SS 316 specimens after 168 h at 80°C (+0.01%) in bio-oil from vacuum pyrolysis of bark residues; moreover, they noticed that also copper was to some extent corroded (-0.06%), and aluminium accounted for the most severe weight loss (-5%) [146]. Zhiru performed extensive degradation tests with metals (430, 304L, 316L, 20Mo4 and SS422) polymers (PTFE, HDPE and PP) and elastomers (SBR, NBR, HNBR, CSM, EPDM, FKM, TFE/P) in pyrolysis oil and blend at several temperature up to 80°C and for as long as 15 days. Among his findings, he showed that stainless steels 430, 304L, 316L and 20Mo4 (ferritic and austenitic families) were not corroded in pyrolysis oil and blended oil at 80°C. The resistance order was 20Mo4 > 304 > 316 > 430. An unusual corrosion behaviour was found associated with the glass bead separations for 430 and 316L and an anticrevice corrosion mechanism was shown. SS422 in Martensitic family was seriously corroded in all pyrolysis fuels [147]. Fuleki and co-workers carried out corrosion studies on aluminium, brass, mild steel and an austenitic stainless steel with bio-oil at several temperatures up to 70°C and up to 360 hours of duration. They found that mild steel and aluminium are highly susceptible to corrosion at any temperature and are not acceptable materials for bio-fuel applications. In addition, the formation and adherence of deposits observed on the mild steel would also negatively affect its operating characteristics and decrease its applicability. The weight change of brass and stainless steel in bio-fuel was relatively unaffected at any temperature. Both brass and austenitic stainless steel materials are acceptable for bio-fuel applications, though, they noticed, in real working conditions high pressure, continuous flow and longer duration might be of concern for these two metals [145].

Our test with pine chips pyrolysis oil at 80°C substantially confirms the aforementioned results for lignocellulosic feedstock. Aluminium suffered the most severe mass loss after 72h ($-1.29 \pm 0.07\%$), while copper mass loss was barely

noticeable ($-0.02 \pm 0.005\%$). For stainless steels 304 and 316L a slight uptake of weight was registered, $0.02 \pm 0.03\%$ and $+0.01 \pm 0.02\%$ respectively, but both figures were of the same order of magnitude of the measurement error to be negligible. In comparable conditions (70°C, 72 h), Fuleki measured the following weight changes for the metal specimens used in his tests: -2.5% for aluminium (AN-A-13 Alclad 24S-T), +0.004% for stainless steel (Shim stock #603-812, T302 cold-rolled), -0.01% for brass (Shim stock #603-510, R30T cold-rolled).

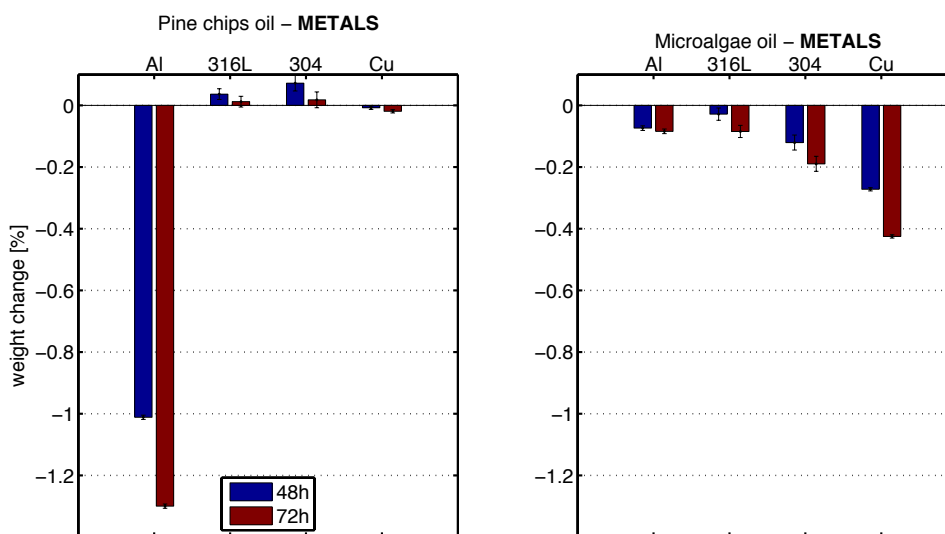


Figure 3.12: Weight change of metals after 48 and 72 hours of immersion at 80°C.

A very different and peculiar aggression pattern was noticed in our tests with the bio-oil from microalgae compared to the one from pine chips. Aluminium and stainless steel 316L specimens were not significantly affected by the contact with bio-oil from microalgae, as revealed by their weight change: $-0.084 \pm 0.007\%$ and $-0.08 \pm 0.02\%$ respectively. Conversely, 304 and especially copper specimens experienced more severe aggressions. 304's mass loss was assessed at $-0.19 \pm 0.02\%$, and copper weight change was $-0.425 \pm 0.005\%$.

In Figure 3.13 are shown the magnifications of the surfaces of both specimens after 72h in microalgae bio-oil (left, letters a,c) and pine chips bio-oil (right, letters b,d). The 304 specimen kept in microalgae bio-oil (a) had its surface attacked, with diffuse pitting, whereas no modifications of the surface could be found in the specimen kept in pine chips bio-oil (b). Conversely, the aluminium specimen kept in pine chips bio-oil

(d) presented a severe and distributed pitting, whereas the surface of the sample kept in microalgae bio-oil (c) was covered by a quite homogeneous layer of coating, which probably acted as a preservative to further chemical attack by the oil, as the weight change between 48 and 72h was limited. Slight tarnishing of the surface of 316L was observed in the specimen kept in microalgae bio-oil (e), compared to the almost intact one that was immersed in pine chips bio-oil.

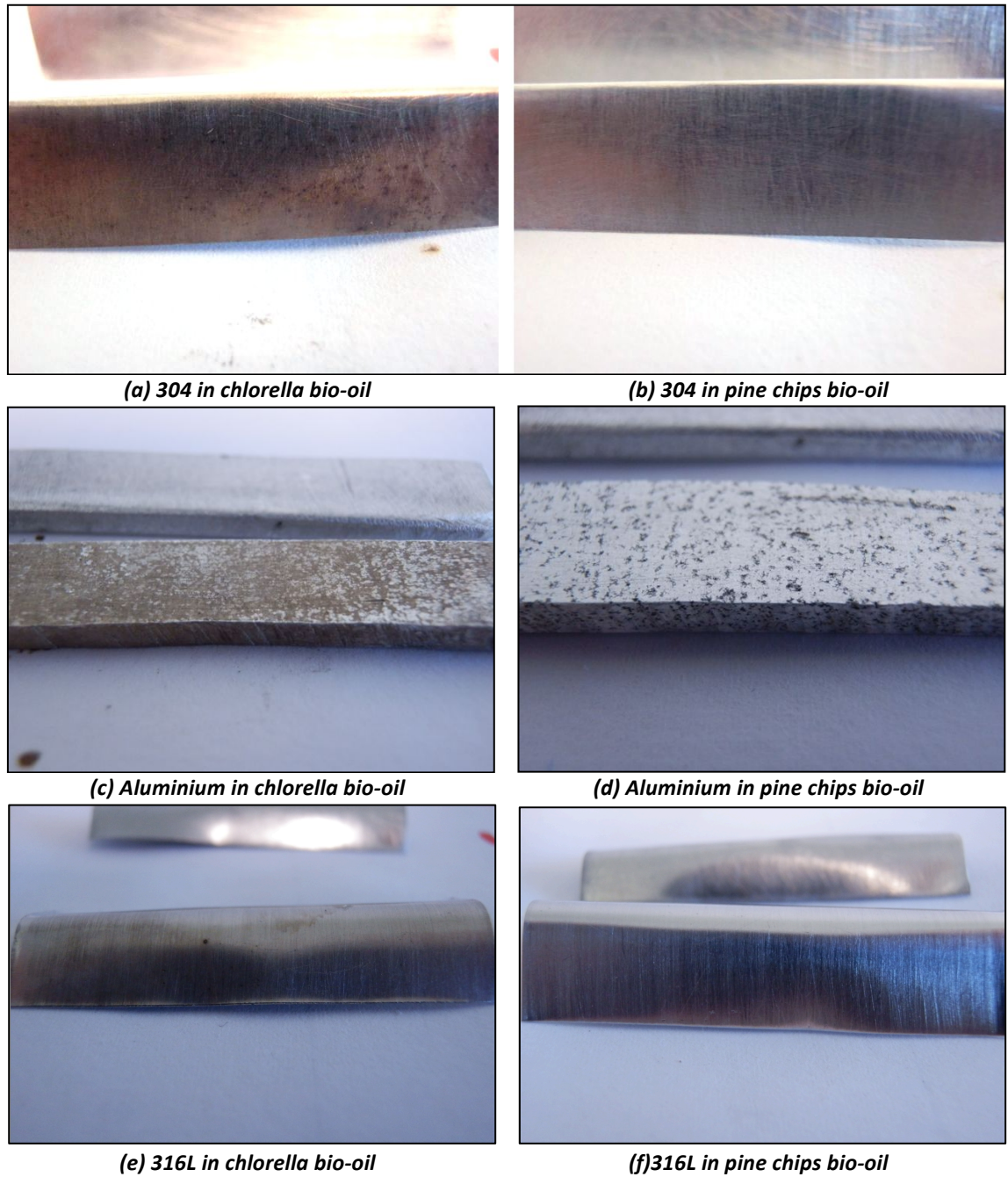


Figure 3.13: Selected metal specimens after 72 h immersion at 80°C in bio-oils.

4 Use of bio-oils in a modified micro gas turbine

As discussed in the chapter “Pyrolysis for fuel, energy and chemicals”, fast pyrolysis produces a liquid as an intermediate which could be potentially used in a wide variety of applications [47], has a more consistent quality compared to any solid biomass, can be used as an efficient energy carrier [10] and contains less inorganic compounds than the raw material, since these are retained in the solid residue during conversion. The handling and processing of liquid fuel has many advantages in comparison with processing solid or gaseous feed streams. Interest in the production of pyrolysis liquids from biomass has grown rapidly in recent years, due to the potential possibilities of de-coupling liquid fuel production from its utilization in scale, time, and location and producing a renewable fuel which could be used for heat and power generation in boilers, engines, and turbines [38]. Nonetheless, if it is clear that combustion of pyrolysis oil attained a reasonable technological maturity, and two major demonstration plants are unwinding in the EU (EMPYRO in The Netherlands and Valmet/Fortum in Finland) and expected to start production in 2015, power generation from pyrolysis oil in engines or turbines is still in its dawn, and to date the problems associated with the challenging chemical properties of pyrolysis oil, highlighted in the chapter “Material compatibility test of bio-oil samples” have been only partially solved [48,59].

This chapter discusses the experimental results obtained in a preliminary test campaign on a micro gas turbine fed with two different bio-oils, the first of biogenic origin, produced by Biomass Technology Group (The Netherlands) from pine chips in their fast pyrolysis demonstration plant, the second produced from the pyrolysis of scrap tires, a waste material. Firing tests were conducted in a dedicated biofuel test bench, which in previous studies was used to investigate the challenges associated with power generation from first and second generation biofuels on emissions at the exhaust [150–153]. The interested reader wishing to go into the matter more thoroughly is encouraged to refer to the suggested bibliography.

4.1 Description of the biofuel test bench

Here the rationale of the design choices worked out in the construction of the biofuels test bench is presented. The working principle of the system is described, major components are detailed along with their interconnections, and measuring instruments and data acquisition system are also discussed.

The bench is based on an overhauled micro gas turbine powering a military auxiliary power unit (APU) by AiResearch-Garrett Corporation, model GTP 30-67; the engine was acquired from Avon Aero Supply, Inc. (USA) after a preliminary selection phase. One of the main issues addressed as regards the engine selection was the design of the combustion chamber. The current trend in the design of micro gas turbines combustion chamber is to adopt annular combustors with multiple fuel injectors, or an annular arrangement of tubular combustors, each of them equipped with its own injector (the so called “tubo-annular layout”) [154]. These kinds of set-up are the outcomes of R&D efforts toward increased performance and effectiveness with lower pollutant emissions (CO, THC, NO_x, etc.), and the geometry of the system has been developed explicitly to accept fuels with very stringent requirements on quality and characteristics, since standardized fuels allow for an optimization of the combustion process.

Basically, the micro gas turbine test bench for biofuel testing is composed of the engine sub-assembly, multi-fuel line, control panel, AC generator, and resistive load bench. The engine sub-assembly drives the AC generator, which produces three-phase power that is converted to heat by the bank of resistors in the load bench; control panel provides basic functions to engine and generator, e.g. start-up and shut down, and allows monitoring relevant operating parameters like rotational speed and minimum oil pressure. Interconnection of sub-assemblies is reported in Figure 4.1.

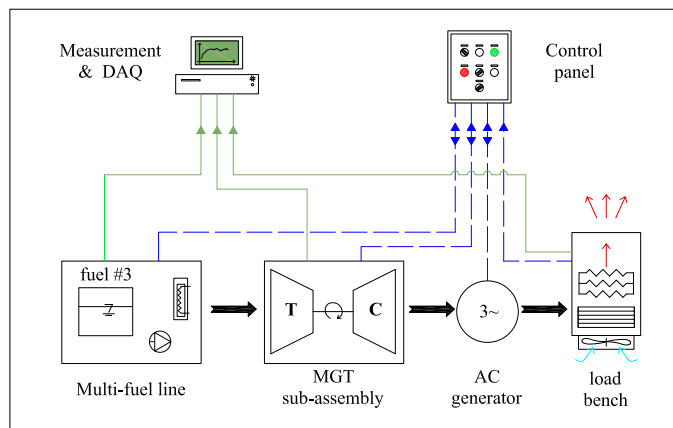


Figure 4.1: Layout of the interconnection of test bench basic sub-assemblies.

Measurements of pressure, temperature, actual power output, fuel flowrate and gas concentration in the exhaust stream (CO , CO_2 , O_2 , NO-NO_x , THC) are carried out on the test bench by independent instruments, while data logging is accomplished with National Instrument hardware and software. A schematic of the test bench with the position of measurement points is shown in Figure 4.2

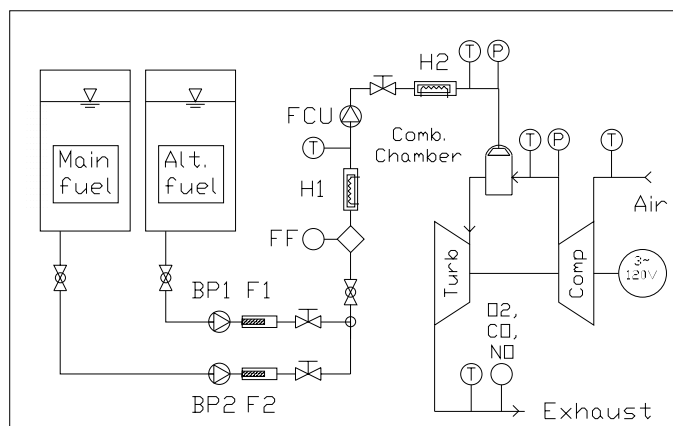


Figure 4.2: Schematic of the biofuel test bench and measurement points.

4.2 Turbine test of pine chips pyrolysis oil

Within the framework of the European FP7 project bioliquids-CHP, in 2010 a R&D project was started at the University of Florence for the adaptation of a micro gas turbine to pyrolysis oil. In a preliminary phase, the combustor of the unit was redesigned in order to achieve higher temperatures in the primary combustion zone. Details of the combustor re-design activities are given in the publication by Cappelletti et al. [56] from CREAR/University of Florence. The engine, equipped with the new combustor, was then tested with reference fuels (diesel and ethanol) to provide feedback for the design. Once measurement with reference fuels gave the expected results, testing of pure pyrolysis oil and a blend of ethanol/pyrolysis oil were tested. The pyrolysis oil used for designing and testing was a sample of fast pyrolysis oil produced by BTG from pine chips; analysis of the oil is reported in Table 3.10 on page 67.

4.2.1 Combustor redesign procedure

Combustor re-design was carried out in cooperation with the Computational Fluid Dynamics group at CREAR. Starting from the existing combustor, the new prototype was designed and then verified by means of RANS CFD modelling. The first activity was the CFD analysis of the original component operated with diesel fuel to understand its aerodynamic and thermal field, this task accompanied by a mono-dimensional investigation. In a later stage, two distinct CFD simulations with vegetable oil and a pseudo-pyrolysis oil (i.e. a model of the liquid with a chemical composition similar to that of the actual pyrolysis oil, but physical behaviour of an ordinary liquid) were performed to understand their effect on flame development during combustion. The final part of the activity was focused on the definition of the modifications on the combustor and to the verification of the new geometry by CFD analysis.

A mono-dimensional model was built to define some dimensionless numbers, which characterize the combustor.

A reverse engineering on the combustor's geometry was performed to obtain the solid model of the unit, this model was simplified to reduce the number of mesh elements and therefore the computational cost.

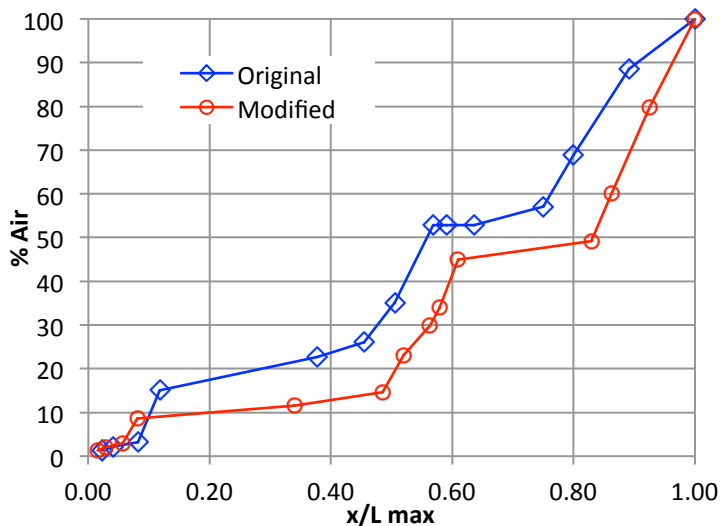


Figure 4.3: Cumulative area of air passages along the axial direction of the combustor.

An isothermal analysis was performed to understand the aerodynamics inside the combustor, which was used to investigate fuel evaporation and flame position.

After, combustion simulations were performed with diesel, vegetable oil and pseudo-pyrolysis oil, and results from post processing of these studies were used to improve the mono-dimensional model.



Figure 4.4: Original and modified reverse flow, silo combustor of the micro gas turbine.

With the support of the simplified model, some adjustments were defined with the aim to allow the development of a stable flame when feeding the unit with biofuels; in particular, these modifications were oriented to adjust the number and diameter of air passages for a better air distribution, and to lengthen the combustor in order to achieve longer residence time. In Figure 4.3 is reported the cumulative area of air passages along the axial direction of both the modified and original combustors. As can be seen from the analysis of the picture, air entrance into the combustor is moved from the primary and secondary zone to the dilution zone at the very end of the combustor. The picture of the original and modified combustor is shown in Figure 4.5

Table 4.1: Equivalence ratio (Φ) in the original and modified combustor at 20 and 12 kWe load.

Zone	Φ Original combustor		Φ Modified combustor	
	diesel Φ 20 kWe	diesel 12 kWe	bio-oil Φ 12 kWe	Bio-oil Φ 12 kWe
Primary	0.91	0.54	0.49	0.92
Secondary	0.42	0.25	0.23	0.51
Dilution	0.17	0.10	0.09	0.09

In Table 4.1 are reported the calculated equivalence ratios (Φ) at several loads for the new and original configurations with diesel and bio-oil. As it can be noticed, the modified combustor features a very high value of Φ in the primary and secondary zone compared to the original configuration (0.92 vs. 0.49 and 0.51 vs. 0.23 respectively). The basic idea was to increase the temperature near the fuel injector (primary zone) to ease the evaporation of bio-oil droplets, thus allowing a faster completion of the combustion process.

4.2.2 Firing test of new combustor with reference fuels

To experimentally validate the performance of the modified combustor of the micro gas turbine, the engine was fitted with the new combustor and run on diesel fuel and ethanol at varying loads while measuring, among others, the carbon monoxide and nitrogen oxides (NO_x) concentrations in the exhaust. Results of measurements are reported in Figure 4.5 for CO and Figure 4.6 for NO_x . Measured concentrations were

then compared with those corresponding to the same load level but with the engine equipped with the original combustor.

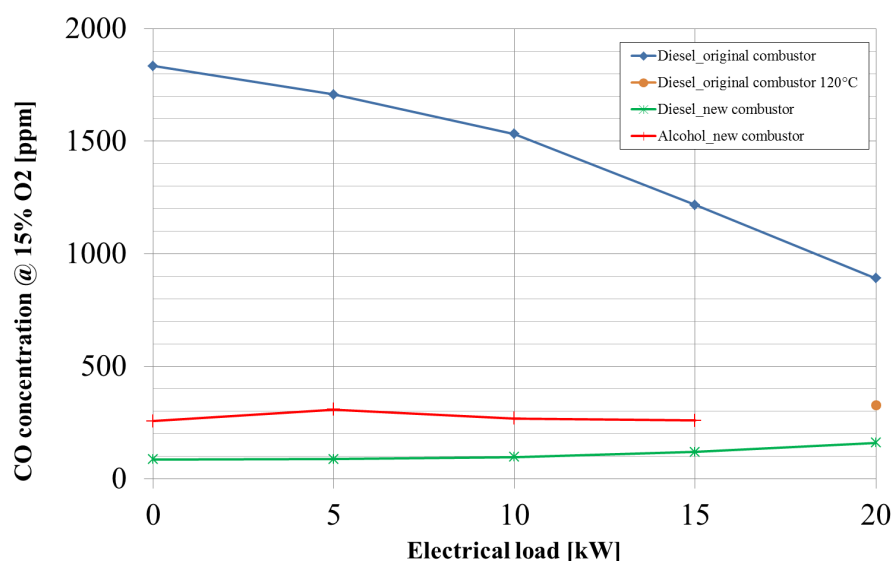


Figure 4.5: CO concentration @15 %vol oxygen in the exhaust for the original and modified combustor.

It was found that even without fuel preheating, the new combustor featured an impressive reduction in CO emissions, inverting the trend that was measured with the original combustor at increasing load; in particular, with the new combustor, emission of CO is almost constant on the whole load range between idle and 20 kW electric. Quite impressive, at 20 kW the new combustor fed with diesel featured an almost six-fold reduction of CO concentration, and even higher at partial load. This was the evidence of an increased flame temperature, which led to a better combustion of the diesel spray. With ethanol, CO concentration in the exhaust attained 2-3 times the corresponding level that it was measured when feeding the engine with diesel in the same (modified) combustor. This can be attributed to the high value of the latent heat of vaporization of ethanol, which reduces the average flame temperature.

NO_x concentration for the modified combustor confirmed the evidence of increased combustion temperature, since a significant increase in NO_x was observed at all loads with diesel fuel.

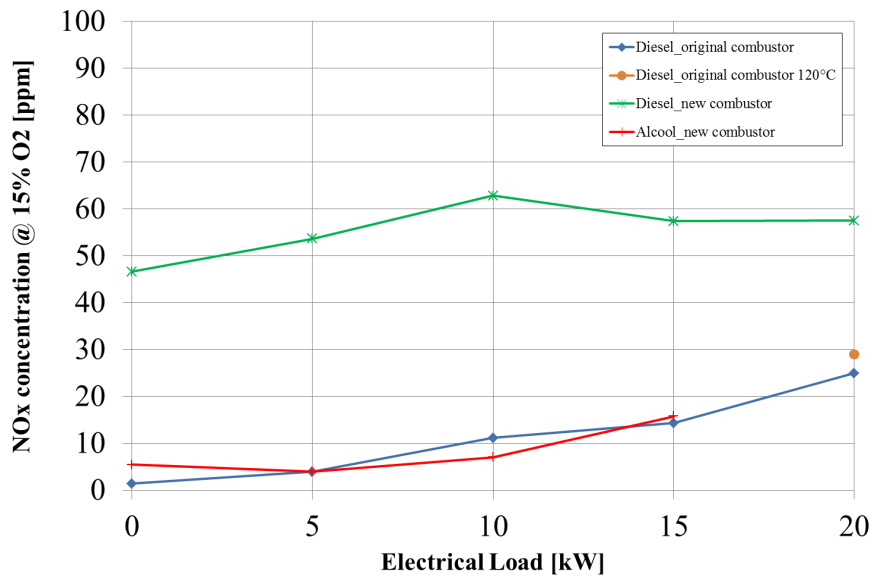


Figure 4.6: NOX concentration @15 %vol oxygen in the exhaust for the original and modified combustor.

4.2.3 Firing test of new combustor with bio-oil and bio-oil blends

Since pyrolysis oil is not miscible in diesel, a specific start up procedure was designed for pure pyrolysis oil. At first, the engine is started with diesel. Once stability is reached, the engine switches to ethanol, that is miscible with both diesel and pyrolysis oil. Once the first transition is completed, and the engine runs solely on ethanol, pyrolysis oil is gradually added until attaining 100%. To shutdown the micro gas turbine, the procedure is reversed.

After the positive results of the tests on the new combustor, several attempts were made to feed pyrolysis oil to the engine. At first, it was tried with pure pyrolysis oil, then with three blends of pyrolysis oil and ethanol with increasing amounts of ethanol (25 %wt, 50 %wt, 75 %wt). Unfortunately, stable operation of the engine was not achieved for any of the tested configurations; the longest run that was obtained was with the blend containing 75 %wt ethanol, and measurement of exhaust gas temperature and fuel flowrate are reported in Figure 4.7, while CO and NO_x concentrations are reported in Figure 4.8.

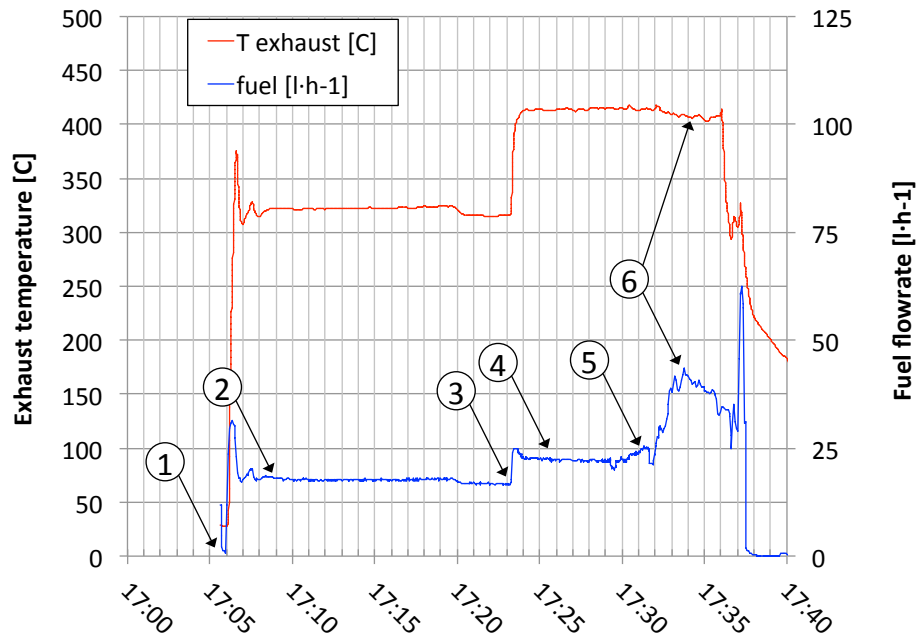


Figure 4.7: Exhaust temperature and fuel flowrate during the blend test (PO:Ethanol 25:75).

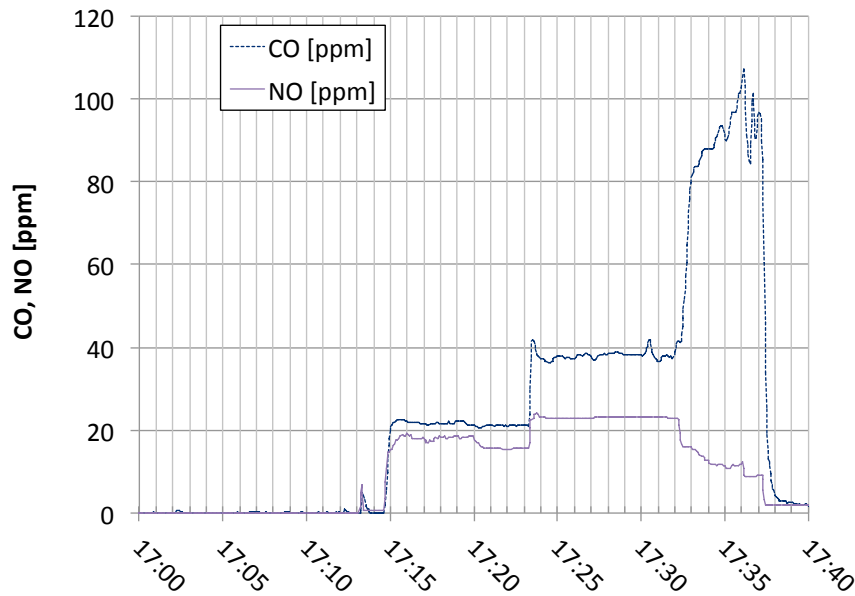


Figure 4.8: CO and NO concentration during the blend test (PO:Ethanol 25:75).

With reference to the numbered events of Figure 4.7, the test was started at around 17:05 (1) with diesel and the engine was let to warm up at 10 kWe (2). At around 17:15 the gas analyser was put on-stream. At 17:23 the load was increased to 15 kWe (3), to increase the combustion chamber temperature ahead of starting the fuel-switch procedure at 17:26 (4). At around 17:30 the blend started to be burned, and the flowrate was gradually increased to compensate for the decreased heating

value (5). At around 17:32 the blend flowrate exceeded $35 \text{ l}\cdot\text{h}^{-1}$, and three major effects could be observed: a sharp increase in CO concentration (from 40 to 80 ppm) indicating that the quality of combustion was worsening; NO concentration decreased around -20% and the temperature of the exhaust dropped around $10 \text{ }^\circ\text{C}$, both indicating that heat release was decreasing. At around 17:34 the rotational speed of the engine was decreasing and the flowrate was increased to compensate for the variation; flame instabilities started to develop and could be heard like small explosions; a sudden increase in rotational speed led to decrease the flowrate (6); however, it was not possible anymore to follow the variation of rotational speed, CO concentration at the exhaust increased again and reached around 110 ppm, when the rotational speed dropped, the flame extinguished and the engine stopped.

In Figure 4.9 are represented the fuel injector (left) and the flame tube exit (right) after the failed test with the 75 %wt ethanol blend. It can be noticed that a sticky, dark deposit was formed on the surfaces from the high temperature repolymerisations of un-burned bio-oil.



Figure 4.9: Fuel injector before and after the test (left), and flame tube exit after test (right).

4.3 Turbine test of scrap tire pyrolysis oil

4.3.1 Firing test of STPO

Here are presented the experimental results from a short duration test of pure STPO in a modified micro gas turbine, a Garrett AiResearch GTP 30-67 originated from an overhauled military APU unit. This work, to our best knowledge, is probably the first to use whole STPO oil in a real-size test bench.

Table 4.2: Chemical analysis of scrap tire pyrolysis oil.

Parameter		STPO	Diesel EN 590	reference norm or standard
<i>Elemental analysis</i>				
C	%wt	86.4	≈86	ASTM D5291
H	%wt	10.4	≈13	ASTM D5291
N	%wt	0.8	-	ASTM D5291
O	%wt	1.4	≈1 ^a	by difference
S	%wt	1.0	< 0.001	int. method
Solid content	%wt	0.6	-	int. method [26]
Water content	%wt	2.2	< 0.02	UNI 8534
HHV	$MJ \cdot kg^{-1}$	42.2		DIN 51900-2
LHV	$MJ \cdot kg^{-1}$	39.9		DIN 51900-2
Viscosity @40°C	cSt	4.2	2 - 4.5	UNI 3104
pH		5.2		-
Density	$g \cdot cm^3$	0.939	0.82 - 0.85	UNI 3675

^a: due to FAME content.

Results from the analysis of the STPO are reported in Table 4.2 along with relevant data for diesel fuel. Due to the limited amount of STPO that was made available (≈8 l) and considering the specification of the test bench, which has a minimum fuel consumption of 16 lh⁻¹ of diesel-equivalent at 20°C ambient temperature, the firing test was carried out at idle, i.e. with the engine running at nominal rotational speed, but without load, to allow for the longest possible run. Test conditions and timeline are reported in Table 4.3 and Table 4.4 respectively.

The engine was started with diesel and let to warm up for 15 min, until constant reading of the two main engine indicators, i.e. compressor delivery (T_{CD}) and exhaust temperature (T_E). Once the stationary operating condition was reached, the gas

analysis probe was inserted at the exhaust port and the system started gathering exhaust concentration data, i.e. CO, total unburned hydrocarbons (THC) and NO and total nitrogen oxides (NO_x). The sampling instrument was allowed to complete its transient phase and stable measurement was achieved at around h12:14:30.

Table 4.3: Test conditions for the STPO test in micro gas turbine.

Parameter	Value/set point
Nominal load	0 kW (idle)
Fuel preheating temperature (before injector, T _f)	50°C
Prevailing ambient temperature (T _A)	14.5 °C
Warm-up time	15 min
Preheating fuel	diesel

As per procedure with miscible fluids, co-feeding of STPO and diesel was initiated by opening the admission valve; the set point of the pump was then slowly adjusted to maintain a constant rotational speed of the engine and allow for a smooth transition between the two fluids. Co-feeding lasted around 3 minutes and by h12:19 was completed. From about h12:19 to h12:28 the microturbine was operated on 100% STPO and the only macroscopic observable variation in operating parameter was a slight increase of fuel flowrate, due to the reduced calorific content of the STPO compared to diesel. After h12:28 reverse co-feeding was initiated again and after 3 min the engine was running on diesel fuel until shut-down.

Table 4.4: Timeline of STPO test in micro gas turbine.

Event	Time (hh:mm:ss)
Measurement of gas concentration at the exhaust begins	12:13
Gas analyser reaches a steady state	12:14:30
Co-feeding of STPO and diesel starts	12:16:30
Co-feeding stops, 100% STPO feeding starts	12:19
Co-feeding starts, 100% STPO feeding stops	12:28
Co-feeding stops, 100% diesel feeding	12:31
End of test	12:34

In Figure 4.10 are reported the measured values of CO, NO_x and exhaust temperature (T_E) during the firing test. CO concentration in the exhaust when feeding STPO resulted pretty constant in the range of 25-35 ppm, the same attained with diesel fuel. It is noteworthy to observe that even during co-feeding of STPO and diesel

no statistically significant difference could be detected in the CO figure, indicating that both fuels behaved in a very similar fashion during combustion and that they can blend very well. Total unburned hydrocarbons were below detection level (0.01% vol) for the whole run, thus indicating that no adverse phenomenon were taking place in the combustion chamber. NO accounted for more than 98% of measured total NO_x; a remarkable increase in NO_x concentration in the exhaust was observed when switching from diesel to STPO and vice versa, moving from 23 ppm to 59 ppm, i.e. a +103% increase. Since no observable trend was observed on CO emission at the same time, such increment cannot be ascribed to any effect of STPO on firing temperature, but more realistically to the nitrogen content of the STPO (around 1%). Supporting this observation is that the exhaust temperature was not affected by the nature of the fuel.

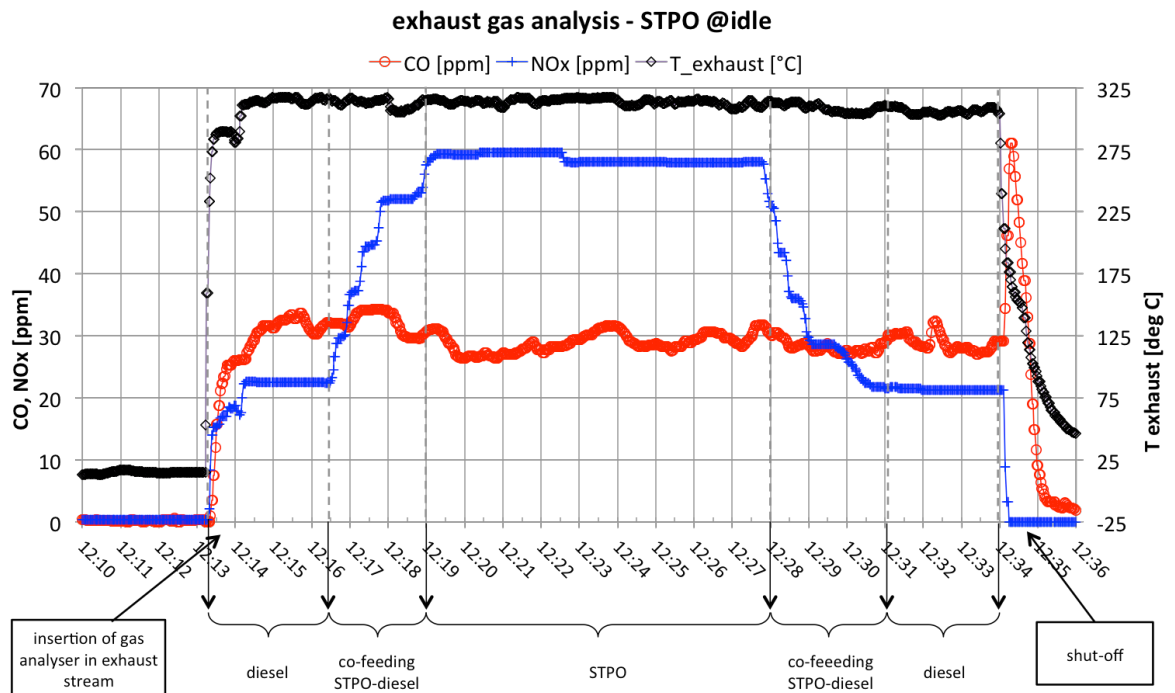


Figure 4.10: Extract of exhaust gas measurements during a STOP firing test.

5 Conclusions

Bio-oils from lignocellulosic biomasses and three distinct microalgae strains were produced in a pilot intermediate pyrolysis unit at several process conditions. By properly tuning the process conditions, with lignocellulosic biomass it was possible to obtain a bio-oil with valuable physical properties, though with low yield. Organic phase of the bio-oils from microalgae showed several very distinctive properties, such as low oxygen content, good calorific value, basic pH, intermediate viscosity, good mass yield. The aqueous phase was too rich in water and too low in calorific content to be used as a fuel-substitute and therefore should be evaluated for the recovery of nutrients or other chemicals. To the best of our knowledge, it was the first time that large amount of microalgae (around 7 kg) were processed to obtain a pyrolysis liquid.

Material compatibility tests have been carried out on 4 metallic and 3 elastomeric specimens with both a commercial bio-oil from pine chips and the bio-oil from freshwater chlorella (microalgae). Bio-oil from microalgae exhibited very distinct properties and aggressiveness pattern, and potential compatible and incompatible materials were identified.

The possibility to use pyrolysis oils from wood and scrap tires have been tested in a modified micro gas turbine and relevant gas concentration measurement carried out. The combustion chamber of the engine was modified to increase the combustion temperature in the primary and secondary zone and to increase the residence time, to allow for burning alternative fuels such as biodiesel and pyrolysis oil.

Scrap tire pyrolysis oil (STPO) was successfully fed to the micro gas turbine and exhibited interesting properties as fuel for energy generation; only minimal differences could be noticed in terms of NO_x concentration in the exhaust. The effect of increased NO_x was attributed to the presence of nitrogen in the liquid; no differences with diesel could be measured in terms of CO and unburned hydrocarbons concentrations. According to literature and to the best of our knowledge, STPO was tested for the first time in a real microturbine in relevant condition.

Pyrolysis oil from pine chips and blends of pyrolysis oil and ethanol were tested in the modified micro gas turbine. In spite of the modifications on the combustion chamber, test of pyrolysis oil from pine chips was not successful and the engine did not reach the expected stability even when fed with a blend of pyrolysis oil and ethanol up to 25%wt_{bio-oil} : 75%wt_{ethanol}.

6 References

- [1] Bridgwater A. V., and Peacocke G. V. ., 2000, "Fast pyrolysis processes for biomass," *Renew. Sustain. Energy Rev.*, **4**(1), pp. 1–73.
- [2] Kersten S., and Garcia-Perez M., 2013, "Recent developments in fast pyrolysis of ligno-cellulosic materials.," *Curr. Opin. Biotechnol.*, **24**(3), pp. 414–20.
- [3] Antal, Jr. M. J., Helsen L. M., Kouzu M., Lédé J., and Matsumura Y., 2014, "Rules of Thumb (Empirical Rules) for the Biomass Utilization by Thermochemical Conversion," *J. Japan Inst. Energy*, **93**(8), pp. 684–702.
- [4] Mohan D., Pittman C. U., and Steele P. H., 2006, "Pyrolysis of Wood/Biomass for Bio-oil: A Critical Review," *Energy & Fuels*, **20**(3), pp. 848–889.
- [5] Lédé J., and Authier O., 2011, "Characterization of biomass fast pyrolysis," *Biomass Convers. Biorefinery*, **1**(3), pp. 133–147.
- [6] Violette M., 1853, "Memoire sur les charbons de bois," *Ann Chim Phys*, **32**, p. 304.
- [7] Kammen D. M., and Lew D. J., 2005, Review of Technologies for the Production and Use of Charcoal.
- [8] Antal M. J., and Grønli M., 2003, "The Art, Science, and Technology of Charcoal Production," *Ind. Eng. Chem. Res.*, **42**, pp. 1619–1640.
- [9] Antal M. J., and Mok W. S. L., 1990, "Review of methods for improving the yield of charcoal from biomass," *Energy & Fuels*, **4**, pp. 221–225.
- [10] Bridgwater A. V., 2012, "Review of fast pyrolysis of biomass and product upgrading," *Biomass and Bioenergy*, **38**, pp. 68–94.
- [11] Shafizadeh F., and Chin Peter P S., 1977, "Thermal Deterioration of Wood," *Wood Technology: Chemical Aspects*, pp. 57–81.
- [12] Várhegyi G., Antal M. J., Jakab E., and Szabó P., 1997, "Kinetic modeling of biomass pyrolysis," *J. Anal. Appl. Pyrolysis*, **42**, pp. 73–87.
- [13] Venderbosch R. H., and Prins W., 2011, "Fast Pyrolysis," *Thermochemical Processing of Biomass: Conversion into Fuels, Chemicals and Power*, R.C. Brown, ed., John Wiley & Sons, Ltd.

- [14] Ripberger G. D., Kirwan C., Jones J. R., and Paterson A. H. J., 2014, "The Intricate Relationship between Vapour Phase Residence Time and Biochar/Biofuel Yield Properties," TCS Symposium, Denver, Colorado, September 2-5.
- [15] Colomba, and Blasi D., 2008, "Modeling chemical and physical processes of wood and biomass pyrolysis," *Prog. Energy Combust. Sci.*, **34**(1), pp. 47–90.
- [16] Grønli M. G., Várhegyi G., and Blasi C. Di, 2002, "Thermogravimetric Analysis and Devolatilization Kinetics of Wood," *Ind. Eng. Chem. Res.*, **41**(17), pp. 4201–4208.
- [17] Antal M. J. J., and Varhegyi G., 1995, "Cellulose Pyrolysis Kinetics: The Current State of Knowledge," *Ind. Eng. Chem. Res.*, **34**(3), pp. 703–717.
- [18] Biagini E., and Tognotti L., 2014, "A Generalized Procedure for the Devolatilization of Biomass Fuels Based on the Chemical Components," *Energy & Fuels*, **28**(1), pp. 614–623.
- [19] Mullen C. a., Boateng A. a., and Goldberg N. M., 2013, "Production of Deoxygenated Biomass Fast Pyrolysis Oils via Product Gas Recycling," *Energy & Fuels*, **27**(7), pp. 3867–3874.
- [20] Bridgwater A. V., 2011, "Upgrading Fast Pyrolysis Liquids," *Thermochemical Processing of Biomass: Conversion into Fuels, Chemicals and Power*, R. Brown, ed., John Wiley & Sons, Ltd.
- [21] Bridgewater A., 2004, "Biomass fast pyrolysis," *Therm. Sci.*, **8**, pp. 21–50.
- [22] Sipilä K., Kuoppala E., Fagnäs L., and Oasmaa A., 1998, "Characterization of biomass-based flash pyrolysis oils," *Biomass and Bioenergy*, **14**(2), pp. 103–113.
- [23] Vispute T., 2011, "Pyrolysis Oils: Characterization, Stability Analysis, and Catalytic Upgrading to Fuels and Chemicals."
- [24] Meier D., Beld B. van de, Bridgwater A. V., Elliott D. C., Oasmaa A., and Preto F., 2013, "State-of-the-art of fast pyrolysis in IEA bioenergy member countries," *Renew. Sustain. Energy Rev.*, **20**, pp. 619–641.
- [25] Demirbas A., 2004, "Effect of initial moisture content on the yields of oily products from pyrolysis of biomass," *J. Anal. Appl. Pyrolysis*, **71**(2), pp. 803–815.
- [26] Oasmaa A., and Peacocke C., 2010, "Properties and fuel use of biomass-derived fast pyrolysis liquids. A guide," *VTT Publ.*, **731**, p. 79 p. + app. 46 p.
- [27] Oasmaa A., and Peacocke C., 2010, *Properties and fuel use of biomass-derived fast pyrolysis liquids. A guide.*
- [28] Chiaramonti D., Bonini M., Fratini E., Tondi G., Gartner K., Bridgwater A. V., Grimm H. P., Soldaini I., Webster A., and Baglioni P., 2003, "Development of emulsions from biomass pyrolysis liquid and diesel and their use in engines— Part 1 : emulsion production," *Biomass and Bioenergy*, **25**(1), pp. 85–99.
- [29] Chiaramonti D., Bonini M., Fratini E., Tondi G., Gartner K., Bridgwater A. V., Grimm H. P., Soldaini I., Webster A., and Baglioni P., 2003, "Development of emulsions from biomass pyrolysis liquid and diesel and their use in engines— Part 2: tests in diesel engines," *Biomass and Bioenergy*, **25**(1), pp. 101–111.

- [30] Ikura M., 2003, "Emulsification of pyrolysis derived bio-oil in diesel fuel," *Biomass and Bioenergy*, **24**(3), pp. 221–232.
- [31] Calabria R., Chiariello F., and Massoli P., 2005, Emulsion of pyrolysis oil in diesel oil: tests in the drop tube furnace.
- [32] Qi G., Dong P., Wang H., and Tan H., 2008, "Study on Biomass Pyrolysis and Emulsions from Biomass Pyrolysis Oils and Diesel," 2008 2nd Int. Conf. Bioinforma. Biomed. Eng., pp. 4735–4737.
- [33] Daugaard D. E., and Brown R. C., 2003, "Enthalpy for Pyrolysis for Several Types of Biomass," *Energy & Fuels*, **17**(4), pp. 934–939.
- [34] Yang H., Kudo S., Kuo H.-P., Norinaga K., Mori A., Mašek O., and Hayashi J., 2013, "Estimation of Enthalpy of Bio-Oil Vapor and Heat Required for Pyrolysis of Biomass," *Energy & Fuels*, **27**(5), pp. 2675–2686.
- [35] Grierson S., Strezov V., Ellem G., McGregor R., and Herbertson J., 2009, "Thermal characterisation of microalgae under slow pyrolysis conditions," *J. Anal. Appl. Pyrolysis*, **85**(1-2), pp. 118–123.
- [36] Onarheim K., Solantausta Y., and Lehto J., 2014, "Integrated fast pyrolysis plant performance," TCS Symposium, Denver, Colorado, September 2-5.
- [37] Rogers J. G., and Brammer J. G., 2012, "Estimation of the production cost of fast pyrolysis bio-oil," *Biomass and Bioenergy*, **36**, pp. 208–217.
- [38] Venderbosch R., and Prins W., 2010, "Fast pyrolysis technology development," *Biofuels, Bioprod. Biorefining*, **4**(2), pp. 178–208.
- [39] Bridgwater A. V., 2013, "Fast Pyrolysis of Biomass for the Production of Liquids," *Biomass Combustion Science, Technology and Engineering*, L. Rosendahl, ed., Woodhead Publishing.
- [40] Ringer M., Putsche V., and Scahill J., 2006, Large-Scale Pyrolysis Oil Production: A Technology Assessment and Economic Analysis. NREL/TP-510-37779.
- [41] Peacocke G., Bridgwater A., and Brammer J., 2006, "Techno-economic assessment of power production from the Wellman and BTG fast pyrolysis process," *Thermal and Chemical Biomass Conversion*, B.A. and B. DGB, ed., CPL Press.
- [42] Lehto J., Oasmaa A., Solantausta Y., Kytö M., and Chiaramonti D., 2014, "Review of fuel oil quality and combustion of fast pyrolysis bio-oils from lignocellulosic biomass," *Appl. Energy*, **116**, pp. 178–190.
- [43] Sturzl R., 1997, The commercial co-firing of RTP bio-oil at the Manitowoc Public Utilities power generation station.
- [44] Wagenaar B., Venderbosch R., Prins W., and Penninks F., 2002, "Bio-oil as a coal substitute in a 600 MWe Power Station," 12th European Conference and technology Exhibition on Biomass for Energy, Industry and Climate Protection.
- [45] Solantausta Y., Oasmaa A., Sipilä K., Lindfors C., Lehto J., Autio J., Jokela P., Alin J., and Heiskanen J., 2012, "Bio-oil production from biomass: Steps toward demonstration," *Energy and Fuels*, pp. 233–240.

- [46] Shaddix C. R., and D.R. Hardesty, 1999, Combustion Properties of Biomass Flash Pyrolysis Oils. Sandia Report SAND99-8238.
- [47] Czernik S., and Bridgwater A. V., 2004, "Overview of Applications of Biomass Fast Pyrolysis Oil," *Energy & Fuels*, **18**(2), pp. 590–598.
- [48] Chiaramonti D., Oasmaa A., and Solantausta Y., 2007, "Power generation using fast pyrolysis liquids from biomass," *Renew. Sustain. Energy Rev.*, **11**(6), pp. 1056–1086.
- [49] Venderbosch R., and Helden M. van, 2001, Diesel engines on bio-oil: a review.
- [50] Kasper J. M., Jasas G. B., and Trauth R. L., 1983, "Use of Pyrolysis-Derived Fuel in a Gas Turbine Engine," ASME Paper No. 83-GT-96, ASME.
- [51] Ardy P. L., Barbucci P., Benelli G., Rossi C., and Zanforlin G., 1995, "Development of gas turbine combustor fed with bio-fuel oil," SECOND BIOMASS CONFERENCE OF THE AMERICAS: ENERGY, ENVIRONMENT, AGRICULTURE, AND INDUSTRY, NREL, Portland, OR (USA), pp. 429–438.
- [52] Andrews R. G., Zukowski S., and Patnaik P. C., 1997, "Feasibility of Firing an Industrial Gas Turbine Using a Bio-Mass Derived Fuel," *Developments in Thermochemical Biomass Conversion* SE - 39, A. V Bridgwater, and D.G.B. Boocock, eds., Springer Netherlands, Dordrecht, pp. 495–506.
- [53] Andrews R. G., Fuleki D., Zukowski S., and Patnaik P. C., 1997, "Results of Industrial Gas Turbine Tests Using a Biomass-Derived Fuel," *Making a Business from Biomass in Energy, Environment, Chemicals, Fibers, and Materials*, R.P. Overend, and E. Chornet, eds., Elsevier Science Inc., New York, p. 425–435.
- [54] Lupandin V., Thamburaj R., and Nikolayev A., 2005, "Test results of the GT2500 gas turbine engine running on alternative fuels: bio oil, ethanol, bio diesel and heavy oil," *Proc. of the ASME TURBO EXPO 05*, ASME, pp. 421–426.
- [55] Strenziok R., Hansen U., and Kunster H., 2001, *Progress in Thermochemical Biomass Conversion*, Blackwell Science Ltd, Oxford, UK.
- [56] Cappelletti A., Rizzo A. M., Chiaramonti D., and Martelli F., 2013, "CFD redesign of micro gas turbine combustor for bio-fuels fueling," XXI International Symposium on Air Breathing Engines (ISABE), Busan, Korea, pp. 1199 – 1206.
- [57] Chiaramonti D., Rizzo A. M., Spadi A., and Prussi M., 2013, "Testing of pyrolysis oil, vegetable oil and biodiesel in a modified micro gas turbine: preliminary results. Oral presentation 2B010.5, 21st European Biomass Conference, Copenhagen."
- [58] Beran M., and Axelsson L.-U., 2014, "Development and Experimental Investigation of a Tubular Combustor for Pyrolysis Oil Burning," *J. Eng. Gas Turbines Power*, **137**(3), p. 031508.
- [59] Beld B. Van de, Holle E., and Florijn J., 2013, "The use of pyrolysis oil and pyrolysis oil derived fuels in diesel engines for CHP applications," *Appl. Energy*, **102**, pp. 190–197.

- [60] Bertoli C., Alessio J. D., Giacomo N. Del, Lazzaro M., Massoli P., Moccia V., and R. I. M. C. N., 2000, "Running Light-Duty DI Diesel Engines with Wood Pyrolysis Oil," *Combustion*, (724).
- [61] Shihadeh A. L., 1998, "Rural electrification from local resources : biomass pyrolysis oil combustion in a direct injection diesel engine," Massachusetts Institute of Technology.
- [62] Jay D. C. ., Rantanen O. A. ., Sipilä K. ., and Nylund N. O., 1995, "Wood Pyrolysis Oil for Diesel Engines," *Proceedings of the ASME Fall Technical Conference, American Society for Mechanical Engineers (ASME)*, New York.
- [63] Calabria R., Chiariello F., and Massoli P., 2007, "Combustion fundamentals of pyrolysis oil based fuels," *Exp. Therm. Fluid Sci.*, **31**(5), pp. 413–420.
- [64] Linck M., Felix L., Marker T., Ortiz-Toral P., Roberts M., and Wangerow J., 2014, "Integrated Hydrolysis and Hydroconversion Pilot Studies: Feedstock Types and Yield Profiles," *TCS Symposium, Denver, Colorado, September 2-5*.
- [65] Jones S. B., Valkenburg C., Walton C. W., Elliott D. C., Holladay J. E., Stevens D. J., Kinchin C., and Czernik S., 2009, *Production of gasoline and diesel from biomass via fast pyrolysis, hydrotreating and hydrocracking: a design case*, Pacific Northwest National Laboratory Richland, WA.
- [66] Huber G. W., Iborra S., and Corma A., 2006, "Synthesis of transportation fuels from biomass: chemistry, catalysts, and engineering.," *Chem. Rev.*, **106**(9), pp. 4044–98.
- [67] Huber G. W., and Corma A., 2007, "Synergies between bio- and oil refineries for the production of fuels from biomass.," *Angew. Chem. Int. Ed. Engl.*, **46**(38), pp. 7184–201.
- [68] French R., and Czernik S., 2010, "Catalytic pyrolysis of biomass for biofuels production," *Fuel Process. Technol.*, **91**(1), pp. 25–32.
- [69] Mortensen P. M., Grunwaldt J.-D., Jensen P. A., Knudsen K. G., and Jensen A. D., 2011, "A review of catalytic upgrading of bio-oil to engine fuels," *Appl. Catal. A Gen.*, **407**(1-2), pp. 1–19.
- [70] Amen-Chen C., Pakdel H., and Roy C., 2001, "Production of monomeric phenols by thermochemical conversion of biomass: a review," *Bioresour. Technol.*, **79**(3), pp. 277–299.
- [71] Effendi A., Gerhauser H., and Bridgwater A. V., 2008, "Production of renewable phenolic resins by thermochemical conversion of biomass: A review," *Renew. Sustain. Energy Rev.*, **12**(8), pp. 2092–2116.
- [72] Wei Q., Ma X., and Dong J., 2010, "Preparation, chemical constituents and antimicrobial activity of pyroligneous acids from walnut tree branches," *J. Anal. Appl. Pyrolysis*, **87**(1), pp. 24–28.
- [73] Sukhbaatar B., Steele P. H., Ingram L. L., and Kim M. G., 2009, "An exploratory study on the removal of acetic and formic acids from bio-oil," *BioResources*, **4**, pp. 1319–1329.

- [74] Freel B., and Graham R., 2002, "Bio-oil preservatives. US 6,485,841 B1."
- [75] Ecn P. D. W., Laan R. Van Der, Rug K., and Heeres E., 2009, "Lignin Valorisation for Chemicals and (Transportation) Fuels via (Catalytic) Pyrolysis and Hydrodeoxygenation," *Environ. Prog.*, **28**(3), pp. 461–469.
- [76] Wittcoff H. A., Reuben B. G., and Plotkin J. S., 2012, *Industrial organic chemicals*, John Wiley & Sons.
- [77] Demirbas A., and Demirbas M. F., 2010, *Algae Energy*, Springer.
- [78] Tredici M., 2010, "Photobiology of microalgae mass cultures: understanding the tools for the next green revolution," *Biofuels*, **1**(1), pp. 143–162.
- [79] IEA task 39, and AMF, 2011, *Algae as a Feedstock for Biofuels - An Assessment of the Current Status and Potential for Algal Biofuels Production*.
- [80] Molina Grima E., Belarbi E.-H., Acién Fernández F. G., Robles Medina a, and Chisti Y., 2003, "Recovery of microalgal biomass and metabolites: process options and economics.," *Biotechnol. Adv.*, **20**(7-8), pp. 491–515.
- [81] Reith J. H., 2004, *Renewable co-production of fine chemicals and energy from microalgae. Public final report E.E.T. project K99005/398510-1010 (In Dutch)*, Petten (NL).
- [82] Rodolfi L., Chini Zittelli G., Bassi N., Padovani G., Biondi N., Bonini G., and Tredici M. R., 2009, "Microalgae for oil: strain selection, induction of lipid synthesis and outdoor mass cultivation in a low-cost photobioreactor.," *Biotechnol. Bioeng.*, **102**(1), pp. 100–12.
- [83] Metting F. B., 1996, "Biodiversity and application of microalgae," *J. Ind. Microbiol. Biotechnol.*, **17**(5), pp. 477–489.
- [84] Spolaore P., Joannis-Cassan C., Duran E., and Isambert A., 2006, "Commercial applications of microalgae," *J. Biosci. Bioeng.*, **101**(2), pp. 87–96.
- [85] H. R., and Wijffels, 2008, "Potential of sponges and microalgae for marine biotechnology," *Trends Biotechnol.*, **26**(1), pp. 26–31.
- [86] Sawayama S., Inoue S., Dote Y., and Yokoyama S.-Y., 1995, "CO₂ fixation and oil production through microalga," *Energy Convers. Manag.*, **36**(6-9), pp. 729–731.
- [87] Ginzburg B.-Z., 1993, "Liquid fuel (oil) from halophilic algae: a renewable source of non polluting energy," *Renew. Energy*, **3**(2/3), pp. 249–252.
- [88] Miao X., Wu Q., and Yang C., 2004, "Fast pyrolysis of microalgae to produce renewable fuels," *J. Anal. Appl. Pyrolysis*, **71**(2), pp. 855–863.
- [89] Amin S., 2009, "Review on biofuel oil and gas production processes from microalgae," *Energy Convers. Manag.*, **50**(7), pp. 1834–1840.
- [90] 2009, *Algae-based biofuels: A Review of Challenges and Opportunities for Developing Countries*.
- [91] Peng W., Wu Q., and Tu P., 2000, "Effects of temperature and holding time on production of renewable fuels from pyrolysis of *Chlorella protothecoides*," *J. Appl. Phycol.*, **12**, pp. 147–152.

- [92] Peng W., Wu Q., and Tu P., 2001, "Pyrolytic characteristics of heterotrophic *Chlorella protothecoides* for renewable bio-fuel production," *J. Appl. Phycol.*, **13**(1), pp. 5–12.
- [93] Peng W., Qingyu W., Pingguan T., and Nanming Z., 2001, "Pyrolytic characteristics of microalgae as renewable energy source determined by thermogravimetric analysis," *Bioresour. Technol.*, **80**(1), pp. 1–7.
- [94] Miao X., and Wu Q., 2004, "High yield bio-oil production from fast pyrolysis by metabolic controlling of *Chlorella protothecoides*," *J. Biotechnol.*, **110**(1), pp. 85–93.
- [95] Demirbas A., 2006, "Oily products from mosses and algae via pyrolysis," *Energy Sources, part A*, **28**(10), pp. 933–940.
- [96] Torri C., Samori C., Adamiano A., Fabbri D., Faraloni C., and Torzillo G., 2010, "Bio evaluation of integrated production of hydrogen, fuels and bio-char from *Chlamydomonas Reinhardtii*," 18th European Biomass Conference and Exhibition, Lyon, France, pp. 455–458.
- [97] Torri C., Samorì C., Adamiano A., Fabbri D., Faraloni C., and Torzillo G., 2011, "Preliminary investigation on the production of fuels and bio-char from *Chlamydomonas reinhardtii* biomass residue after bio-hydrogen production," *Bioresour. Technol.*, pp. 1–7.
- [98] Li S.-Q., Yao Q., Chi Y., Yan J.-H., and Cen K.-F., 2004, "Pilot-Scale Pyrolysis of Scrap Tires in a Continuous Rotary Kiln Reactor," *Ind. Eng. Chem. Res.*, **43**(17), pp. 5133–5145.
- [99] Choi G.-G., Jung S.-H., Oh S.-J., and Kim J.-S., 2014, "Total utilization of waste tire rubber through pyrolysis to obtain oils and CO₂ activation of pyrolysis char," *Fuel Process. Technol.*, **123**, pp. 57–64.
- [100] ETRMA, 2014, European Tire and Rubber Manufacturer Association (ETRMA) - Statistics 2014.
- [101] Zabaniotou A., Antoniou N., and Bruton G., 2014, "Analysis of good practices, barriers and drivers for ELTs pyrolysis industrial application," *Waste Manag.*, **34**(11), pp. 2335–46.
- [102] 2013, "RECICLANIP - Coleta e Destinação de Pneus Inservíveis."
- [103] Connor K., Cortesa S., Issagaliyeva S., and Meunier A., 2013, Developing a sustainable waste tire management strategy for Thailand.
- [104] 1999, EC, 1999. European Council Directive, Waste Landfill Directive (1999/31/EC, 1999) Official Journal of the European Communities, European Council.
- [105] Wolfson D., Beckman J., Walters J., and Bennett D., 1973, Destructive distillation of scrap tires - Report 7302, Washington, DC.
- [106] Oasmaa A., Elliott D. C., and Müller S., 2009, "Quality control in fast pyrolysis bio-oil production and use," *Environ. Prog. Sustain. Energy*, **28**(3), pp. 404–409.

- [107] Quek A., and Balasubramanian R., 2013, "Liquefaction of waste tires by pyrolysis for oil and chemicals—A review," *J. Anal. Appl. Pyrolysis*, **101**, pp. 1–16.
- [108] Williams P. T., 2013, "Pyrolysis of waste tyres: a review.," *Waste Manag.*, **33**(8), pp. 1714–28.
- [109] Martínez J. D., Puy N., Murillo R., García T., Navarro M. V., and Mastral A. M., 2013, "Waste tyre pyrolysis – A review," *Renew. Sustain. Energy Rev.*, **23**, pp. 179–213.
- [110] İlkılıç C., and Aydın H., 2011, "Fuel production from waste vehicle tires by catalytic pyrolysis and its application in a diesel engine," *Fuel Process. Technol.*, **92**(5), pp. 1129–1135.
- [111] Doğan O., Çelik M. B., and Özdalyan B., 2012, "The effect of tire derived fuel/diesel fuel blends utilization on diesel engine performance and emissions," *Fuel*, **95**, pp. 340–346.
- [112] Sharma A., and Murugan S., 2013, "Investigation on the behaviour of a DI diesel engine fueled with Jatropha Methyl Ester (JME) and Tyre Pyrolysis Oil (TPO) blends," *Fuel*, **108**, pp. 699–708.
- [113] Martínez J. D., Rodríguez-Fernández J., Sánchez-Valdepeñas J., Murillo R., and García T., 2014, "Performance and emissions of an automotive diesel engine using a tire pyrolysis liquid blend," *Fuel*, **115**, pp. 490–499.
- [114] Sharma A., and Murugan S., 2014, "Influence of Fuel Injection Timing on the Performance and Emission Characteristics of a Diesel Engine Fueled with Jatropha Methyl Ester-Tyre Pyrolysis Oil Blend," *Appl. Mech. Mater.*, **592-594**, pp. 1627–1631.
- [115] Martínez J. D., Ramos Á., Armas O., Murillo R., and García T., 2014, "Potential for using a tire pyrolysis liquid-diesel fuel blend in a light duty engine under transient operation," *Appl. Energy*, **130**, pp. 437–446.
- [116] Koc A. B., and Abdullah M., 2014, "Performance of a 4-cylinder diesel engine running on tire oil–biodiesel–diesel blend," *Fuel Process. Technol.*, **118**, pp. 264–269.
- [117] López F. A., Centeno T. A., Alguacil F. J., and Lobato B., 2011, "Distillation of granulated scrap tires in a pilot plant.," *J. Hazard. Mater.*, **190**(1-3), pp. 285–92.
- [118] Tudu K., Murugan S., and Patel S. K., 2014, "Light Oil Fractions from a Pyrolysis Plant—An Option for Energy Use," *Energy Procedia*, **54**, pp. 615–626.
- [119] Öztop H. F., Varol Y., Altun Ş., and Firat M., 2014, "Using Gasoline-like Fuel Obtained from Waste Automobile Tires in a Spark-ignited Engine," *Energy Sources, Part A Recover. Util. Environ. Eff.*, **36**(13), pp. 1468–1475.
- [120] Murugan S., Ramaswamy M. C., and Nagarajan G., 2008, "The use of tyre pyrolysis oil in diesel engines.," *Waste Manag.*, **28**(12), pp. 2743–9.
- [121] Seljak T., Rodman Oprešnik S., and Katrašnik T., 2014, "Microturbine combustion and emission characterisation of waste polymer-derived fuels," *Energy*, **77**, pp. 226–234.

- [122] Rizzo A. M., Chiaramonti D., Bettucci L., and Marsili Libelli I., 2011, "Characterization of microalga chlorella as a fuel and its thermogravimetric behaviour," Proc. of ISAF XIX - International Symposium on Alcohol Fuels - Verona, 10-14 October 2011, D. Chiaramonti, and V.N. Raina, eds., Verona, pp. 165–167.
- [123] Rizzo A. M., Prussi M., Bettucci L., Marsili Libelli I., and Chiaramonti D., 2013, "Characterization of microalga Chlorella as a fuel and its thermogravimetric behavior," Appl. Energy, **102**, pp. 24–31.
- [124] Rizzo A. M., Chiaramonti D., and Prussi M., 2011, "Oily products from pyrolytic processing of microalgae: an overview," Proc. of the 19th European Biomass Conference and Exhibitions, Berlin, pp. 807–816.
- [125] Rizzo A. M., Nistri R., Buffi M., Marsili Libelli I., Bettucci L., Prussi M., and Chiaramonti D., 2013, "Effect of Feedstock Composition on Quality and Yield of Bio-oil from the Pyrolysis of Three Microalgae Species from Open Pond and Closed Photobioreactor," Proc. of the 21st European Biomass Conference and Exhibitions, pp. 494 – 499.
- [126] Chen G., Yu Q., and Sjöström K., 1997, "Reactivity of char from pyrolysis of birch wood," J. Anal. Appl. Pyrolysis, **40-41**, pp. 491–499.
- [127] Ingram L., Mohan D., Bricka M., Steele P., Strobel D., Crocker D., Mitchell B., Mohammad J., Cantrell K., and Pittman C. U., 2008, "Pyrolysis of Wood and Bark in an Auger Reactor: Physical Properties and Chemical Analysis of the Produced Bio-oils," Energy & Fuels, **22**(1), pp. 614–625.
- [128] Yang Y., Brammer J. G., Mahmood A. S. N., and Hornung A., 2014, "Intermediate pyrolysis of biomass energy pellets for producing sustainable liquid, gaseous and solid fuels.," Bioresour. Technol., **169**, pp. 794–9.
- [129] Buffi M., Rizzo A. M., Chiaramonti D., and Pari L., A comparative study on pyrolysis oil from different feedstock (submitted for publication).
- [130] Westerhof R. J. M., Brilman D. W. F. (Wim), Swaaij W. P. M. van, and Kersten S. R. A., 2010, "Effect of Temperature in Fluidized Bed Fast Pyrolysis of Biomass: Oil Quality Assessment in Test Units," Ind. Eng. Chem. Res., **49**(3), pp. 1160–1168.
- [131] Dauenhauer P. J., Colby J. L., Balonek C. M., Suszynski W. J., and Schmidt L. D., 2009, "Reactive boiling of cellulose for integrated catalysis through an intermediate liquid," Green Chem., **11**(10), p. 1555.
- [132] "Phyllis2, database for biomass and waste. Energy research Centre of the Netherlands."
- [133] Lourenço S. O., Barbarino E., Lavín P. L., Lanfer Marquez U. M., and Aida E., 2004, "Distribution of intracellular nitrogen in marine microalgae: Calculation of new nitrogen-to-protein conversion factors," Eur. J. Phycol., **39**(1), pp. 17–32.
- [134] Jones D. B., 1941, Factors for converting percentages of nitrogen in foods and feeds into percentages of proteins.

- [135] BLIGH E. G., and DYER W. J., 1959, "A rapid method of total lipid extraction and purification.," *Can. J. Biochem. Physiol.*, **37**, pp. 911–917.
- [136] Bigelow N., Barker J., Ryken S., Patterson J., Hardin W., Barlow S., Deodato C., and Cattolico R. A., 2013, "Chrysochromulina sp.: A proposed lipid standard for the algal biofuel industry and its application to diverse taxa for screening lipid content," *Algal Res.*, **2**(4), pp. 385–393.
- [137] Oasmaa A., Elliott D. C., and Mu S., 2009, "Quality Control in Fast Pyrolysis Bio-Oil Production and Use," *Environ. Prog.*, **28**, pp. 404–409.
- [138] BIOTOX (2005). Final technical report. Part I: Publishable final report. Project No S07.16365. An assessment of bio-oil toxicity for safe handling and transportation.
- [139] Elliott D. C., 1983, Analysis and upgrading of biomass liquefaction products. Final report, Vol. 4, IEA Co-operative project D1 Biomass Liquefaction Test Facility Project, Richland, Washington.
- [140] Rick F., and Vix U., 1991, "Product Standards for Pyrolysis Products for Use as Fuel in Industrial Firing Plants," *Biomass Pyrolysis Liquids Upgrading and Utilization SE - 7*, A. V Bridgwater, and G. Grassi, eds., Springer Netherlands, pp. 177–218.
- [141] Peacocke G. V. C., Russell P. A., Jenkins J. D., and Bridgwater A. V., 1994, "Physical properties of flash pyrolysis liquids," *Biomass and Bioenergy*, **7**(1-6), pp. 169–177.
- [142] Oasmaa A., Leppämäki E., Koponen P., Levander J., and Tapola E., 1997, "Physical characterisation of biomass-based pyrolysis liquids application of standard fuel oil analyses," *VTT Publ.*
- [143] Meier D., Oasmaa A., and Peacocke G. V. C., 1997, "Properties of Fast Pyrolysis Liquids: Status of Test Methods," *Developments in Thermochemical Biomass Conversion SE - 31*, A. V Bridgwater, and D.G.B. Boocock, eds., Springer Netherlands, pp. 391–408.
- [144] 2012, "ASTM D7544-12, Standard Specification for Pyrolysis Liquid Biofuel."
- [145] Fuleki D., 1999, "Bio-fuel system material testing," *PyNe Newsl.*, pp. 5–6.
- [146] Darmstadt H., Garcia-Perez M., Adnot A., Chala A., Kretschmer D., and Roy C., 2004, "Corrosion of Metals by Bio-Oil Obtained by Vacuum Pyrolysis of Softwood Bark Residues. An X-ray Photoelectron Spectroscopy and Auger Electron Spectroscopy Study," *Energy & Fuels*, **18**(5), pp. 1291–1301.
- [147] Zhiru L., 2001, "The degradation effects of pyrolysis liquids on metals, plastics and elastomers," University of Toronto.
- [148] Kirk D. W., Li Z., Fuleki D., and Patnaik P. C., 2001, "Materials Compatibility With Pyrolysis Biofuel," *Volume 2: Coal, Biomass and Alternative Fuels; Combustion and Fuels; Oil and Gas Applications; Cycle Innovations*, ASME, p. V002T01A006.

- [149] Hu X. G., Zhou L. L., Wang Q. J., Xu Y. F., and Zhu X. F., 2011, "On corrosion behaviour of metal in biomass oil," *Corros. Eng. Sci. Technol.*, **46**(4), pp. 400–405.
- [150] Chiaramonti D., Rizzo A. M., Riccio G., Prussi M., and Martelli F., 2011, "Realizzazione di un banco prova didattico policombustibile per microturbina a gas in ciclo semplice.," *Atti 66° Convegno Nazionale ATI*, Cosenza.
- [151] Chiaramonti D., Rizzo A. M., Spadi A., Prussi M., Riccio G., and Martelli F., 2013, "Exhaust emissions from liquid fuel micro gas turbine fed with diesel oil, biodiesel and vegetable oil," *Appl. Energy*, **101**, pp. 349–356.
- [152] Chiaramonti D., Rizzo A. M., Riccio G., Cappelletti A., Prussi M., and Martelli F., 2011, "Adaptation of a micro gas turbine to biofuels and preliminary tests with diesel fuel," *Third International Conference on Applied Energy*, pp. 2057–2066.
- [153] Rizzo A. M., 2011, "Micro gas turbine fed with liquid biofuels: conversion and testing," University of Florence.
- [154] Saravanamutto H., Rogers G., and Cohen H., 2001, *Gas turbine theory*, Pearson Education Ltd.
- [155] 2009, "EN 14918 : Solid biofuels - Determination of calorific value."
- [156] DuBois M., Gilles K. a., Hamilton J. K., Rebers P. a., and Smith F., 1956, "Colorimetric Method for Determination of Sugars and Related Substances," *Anal. Chem.*, **28**(3), pp. 350–356.

Appendix A: analytical procedures

The first appendix is devoted to the experimental and analytical procedures adopted in laboratory for the analysis on the most relevant chemical and physical properties of the bio-oil. Unless differently specified, each analysis was carried out in triplicates.

Calorific value (HHV)

Determination of the higher heating value was carried out according to EN 14918 [155], for solid samples, or DIN 51900-2, for liquid samples, by means of a Leco AC500 isoperibol calorimeter. A sample of about 1 g was weighed with a precision of 0.1 mg in a crucible, then the crucible and a nickel ignition wire were placed into the calorimeter. The equipment was closed and pressurized to 29 bar with high purity oxygen (99,999%), then settled into the bucket, which was previously filled with a fixed volume of distilled water. After a suitable period, required to reach thermal equilibrium, the ignition was automatically started and temperature was measured by an electronic thermometer with an accuracy of 0.0001°C. The higher heating value automatically calculated by the instrument is then corrected to account for the residual length of the nickel wire. Certified calorific standard (benzoic acid) was used both for calibration and as a spike for samples.

Density

Density of bio-oils was measured by means of a calibrated glass hydrometer according to UNI 3675. Bio-oils were kept at 15°C or 20°C in a glass cylinder inside a water bath in order to reach a constant temperature before dunking the hydrometer.

Kinematic viscosity

Kinematic viscosity of oils was measured according to UNI 3104 with a Lauda viscometer, made of an Ubbelohde capillary tube controlled by iVisc software and a Proline PV 15 thermostatic bath filled with deionized water. Thermostatic bath allows keeping a constant temperature with a precision of 0.01°C. Sample was introduced in the capillary tube and allowed to reach the selected temperature in the thermostatic bath before starting the analysis. Each measurement was carried out at the selected temperature for five times: two times in order to precondition the capillary tube, then the last three times for analysis: an interval of 90 s occurred between every measurement.

Due to the combined effect of dark colour and sticky nature, few bio-oil samples could adhere to the glass wall of the capillary, resulting in the impossibility for the optical sensor to detect the passage of the liquid meniscus.

Solid content

Solid content of bio-oils was determined by the method from Oasmaa & Peacocke [26]. Bio-oils samples were dissolved in a solvent solution of methanol-dichloromethane (1:1). The solution was filtrated with a 1 µm pore size micro fiber filter over a Millipore filtration system under vacuum, and washed with the solvent mixture until the filtrate was clear. The filter paper with the residue was then air-dried for 30 minutes.

Moisture

Moisture content of solid feedstock was determined by a Leco TGA 701 instrument according to UNI 14774-3. Leco TGA 701 allows a weight measurement with a precision of 0.0001 g and provides an automatic correction according to the gas density variation as the temperature was increased from ambient final temperature. The instrument can host 19 samples plus and 1 position for the reference crucible. Samples were heated in porcelain crucibles under an air or nitrogen flow of 3,5 l·min⁻¹ from room temperature to 105°C by a heating rate of 10 °C·min⁻¹, then held at 105°C for 2h30' until constant weight measurement.

Ash

Determination of the amount of ash in bio-oils and biomasses were performed in a Leco TGA 701 instrument. Samples of bio-oils were gradually heated in porcelain crucibles under an airflow of 5 l·min⁻¹ heated from room temperature to 775°C at oven heating rates of 10 °C·min⁻¹ in porcelain crucibles, then held at 775°C for at least 1h30' to allow for a complete incineration. Samples of algal cells were analysed according to UNI 14775: algal cells were heated in porcelain crucibles under an air flow of 3,5 l·min⁻¹ from room temperature to 250°C at oven heating rate of 7 °C/min and held at 250°C for 1h, then heated from 250°C to 550°C at 10 °C/min and held at 550°C for at least 2h. Analyses were carried out in triplicates.

Conradson Carbon Residue (CCR)

Determinations of the CCR in bio-oils were performed in a Leco TGA 701 instrument. Samples of bio-oils were gradually heated in porcelain crucibles under a nitrogen (99.999%) flow of 10 l·min⁻¹ from room temperature to 500°C at oven heating rates of 10 °C·min⁻¹ in porcelain crucibles, then held at 500°C for 15'.

Thermo-Gravimetric Analysis (TGA)

Biomass samples were subjected to TGA by means of a Leco TGA 701 instrument; all the analyses were conducted under a flow of $8.5 \text{ l}\cdot\text{min}^{-1}$ of high purity nitrogen gas (99,999%) in order to prevent the oxidation of the samples. The temperature program was a constant heating rate ramp from room temperature to 800°C , at $15^\circ\text{C}\cdot\text{min}^{-1}$ in porcelain crucibles held by a pneumatic carousel; only one crucible was loaded into the carousel at a time, and each TGA test was repeated in triplicates. The temperature of the oven was measured with a precision of $\pm 2\%$ of the reading. Weight loss of each sample was recorded about every 2 min with a precision of 0.0001 g and subjected to an automatic correction according to the nitrogen density variation as the temperature was increased from ambient to 800°C . Records of weight loss of each sample were collected to determine both thermogravimetric (TG) and derivative thermogravimetric (DTG) curves.

Carbohydrates, Lipids and Proteins content

The determination of carbohydrates was performed by the phenol-sulphuric acid method of Dubois *et al.* [156]. The analysis was conducted on freeze-dried samples, weighed and then suspended in water in the ratio 1:5. The samples were shaken to facilitate soaking of the cells and thus obtain a better extraction. In a vial of proper size, 1 ml of phenol and 5 ml of 5% H_2SO_4 were added to 1 ml of sample. After 10 minutes, dipping the vial in a bath of ice and water freezes the reaction. After cooling, the solution was inserted in a spectrophotometer and its absorbance measured at a wavelength of 488nm, using pure water as zero. The concentration of carbohydrates is given by the calibration curve obtained with anhydrous glucose, whose equation is $y = 109.6x - 0,487$, where y is $\text{mg}\cdot\text{l}^{-1}$ of carbohydrates (Abs_{488}).

The determination of lipids was performed by the phenol-sulphuric acid method of Bligh and Dyer [135]. 20 ml methanol and 10 ml chloroform were added to a 100 ml conical flask containing 5 g of sample, and the mixture was shaken for 2 min. 10 ml

chloroform were added a second time and the mixture was shaken vigorously for 2 min. 18 ml of distilled water were added and the mixture was shaken again for 2 min. the layer were separated by centrifugation for 10 min at 2000 rpm. The lower layer was transferred to pear-shaped flask with a Pasteur pipette. A second extraction was done 20 ml 10% (v/v) methanol in chloroform by shaken for 2 min. After centrifugation, the chloroform phase was added to the first extract. Evaporation was done in rotavapor and the residue was dried at 105°C for 1 h.

The determination of proteins was inferred by multiplying the nitrogen content, obtained from elemental analysis, for a conversion factor [133,134].

Appendix B: GC-MS of pyrolysis liquids

GC-MS analysis of bio-oils and aqueous phases were performed in a Shimadzu GCMS-QP 2010 Plus equipped by a Phenomenex Zebron ZB-5HT Inferno (30m x 0.25mm x 0.25 μ m). Setup parameters are as follow:

- Gas carrier: He 99,999%
- Column flow: 2,02 mL/min
- Flow control mode: linear velocity
- Injection: volume 1 μ L , Split mode, 1/150 ratio, T= 250°C
- Scan mode: full scan, 35-550 m/z
- Solvent cut time: 1,5 min

Oven temperature program:

Rate (°C/min)	Temperature (°C)	Hold Time (min)
-	40	10
8	200	10
10	280	30

Sample preparation was different for organic and water phase. For the organic phase some drops of bio-oil were solved in dichloromethane then suspended particles were removed by means of a 0,2 μ m filter. For the water phase some drops of bio-oil were diluted with 2-propanol and suspended particles were removed by means of a

0,2um filter. Internal NIST 08 library was used for the identification of the compounds found in the bio-oil and their categorization into main functional group.

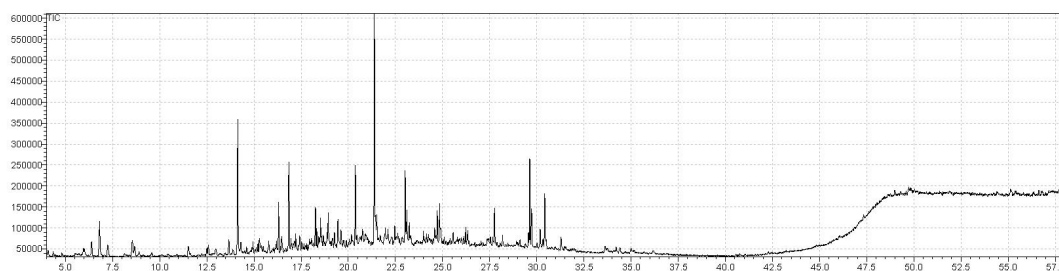


Figure B.1: Chromatogram of the bio oil from Chlorella Ingrepro.

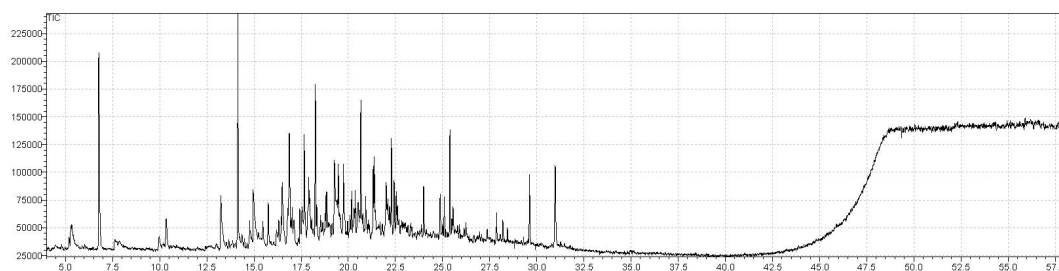


Figure B.2: Chromatogram of the aqueous phase from Chlorella Ingrepro.

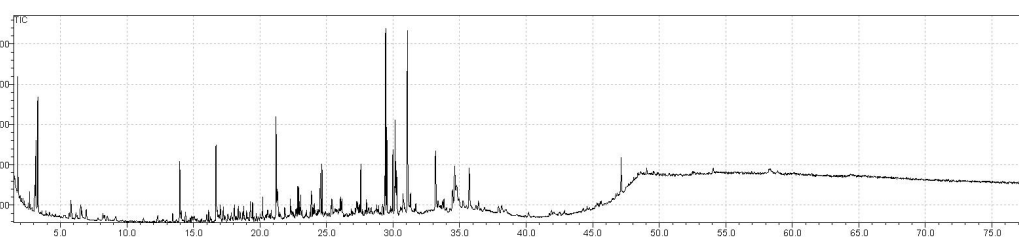


Figure B.3: Chromatogram of the bio oil from Nannochloropsis HCMR.

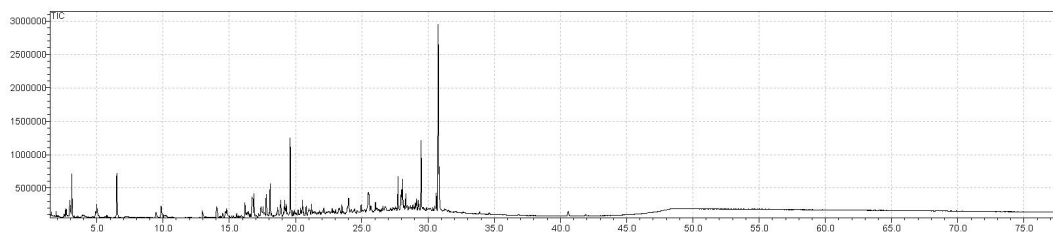


Figure B.4: Chromatogram of the aqueous phase from Nannochloropsis HCMR.

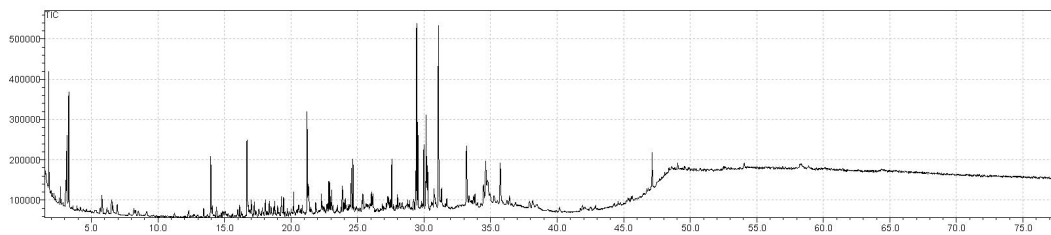


Figure B.5: Chromatogram of the bio-oil from Chlorella HCMR.

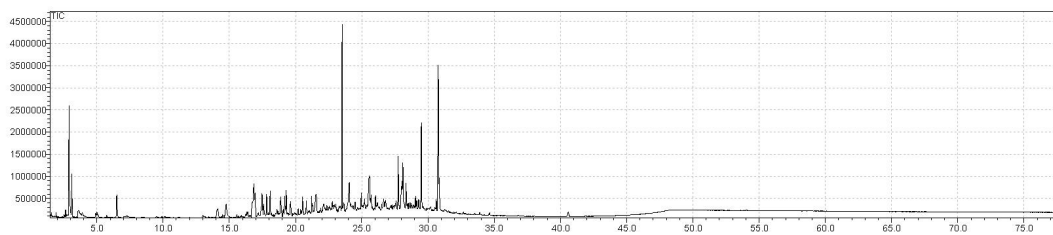


Figure B.6: Chromatogram of the aqueous phase from Chlorella HCMR.